AN EFFICIENT METHOD OF ESTIMATING SEDIMENT DISCHARGE IN RIVERS

by

Hadi Emdad

B.S. in Irrigation Engineering, Shiraz University, Iran, 1975

M. Engineering in Engineering Science, Pennsylvania State University, 1989

Submitted to the Graduate Faculty of

The School of Engineering in partial fulfillment

of the requirements for the degree of

Doctor of Philosophy

University of Pittsburgh

2004

UNIVERSITY OF PITTSBURGH

SCHOOL OF ENGINEERING

This dissertation was presented

by

Hadi Emdad

It was defended on

December 3, 2004

and approved by

Rafael G. Quimpo, Professor, Department of Civil and Environmental Engineering

Tin-Kan Hung, Professor, Department of Civil and Environmental Engineering

William Matlack, Professor, Graduate School of Public and International Affairs

Allan Bullen, Emeritus Professor, Department of Civil and Environmental Engineering

Dissertation Director: Chao-Lin Chiu, Professor, Department of Civil and Environmental Engineering

AN EFFICIENT METHOD OF ESTIMATING SEDIMENT DISCHARGE IN RIVERS

Hadi Emdad, PhD

University of Pittsburgh, 2004

Estimation of sediment discharge by conventional measurement methods is expensive and labor intensive. An efficient method that can estimate the average cross-sectional sediment concentration and discharge in a river channel was developed. This method relies on the Chiu's velocity and sediment distribution models, which are based on the probability concept. The advantage of this approach compared to conventional methods is that the velocity and sediment concentration can be accurately estimated over the entire water depth, from the channel bed to the water surface. This method requires determining the location of a vertical (y-axis), where the maximum velocity of the entire cross section occurs. The correlation between the mean sediment concentration on each vertical and the cross-sectional mean concentration was analyzed. It led to the conclusion that sediment sampling should be conducted on y-axis at a point where sediment concentration is equal to the mean concentration on y-axis. A family of plots for selection of the sampling location was developed. Finally, a method based on Chiu's sediment transport model and data analysis was developed to estimate the mean sediment concentration in a channel section. This cross-sectional mean sediment concentration can be used to calculate the sediment discharge.

TABLE OF CONTENTS

LIST OF TABLES

LIST OF FIGURES

ACKNOWLEDGEMENT

I would like to express my sincere appreciation to my advisor Dr. Chao-Lin Chiu for his advice and patient guidance throughout my graduate program at the University of Pittsburgh. Without his encouragement this dissertation would not be possible. I would like to thank Dr. Allan Bullen, Dr. William Matlack, Dr. Rafael Quimpo and Dr. Tin-Kan Hung for serving on my doctoral committee.

The Missouri River sediment reports and field data were obtained from Mr. Larry J. Morong with Department of the Army, Corps of Engineers, Omaha District. The field data on Mississippi River was obtained from Dr. Albert Molinas. The efforts of Mr. Morong and Dr. Molinas in providing the data are appreciated.

1.0 INTRODUCTION

1.1 PROBLEM AND BACKGROUND

Suspended sediment is a major carrier of many contaminants including nutrients and heavy minerals. Control and mitigation of these problems require understanding of the sediment transport processes. Monitoring of sediment transport of a stream provides useful information concerning changes in the watershed conditions and will determine the quantity of sediment discharge. Quantifying the amount of sediment transport within a watershed is important due to the fact that:

1. Expected capacities for reservoirs may be underestimated.
2. Sedimentation of rivers can cause increase in drinking water treatment costs and may impact the public health.
3. Ecologically sensitive areas can be adversely impacted by excessive sedimentation.

Without a monitoring system, the watershed problems and changes in environmental conditions cannot be measured and addressed adequately. The quantity of sediment in water must be estimated so that the sediment may be removed before the water enters a distribution system. Pesticides and organic materials are adsorbed by sediment, causing potential health hazards in some streams, estuaries, and water reservoirs.

There is not a single sediment transport equation, which is efficient and provides reliable results

without requiring a large number of sampling and complex computations. Many sediment transport equations have been developed: HEC-6 model offers the user a choice of 12 different equations. The Corps of Engineers Sediment Transport Package (ODSET) uses 11 equations.

Unlike hydraulic equations such as Chezy's and Manning's, which give approximately same results, the existing sediment transport equations applied to the same data set can generate estimates of sediment transport rates ranging over more than 2 orders of magnitude [34].

Existing methods of predicting bed material load in sand bed channel flow is unreliable. In field data collection sedimentation quantities have to be separately sampled and measured. Measurements involve collection and transportation of large volumes and numbers of samples to laboratories and methods of analysis are slow and cumbersome. Sediment transport in natural channels is highly variable in space and time, so the accuracy of measurement depends on exposure time and density of sampling. In view of this situation, it is only realistic to expect substantial level of errors in sedimentation data [12].

Because of the costs, difficulties and uncertainties associated with the traditional methods of sediment load measurements and estimate, many environmental groups and government agencies have not adopted a sediment measurement program.

The common method used by U.S. Geological Survey (USGS) is to measure the suspended sediment concentration by depth-and point-integrating samplers. By conducting depth-averaged sampling the vertical mean concentration is determined directly. However, the method is impractical under strong currents in high flows. In addition, a distance of 0.3 to 0.5 foot from the channel bed is left unmeasured due to the sampler's restrictions [14].

The US Geological Survey uses US PS-69 automatic pumping samplers at gaging stations in Pennsylvania to measure the suspended sediment concentration of streams and some small

rivers. Data collected by pumping samplers are taken from a single point in the flow, which represents neither the cross-sectional nor vertical mean sediment concentrations. Without a workable mathematical model of distribution of sediment concentration, it is difficult to establish a stable relation between the concentration at the sample point and the mean sediment concentration in the vertical and the cross-section.

Sediment rating curves are often used to estimate suspended sediment loads where the sampling program is insufficient to define the continuous record of sediment concentration. Use of this technique will involve errors in the values of sediment load produced. Values of annual sediment load estimated by using a rating curve could involve errors of up to 280%. Careful consideration should be given to possible error terms before rating curve estimates of sediment load are used in statistical and other analyses [16, 20].

The widely used Rouse equation- a suspended sediment concentration model is based on the Prandtl-von Karman velocity distribution, which is incapable of predicting maximum velocities near water surface and the channel bed. Rouse equation can not predict sediment concentration at or near the channel bed, where the highest sediment concentration occur [2].

1.2 OBJECTIVE AND SCOPES OF STUDY

The main objective of this research is to develop an efficient method of estimating sediment discharge in rivers based on Chiu's velocity and sediment-distribution models. To achieve this goal, the following objectives have been established:

- Develop a method to estimate a coefficient for converting sediment concentration at the optimal point on y-axis to the cross-sectional mean concentration. This sediment concentration can be used to calculate the sediment discharge.
- Determine the location of the optimal sampling station (hereinafter is referred to as the y-axis) across a river cross section at a monitoring station.
- Determine the optimal depth of sampling on y-axis. Sediment concentration at this depth should represent the mean concentration on y-axis.
- Apply Chiu's sediment transport model to sediment and velocity data obtained from Missouri River Special Point-Integrated Sediment Sampling Program initiated in 1976 by the USGS and the U.S. Corps of Engineers (USACE).
- Apply Chiu's equations to sediment and velocity data on Mississippi River obtained from Lower Mississippi River Sediment Study by USACE and others. Data analysis on other rivers.

2.0 REVIEW OF LITERATURE

2.1 DISCHARGE MEASUREMENT BY CONVENTIONAL METHODS

Determination of water discharge is needed for estimation of sediment discharge. At many locations water discharge can be accurately determined from a stage-discharge relation. If, however, the relation of discharge to stage is not stable, as for most sand bed streams, or an accurate relation is not available, as for a new station, a discharge measurement is necessary at the time sediment concentration is sampled in the cross section [25].

Average velocity is required for calculating water discharge. Direct measurement of the average velocity of an entire cross section is impossible, so the conventional method uses incremental method, which is time consuming.

The discharge of a stream is calculated from measurement of velocity and depth. In the field, a marked line is stretched across the stream. At regular intervals along the line, the depth of the water is measured with a graduated rod or by lowering a weighted line from the surface to the streambed, and the velocity is measured using a current meter [36]. The discharge at a cross section is found by summing the incremental discharges from each measurement i, i = 1, 2, 3,…, n of velocity $\overline{u}_i$ and depth D_i.

$$Q = \sum_{i=1}^{n} \overline{u}_i D_i \Delta w_i \qquad (2\text{-}1)$$

Δw_i =width increment; D_i=water depth; $\overline{u}_i$ = average velocity at a vertical

Each measurement represents the conditions up to halfway between this measurement and the adjacent measurements on each side.

$$\Delta w_i = \frac{1}{2}(b_{i+1} - b_i) + \frac{1}{2}(b_i - b_{i-1}) \quad (2\text{-}2)$$

b_i = horizontal distance in feet of i^{th} velocity vertical from the left water edge; b_1=0; b_n = channel width.

Discharge increment is

$$q_i = D_i \bar{u}_i \Delta w_i \quad (2\text{-}3)$$

The average vertical velocity is computed by averaging point velocities at two points on each vertical. These point velocities are measured by current-meter and located at 0.2 and 0.8 of the total depth below the water surface.

A comprehensive study by the USGS in 1950 making a comparison of mid-section versus the mean-section methods of computing cross-sectional area and/or discharge resulted in USGS adopting the mid-section method as the standard or recommended procedure. The main reason for adopting the mid-section method was time and money savings over the mean-section method[35].

2.1.1 Mid-Section Method

The mid-section method of measurement assumes that the velocity samples at each depth sampling point, represents the mean velocity in partial rectangular cross-sectional area. The partial area extends laterally from half the distance from the preceding meter location to half the distance to the next, and vertically from the water surface to the measured depth (Figure 1). The channel cross section is defined by depths at locations 1,2,3,…n. At each location, the velocities

are measured by current-meter to obtain the mean of vertical distribution of velocities. The partial discharge is now computed for any subsection i as

$$q_i = \bar{u}_i \left[\frac{(b_i - b_{(i-1)})}{2} + \frac{(b_{(i+1)} - b_i)}{2} \right] D_i = \bar{u}_i \left[\frac{b_{(i+1)} - b_{(i-1)}}{2} \right] D_i \qquad (2\text{-}4)$$

where

q_i = discharge through partial section i,

u_i = mean velocity at subsection i,

b_i = distance from initial point to location i,

$b_{(i-1)}$ = distance from initial point to preceding location,

$b_{(i+1)}$ = distance from initial point to next location

D_i = depth of water at location i.

Thus, for example, the discharge through partial section 5 is

$$q_5 = \bar{u}_5 \left[\frac{b_6 - b_4}{2} \right] D_5 \qquad (2\text{-}5)$$

The preceding location at the beginning of the cross section is considered coincident with location 1; the "next location " at the end of the cross section is considered coincident with location n. Thus,

$$q_1 = \bar{u}_1 \left[\frac{b_2 - b_1}{2} \right] D_1 \quad \text{and} \quad q_n = \bar{u}_n \left[\frac{b_i - b_{(n-1)}}{2} \right] D_n \qquad (2\text{-}6)$$

For the example shown in the figure, q_1 is zero because the depth at observation point 1 is zero. The summation of the discharges for all partial sections is the total discharge of t he stream [35].

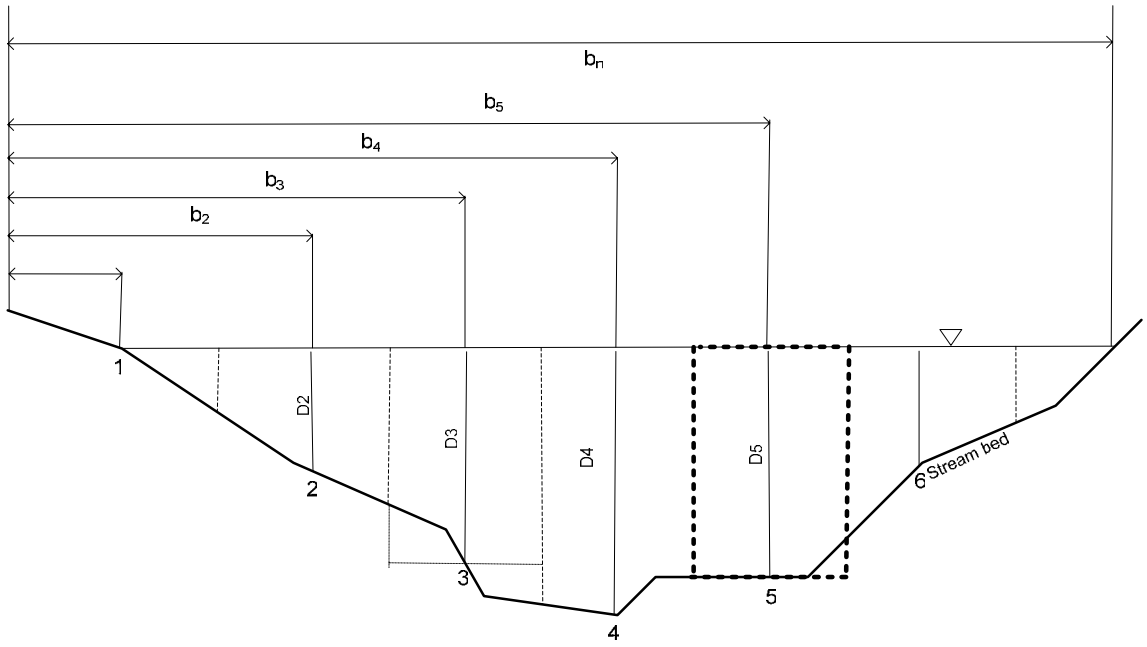

Figure 2-1 Sketch of Mid-section Method of Computing Cross-sectional Area for Discharge Measurement

2.2 MEASUREMENT OF SUSPENDED SEDIMENT DISCHARGE

Sediment concentration may be determined as the ratio of the weight of sediment to the weight of water-sediment and is the method referred in USGS manual [25]. The purpose of collecting sediment samples is to determine the instantaneous sediment concentration at a cross section. USGS uses two basic methods to define the location or spacing of the verticals. One is based on equal increments of water discharge (EDI); the second is based on equal increments of stream or channel width (EWI).

Units of measurement of sediment concentration are reported in the U.S.G.S. Computation of Fluvial-Sediment Discharge [25] as follows: Milligrams of sediment per liter of water-sediment mixture is a concentration unit. However, as a matter of convenience, it is determined in the laboratory in parts per million, which is the dry weight of suspended material per million equal weights of water-sediment mixture, or milligram per kilogram, and is found by the formula:

parts per million = (weight of sediment X 1000000)/(weight of water-sediment mixture)

or

$$1\text{ppm}=\frac{0.001g}{1000g}=\frac{1g}{1000000g}$$

Concentration in milligram per liter is the weight in milligrams (mg) of sediment per thousand milliliters (ml) of mixture and is the ratio of dry weight of sediment to the volume of mixture, or

$$\text{Milligrams per liter}=\frac{0.001g}{1000ml}=\frac{1mg}{1000ml}$$

The numerical values of part per million and milligrams per liter are equal when the density of the mixture is equal to 1.00, and for all practical purposes, 1 liter weighs 1000 g.

2.2.1 The Equal-Discharge–Increment Method (EDI)

In this method, the location of verticals can only be done after the discharge distribution across the width is known. It is then a simple matter to locate the verticals at the middle of strips of equal discharge. Obviously the average of the mean concentrations measured at these verticals gives the average concentration for entire cross section. This value can then be multiplied by the discharge obtained with the help of a stage-discharge curve [30].

In EDI method, the cross-sectional area is divided laterally into a series of subsections, each of which conveys the same water discharge. Depth integration is then carried out at vertical in each subsection where half of the subsection discharge is on one side and half is on the other side. The method requires that we have some knowledge of stream flow distribution in the cross section before sampling verticals can be selected. EDI method can save and labor over the ETR method, especially on the larger streams, because fewer verticals are required. From a discharge measurement, a graph is drawn of cumulative discharge in percent of total discharge versus distance from left or right bank or the station numbers on the cableways or bridges. A decision is made as to the number of verticals required to adequately define the suspended sediment concentration across the stream [13].

The average sediment concentration for the whole cross section in EDI method is calculated as

$$\overline{C}_X = \frac{1}{n}\sum_{i=1}^{n}\overline{C}_i \qquad (2\text{-}7)$$

$\overline{C}_i$ = average concentration at vertical, i =1.. n

If the partial discharge in the subsections is not equal, the discharge distribution weight is not equal to $\frac{1}{n}$.

2.2.2 Equal-Width-Increment Method (EWI)

In this method the measured sediment concentration in a vertical has to be multiplied the discharge through the strip it represents to compute the load passing the strip. The discharge through the strip can be obtained by current meter measurements in the vertical or with the help of a relation between the discharge in the strip and the total discharge in the cross section. The

total discharge could be obtained from the stage-discharge curve. The relation between the discharge through a strip and the total discharge will have to be obtained earlier from extensive current-meter investigations [30].

This method also is called Equal-width-increment method. The EWI method requires that all verticals be traversed using the same transit rate [14]. The number of verticals required for an EWI sediment discharge measurement depends on the distribution of concentration and flow in the cross section at the time of sampling and accuracy of the results. Water discharge measurement is not required preceding use of the EWI method.

If the sampled verticals do not represent centroids of equal discharge (EDI method), the mean concentration is not the average of all measured verticals. In this case (EWI) the mean concentration in the cross section is calculated as:

$$\overline{C}_x = \frac{1}{Q}\int_A uCdA = \frac{1}{Q}\sum_{i=1}^{n}\overline{C}_i q_i = \sum_{i=1}^{n}\overline{C}_i\left(\frac{\overline{u}_i A_i}{Q}\right) = \sum_{i=1}^{n}\overline{C}_i W_i \qquad (2\text{-}8)$$

W_i = discharge distribution weight = $\frac{q_i}{Q}$

$$A_i = D_i \Delta w_i \qquad (2\text{-}9)$$

Δw_i = width of vertical

2.2.3 Suspended Sediment Sampling Methods

The usual purpose of sediment sampling is to determine the instantaneous mean discharge-weighted suspended sediment concentration at a cross section. Such concentrations are combined with water discharge to compute the measured suspended sediment discharge.

In the depth-integration method the sampler traverses the depth of the stream at a uniform speed. At every point in the vertical, a volume of sediment-water mixture proportional to the stream velocity is collected by the sampler. The concentration of the sample thus gives the mean concentration in the vertical. The product of this concentration and discharge corresponding to the strip within which the vertical lies is the suspended sediment load for the strip [14, 30].

Depth-integrated samplers normally collect water and sediment mixture only from the surface to about 0.3 foot from the streambed [29].

In the point-integrating method sediment samples are taken at a number of points along the vertical to obtain the concentration distribution in the vertical. If the velocity distribution in the vertical is known or measured, the concentration and velocity profiles could be combined to prepare the sediment distribution curve for the vertical and the suspended load is calculated. Point-integrating sampler will have to be used on streams, which are too deep or too swift for the depth-integrating sampler [14, 30].

Point-integrated sample is a sample of sediment that is accumulated continuously in a sampler that is held at a relatively fixed point and that admits water and sediment mixture at a velocity about equal to the instantaneous stream velocity at that point [29]. Because of the cost of sampling, this method is used mostly for research programs.

2.2.4 Location of Sampling Points on the Vertical

A precise method of point-integration involves the determination of the velocity and concentration distribution curves in the vertical measurement at a large number of points. But this is too time-consuming to be practicable for routine sediment investigations. Therefore, such detailed profiles are taken for research purposes [14, 30]. In practice point-integration method follows one of the following schemes: One-point method, two-point method, and. three-point method.

In the one-point method the concentration is measured at the surface or at 0.6 times the depth below the surface. An empirical coefficient has to be used to get the mean sediment concentration from known surface concentration. This method is undependable. Sampling at 0.6 depths has been used in the hope that it gives the mean concentration, presumably because the mean velocity occurs approximately at this level. This method is not reliable because the mean sediment concentration varies with the flow and sediment size.

Straub [30, 33] showed that the mean concentration of suspended sediment in a vertical is given by

$$\overline{C_i} = \frac{3}{8} C_{0.8D} + \frac{5}{8} C_{0.2D} \qquad (2\text{-}10)$$

Where $C_{0.8}$ and $C_{0.2}$ are sample concentration taken at 0.8 and 0.2 depth below water surface, respectively.

The three-point method involves the measurement of the concentration at surface, bottom and mid-depth. The two-point and three-point methods do not give a correct idea about the size distribution of the suspended load. Such information can only be obtained using a depth-

integrating sampler or from records of a point-integrating sampler at a number of points in the vertical.

The current method of sediment measurement, which is used widely by USGS is automatic pump sampling [23]. However, when the sampler intake is fixed, without a sediment distribution model, the point sampling does not represent the vertical or cross-sectional mean concentration. It is evident from the vertical distribution of sediment concentration that relative depth of the sampler intake may have a relatively small effect on the measured concentrations of silt and clay it will have a very large impact on all sands, and even coarse silt. The sample intake should be located at a point within the cross-section that approximates the mean concentration across the full range of sampled flows or have an adjustment factor.

Single-point sampling can accurately represent the mean concentration of fine sediment (silt and clay) that exhibits uniform concentration distribution. However, the measurement of sand load presents a difficult problem and can produce very poor correlation between the point samples and the mean concentration.

2.3 ESTIMATION OF SUSPENDED SEDIMENT DISCHARGE

Generally, the mean discharge-weighted concentration ($\overline{C}_x$) of a stream can be used directly to compute the rate of sediment discharge moving in the stream [14, 25].

If water discharge is in cubic feet per second

$$Q_s = 0.0027 Q \overline{C}_x \qquad (2\text{-}11)$$

Q_s = tons per day (English short tons)

If water discharge is in cubic meters per second

$$Q_s = 0.0864 Q \overline{C}_x \quad (2\text{-}12)$$

Q_s = metric tons per day

where

$\overline{C}_x$ = discharge-weighted mean concentration (whole cross-section), in mg/L

Q = stream flow rate, in cubic feet per second, or cubic meters per second.

2.3.1 Calculation of Cross-sectional Concentration (Single Vertical Method)

Ideally, one must measure the suspended sediment concentration at all points in a cross section. Because of the cost constraints, and difficulties of sampling during floods, measuring along a fixed vertical or at a single point is a more practical option.

USGS uses a coefficient, which is computed by dividing the mean concentration of the cross section by the concentration obtained from the point or single-vertical sample. This coefficient is called cross-section or box coefficient. The average cross-sectional concentration is measured by means of depth/width integrating technique, which is known as EWI or EDI methods. The coefficient is multiplied by a concentration obtained from a point or single- vertical in order to obtain an estimate of the mean sediment concentration in the stream cross section [24, 25].

The USGS method does not use a sediment transport model to convert the single-sample to the mean vertical concentration. Moreover, the locations of single-vertical and the single- point sampling should be investigated to determine the correlations between their concentrations and cross-sectional concentrations especially for streams with sand size (coarser than 0.062 mm)

suspended sediment. This method may cause errors when used in rivers with coarse suspended sediment, because the sediment size distribution is non-uniform across the channel and along the water depth. According to Morris, G. and Fan [34], one possible approach is to separate samples into fine and coarse fractions, and to establish relationships for each individually.

L.Yuqian [22] suggested that for a sediment size of less than 0.075 mm, the vertical distribution is rather uniform and sampling at any point in the vertical can be considered representative of the average sediment concentration in the vertical, however, it does not apply to certain rivers.

2.3.2 Rating Curve Method

After collecting sufficient sediment and water data, average sediment and average water discharge are computed for each cross section. Then, they are plotted against each other. By using least square method, the best line is fitted through the data on a log-log paper.

The relation between suspended sediment and water discharge is defined by a power function, $C = a Q^b$ and referred to rating curve[16, 20]. Normally this function is formulated as linear model to find the solution of the rating curve parameters (a and b). Formulation of the power function as a linear model requires a logarithmic transformation to linearize the function and a subsequent correction for transformation bias (by the method of least square).

In order to use the rating curve method for estimating the suspended sediment loads and sediment discharge of streams, parameters a and b of the power function must be determined at high and low-flow periods.

Even when rating curves differentiated by season and stage, errors can be expected in estimates of annual suspended sediment loads. If rating curve approach produces unacceptable errors, then

at present the only viable alternative is some form of field monitoring enabling the direct calculation of loads as there is no viable prediction model for stream sediment transport [16, 20].

3.0 DESCRIPTION OF DATA

Sediment data on Missouri [10], Mississippi [27], Atchafalaya [27], Sacramento [17], Niobrara [29] and Middle Loup Rivers [37] as well as Rio Grande Channel [38], 8-ft McQuivery Flume [19] and Coleman Flume [21] were analyzed.

The Missouri River sediment data was provided by USACE, Omaha District [10].

The U.S. Geological Survey, under a cooperative stream gaging program with the U.S. Corps of Engineers, has collected bed material and suspended sediment samples since 1976 at two locations on Missouri River: Omaha, Nebraska, and Nebraska City, Nebraska. They have collected data at Sioux City, Iowa since 1979. The data collected from 1979 to 1986 used by USACE to estimate the bed material loads in order to study the degradation problems and to define the balance of sediment load between different stations of Missouri River.

The sediment data includes the size distribution of the suspended sediment and the laboratory results such as total weight of the sample, volume of the sample, plus cumulative weight retained on the various sieves. Also, the actual concentration of sediment retained on each sieve was included.

Data collected include five to seven point-integrated samples per stream vertical at five locations in the cross-section (Figure 3.1). Each station was sampled by boat at about six week intervals during the open water season.

In addition to the sediment data, velocity measurements, discharge measurements, water surface elevation and slope, sonic soundings and temperature data were collected at each station. Laboratory analyses of the sediment were conducted and recorded.

Suspended sediment samples were collected with a US P-61 point-integrating suspended sediment sampler.

Discharge distribution data across the channel was included with the data. This is used in this study to compute weight factors for different sample verticals. The factors are then used to calculate sediment load across the section. This data is needed for calculation of sediment load by the new sediment transport model as well as the traditional method.

The velocity and sediment data collected by USGS at Nebraska City, Omaha, Sioux City, Gayville, and Ponca stations were selected for analysis in this research. These stations are briefly described below [8, 9, 11].

The Nebraska City Station (River Mile 561.8) is at the Waubonsie Highway Bridge (Nebraska-Iowa State Highway 2). The station was established in 1957.

Omaha Station is in Douglas County, Nebraska. The station is on the left side of the concrete floodwall on the right bank, 275 feet downstream from the Interstate 480 highway bridge in Omaha, at River Mile 615.9. The drainage area upstream of this station is approximately 322,800 mi^2 . The station has been in operation since 1939 [8,9].

Sioux City Station is located in Dakota County, Nebraska, on the right bank on the upstream side of the bridge on US Highway 77 at South Sioux City. At River Mile 732.3 mi downstream of Big Sioux River, the Missouri River drains an area of 314.6 mi^2. The Sioux City Station was established in 1954.

The basic measurements in the point-integrated sampling on Missouri River comprise the depth of flow at sampling vertical; the number of sampling points; the velocity and distance from the local bed for each sampling point and for each sample, the measured point-integrated sample volume, weight of sediment in the point-integrated sample and its particle size distribution.

These data are used to compute the suspended bed material load from water surface up to a specified distance from the bed. The distance is the outer limit of the bed layer for computing the suspended bed material load and is 0.5 ft [10,11,12].

The Mississippi River [27] data included data on Old River Complex (ORCC). The discharge and sediment data were collected at seven ranges along the Mississippi River and ORCC (Union Point, Hydropower Station, Line 13, Low Sill, Auxiliary, Line 6 and Tarbert).

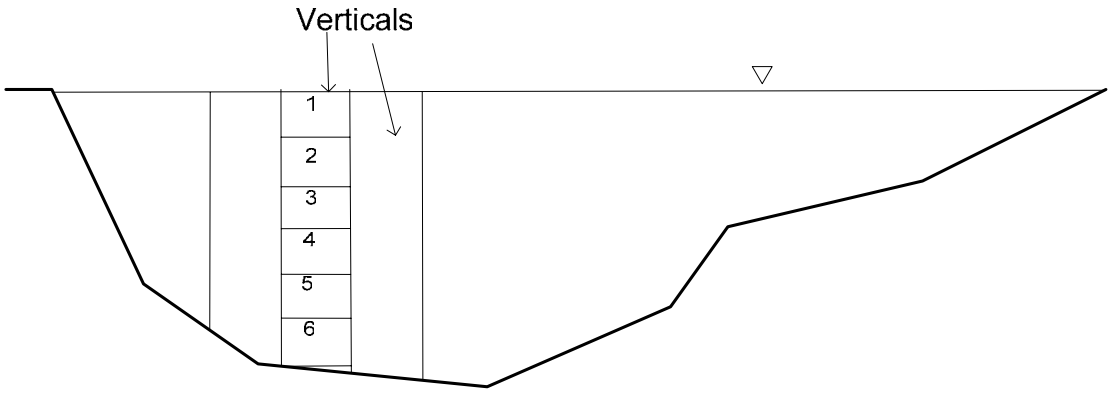

Six-point sediment samples and velocity measurements collected in each of five verticals.
(Obtained from US Army Corps of Engineers Missouri River Division)

Figure 3-1 Sampling Schematic Missouri River

4.0 MATHEMATICAL MODELS OF VELOCITY DISTRIBUTION

A velocity distribution model is required for calculating sediment discharge in rivers. Many researchers have studied the velocity distribution in open channel flow. The most widely used conventional equation for velocity distribution is Prandtl-von Karman Universal velocity equation. USACE used this logarithmic velocity profile for calculating sediment discharge of Missouri River [8, 9]. Toffaleti (1969) suggested the velocity distribution in the form of power law[9]. The existing equations cannot predict the maximum velocity below the water surface. Also, they are deficient near the channel bed and in sediment-laden water. Chiu developed a velocity distribution by using entropy maximization, which can describe the vertical velocity profile from the water surface to the channel bed and is applicable in steady and unsteady flows with or without sediment [1].

4.1 SIMPLE POWER LAW VELOCITY DISTRIBUTION

The simplest form of power law is [4]

$$u = ay^b \tag{4-1}$$

$$\frac{du}{dy} = \frac{ab}{y^{1-b}} \tag{4-2}$$

This velocity distribution goes to infinity at y = 0 which is considered the weakness of power law, considering the fact that the velocity is zero at the bed. Toffalete (1969) suggested that

$$\frac{u}{\bar{u}} = n_1 (\frac{y}{D})^{n_2} \tag{4-3}$$

Many attempts have been made to divide flow velocity into several regions, but it is difficult with only five or six data measurements at different levels [8].

4.2 PRANDTL-VON KARMAN UNIVERSAL VELOCITY EQUATION

The well-known von Karman equation is [3, 4]

$$u = \frac{u_*}{k} \ln \frac{y}{y_0} \tag{4-4}$$

then

$$\frac{du}{dy} = \frac{u_*}{ky} \tag{4-5}$$

u_* = shear velocity; k = von Karman's constant, $k \approx 0.4$ for clear water.

For sediment-laden water, k is less than 0.4, and k decreases with sediment concentration. At the channel bed, the velocity gradient goes to infinity, which is the weakness of this velocity distribution. The velocity is zero at a distance y_0 above the channel bed

4.2.1 Parameter Estimation of the Logarithmic Velocity Distribution

This research also investigates the applicability of velocity distributions near channel beds. The logarithmic equation was applied to velocity data of Missouri River. As it was shown in Figure 4.1, the velocity at a distance equal to y_0 becomes zero.

The parameters of the logarithmic velocity profile are estimated as follows:

The Prandtl-von Karman equation can be written in the form of

$$u = A_1 \ln(y) + A_2 \tag{4-6}$$

where

$$A_1 = \frac{u_*}{k} \quad \text{and} \quad A_2 = -\frac{u_*}{k}\ln(y_0) \tag{4-7}$$

The two parameters are estimated from regression. u_* (Shear Velocity) is obtained from

$$u_* = \sqrt{gRS} \tag{4-8}$$

where

g = gravity acceleration, R= hydraulic Radius, and S = water surface slope (in the case of Missouri River). Therefore, k can be calculated.

To illustrate applicability of the logarithmic velocity profile, the 6-point velocity data at a vertical with the depth of 15.7 feet, was analyzed (Missouri River, Omaha Station, dated 4/16/80). As the result, the following logarithmic equation was calculated

$$u = 0.599 \ln(y) + 3.819 \tag{4-9}$$

From A1 and A2, the parameters, k=0.389 and $y_0 = 0.0017$ ft were calculated (u_*=0.233 ft/s).

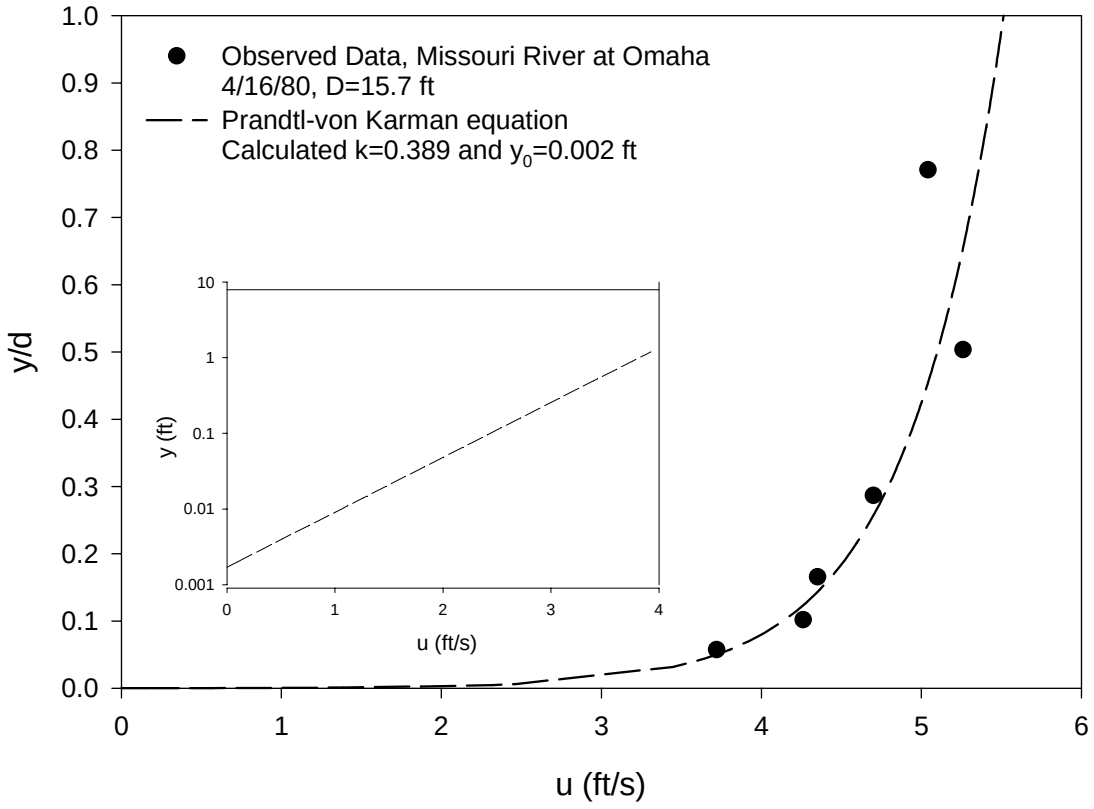

Figure 4-1 Prndlt-von Karman Velocity Distribution near Channel Bed

4.3 CHIU'S VELOCITY DISTRIBUTION

4.3.1 Model Formulation

Chiu pioneered the probability-based mathematical models of velocity distribution, which was published in several papers in conference proceedings and journal papers. Chiu's velocity distribution equation was presented as [4, 5, 6]

$$u = \frac{u_{\max}}{M} \ln\left[1 + (e^{M} - 1)\frac{\xi - \xi_0}{\xi_{\max} - \xi_0}\right] \tag{4-10}$$

in which

$$\xi = \frac{y}{D-h}\exp(1 - \frac{y}{D-h}) \tag{4-11}$$

D = water depth at the y-axis; h = a parameter

Chiu derived the velocity distribution equation (4-10) as below

$$\frac{\xi - \xi_0}{\xi_{\max} - \xi_0} = \int_0^u p(u)du = \int_0^u e^{(a_1 + a_2 u)}du \tag{4-12}$$

Where a_1 and a_2 = parameters, $0 \le \xi \le 1$; ξ = is a value attached to an isovel on which the velocity is u; ξ_0 is the value of ξ when u = 0; and $\xi_{\max}$ = the value of ξ when u is the maximum velocity.

The probability of velocity less than or equal to u, is the area between the isovels of ξ and ξ_0, divided by the total area of the channel section. In wide channels this probability is equal to $\frac{y}{D}$.

Chiu's probability-based velocity distribution equation was determined by maximizing Shannon's information entropy [3,5]. Shannon's information entropy, which is the average information content in a massage, or the measure of uncertainty can be expressed in discrete form as

$$H = -\sum_{j} p(x_j) \ln p(x_j) \tag{4-13}$$

where H is the mean value of $-\ln p(x_j)$; x_j is the value of discrete random variable X; and $p(x_j)$ is the prior probability of X being equal to x_j. For a continuous random variable, the information entropy can be expressed as

$$H = -\int_{0}^{u_{\max}} p \ln p(u) d(u) \tag{4-14}$$

where p(u) is the probability density function of continuous random variable U.

A system has the tendency to move toward chaos or uncertainty rather than toward order. p(u) can be determined so that H is maximized subject to a set of constraints [3]:

$$\int_{0}^{u_{\max}} p(u) d(u) = 1 \tag{4-15}$$

and

$$\int_{0}^{u_{\max}} up(u) du = \overline{u} = \frac{Q}{A} \tag{4-16}$$

A=Cross-sectional Area

The entropy can be maximized by the method of Lagrange multipliers, and the probability density function can be determined as

$$p(u) = e^{(\lambda_1 - 1)} e^{\lambda_2 u} \tag{4-17}$$

in which λ_1 and λ_2 are the Lagrange multipliers.

Substitution of (4-17) in to (4-12) yields:

$$\int_0^{u_{\max}} e^{(\lambda_1 - 1)} e^{\lambda_2 u} du = 1 \tag{4-18}$$

or

$$e^{\lambda_1 - 1} = \frac{\lambda_2}{e^{\lambda_2 u_{\max}} - 1} \tag{4-19}$$

By defining $M = \lambda_2 u_{\max}$ and substituting (4-19) in to (4-17), the probability density function becomes

$$p(u) = \frac{M e^{M \frac{u}{u_{\max}}}}{u_{\max}(e^M - 1)} \tag{4-20}$$

$$\int_0^u p(u) d(u) = \frac{e^{M \frac{u}{u_{\max}}} - 1}{e^M - 1} \tag{4-21}$$

Through mathematical manipulation of these equations, Chiu (1989) derived a velocity distribution as:

$$\frac{u}{u_{\max}} = \frac{1}{M} \ln\left[1 + (e^M - 1)\frac{\xi - \xi_0}{\xi_{\max} - \xi_0}\right] \tag{4-22}$$

Equation (4-20) gives

$$\int_0^{u_{\max}} u \frac{M e^{M \frac{u}{u_{\max}}}}{u_{\max}(e^M - 1)} du = \bar{u} \tag{4-23}$$

which, when integrated, can be expressed as

$$\frac{\bar{u}}{u_{\max}} = \frac{e^M}{e^M - 1} - \frac{1}{M} = \phi \tag{4-24}$$

4.3.2 Location of y-axis

y-axis is a vertical on which the maximum velocity of the cross section occurs. In order to illustrate the procedure of determining the location of y-axis, this research used velocity data of Missouri River at Nebraska City, Sioux City, Gayville, Ponca and Omaha stations, and Mississippi River at Union Point, Range 362.2 and Tarbert. Data collected on Missouri River by USGS include five to seven point velocities on each of the five verticals in the channel section. The velocities were measured by Price current-meter. Because of the operational restriction of current-meters, velocity measurements were conducted approximately between 0.07 and 0.77 of the total water depth. The measured velocities were used to plot the isovels in the cross sections. Figures 4.2 and 4.3 show the isovel pattern and indicate the location of the y-axis.

The maximum velocities were estimated at the average location of the y-axis. Figures 4.4 to 4.8 show the locations of the y-axis on different dates. The figures demonstrate that even for a sand bed channels such as Missouri River, the location of y-axis was stable. Figures 4.9 and 4.10 show the channel cross sections of Missouri River at Sioux City and Nebraska City at different discharges. The location of y-axis is shown on theses channel sections.

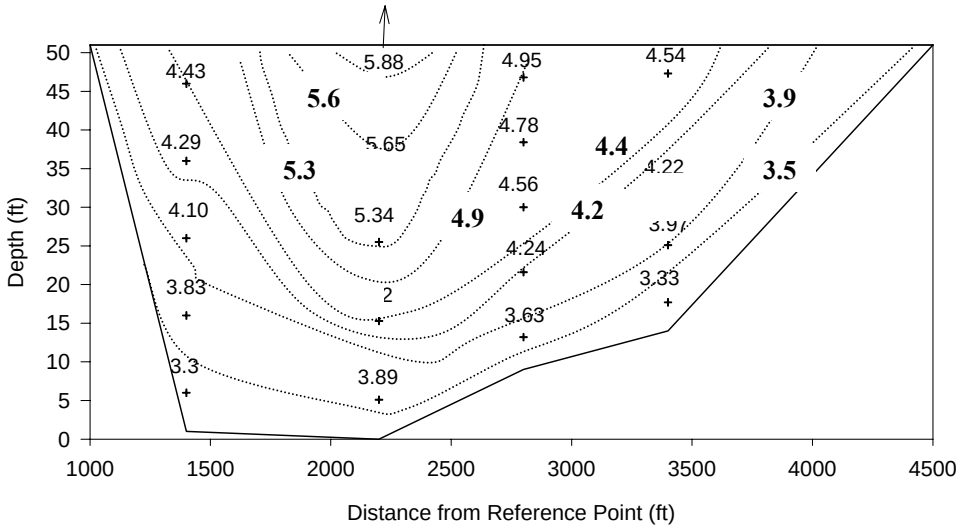

Figure 4-2 Isovels Showing Location of y-axis Mississippi River at Tarbert (2/1/1996)

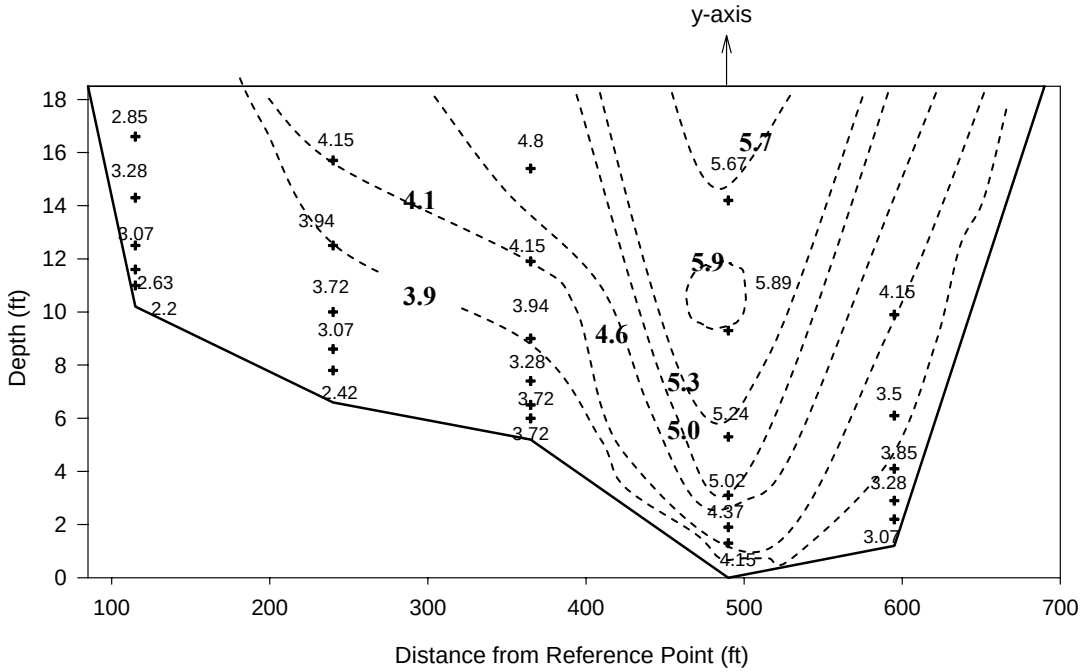

Figure 4-3 Isovels Showing Location of y-axis Missouri River at Omaha (4/26/1978)

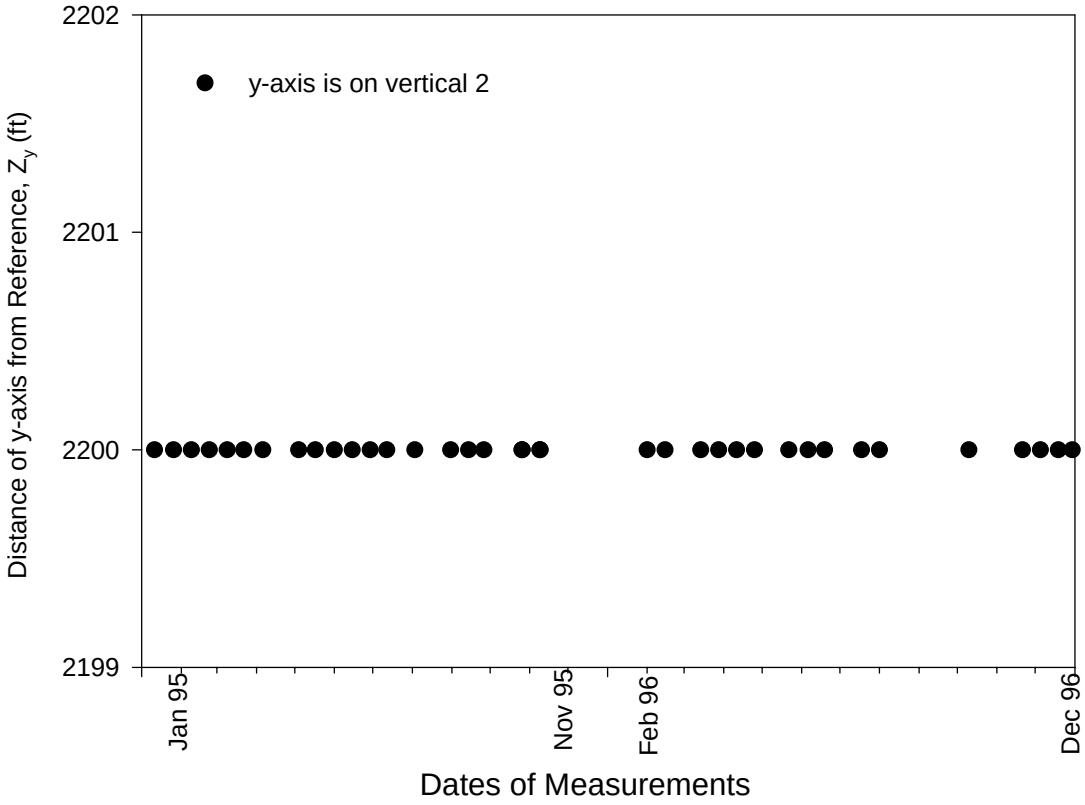

Figure 4-4 Location of y-axis, Mississippi River at Tarbert

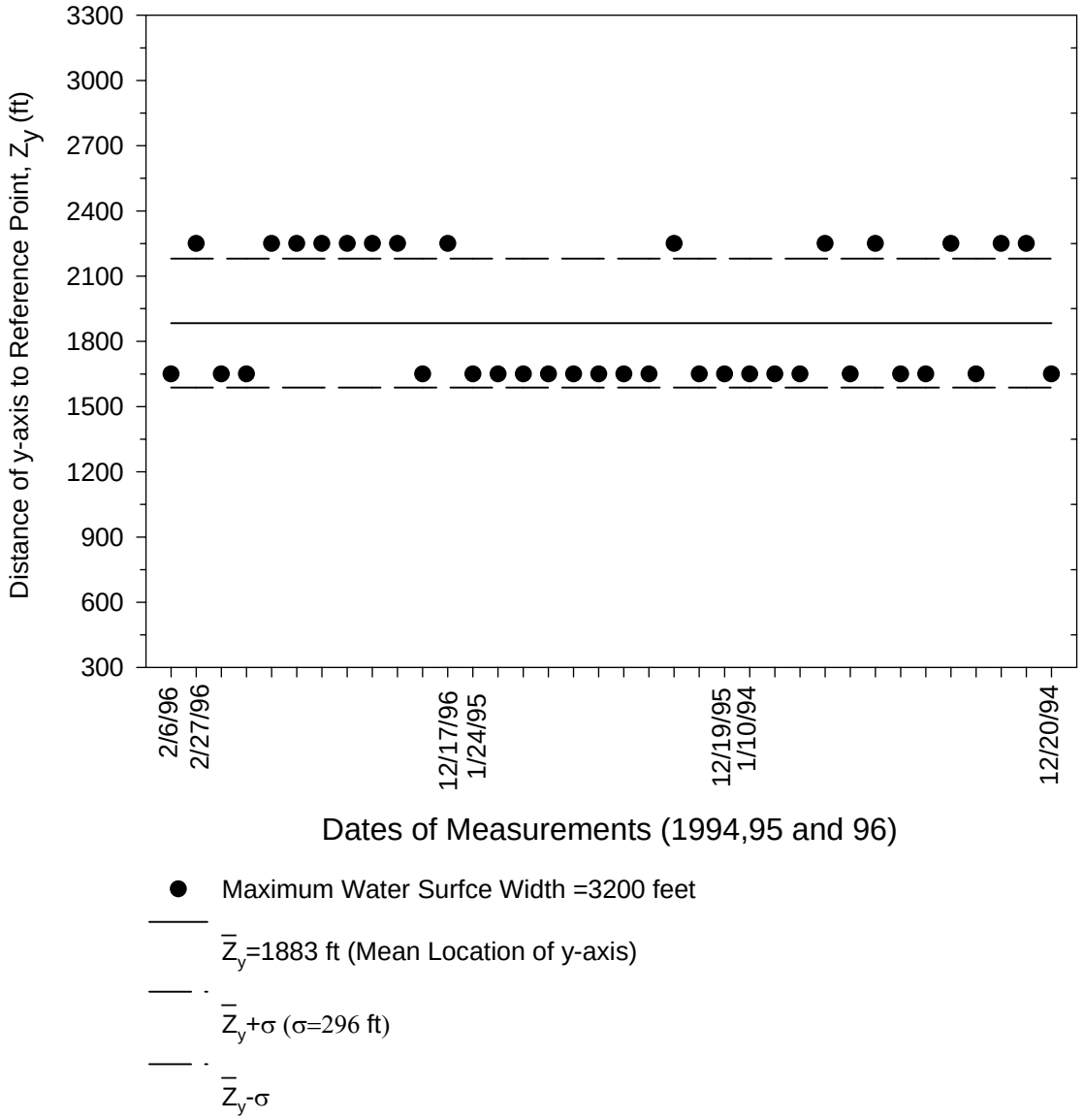

Figure 4-5 Location of y-axis, Mississippi River at Union Point

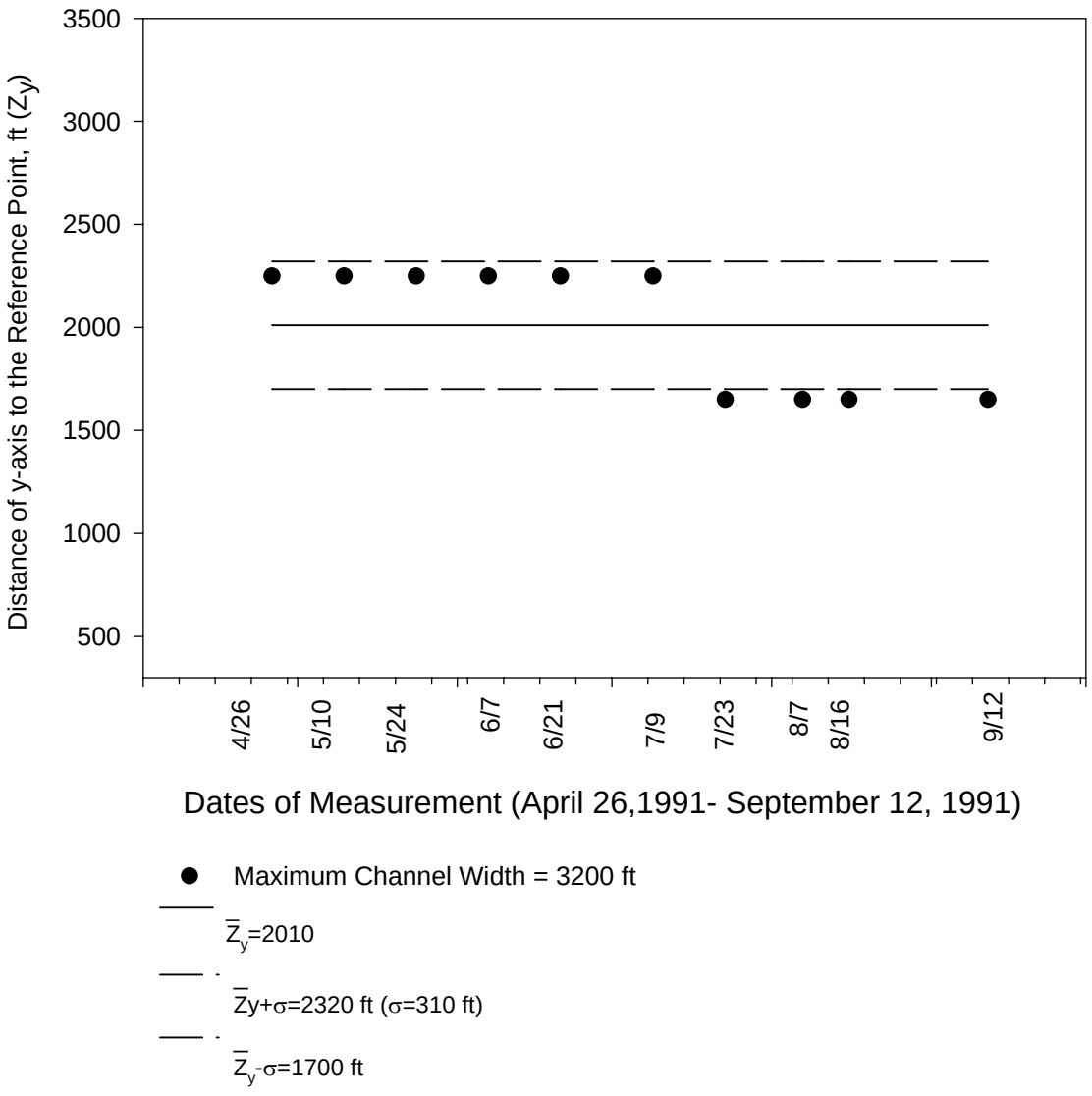

Figure 4-6 Location of y-axis, Mississippi River at Range 362.2

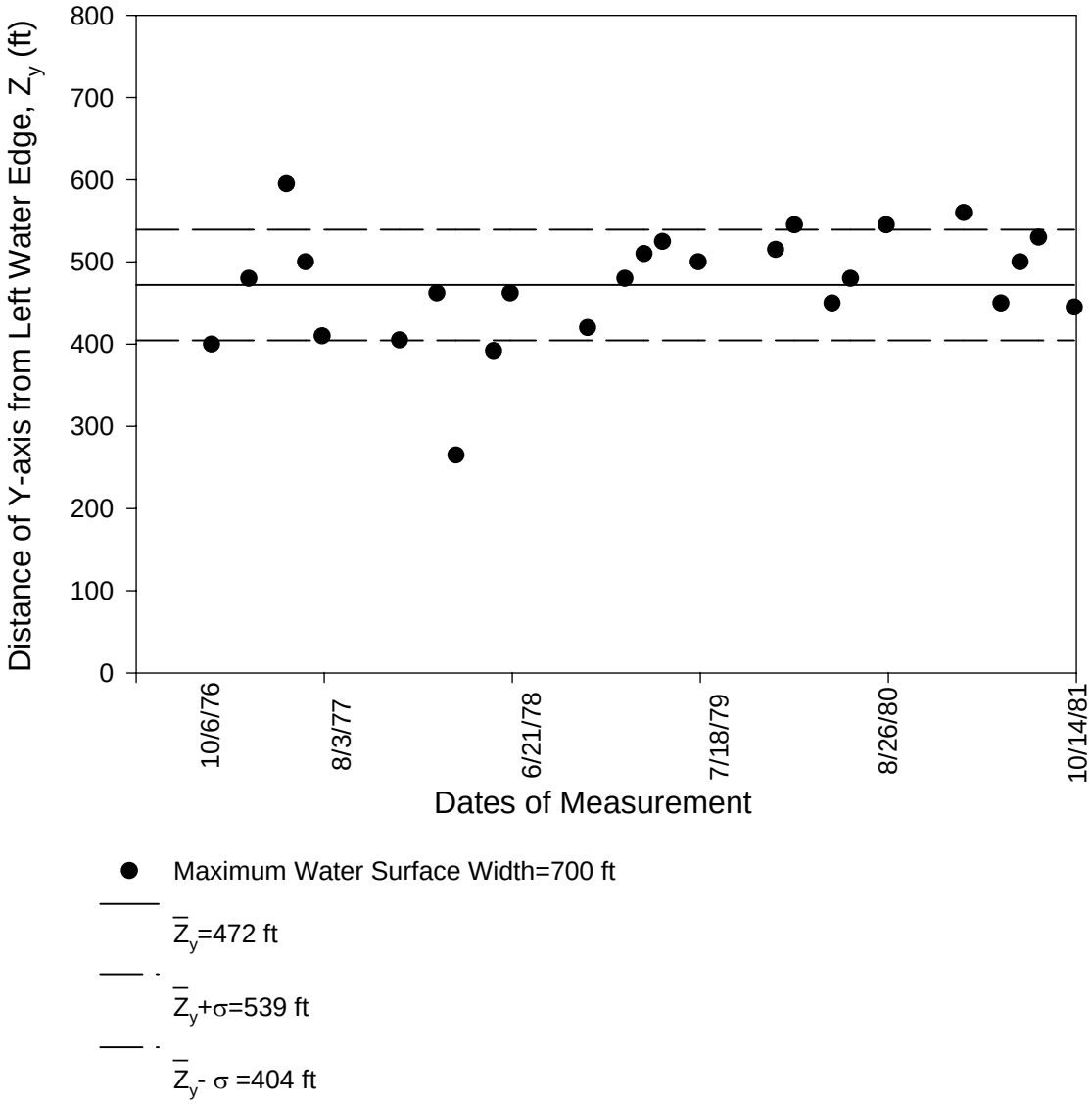

Figure 4-7 Location of y-axis, Missouri River at Omaha

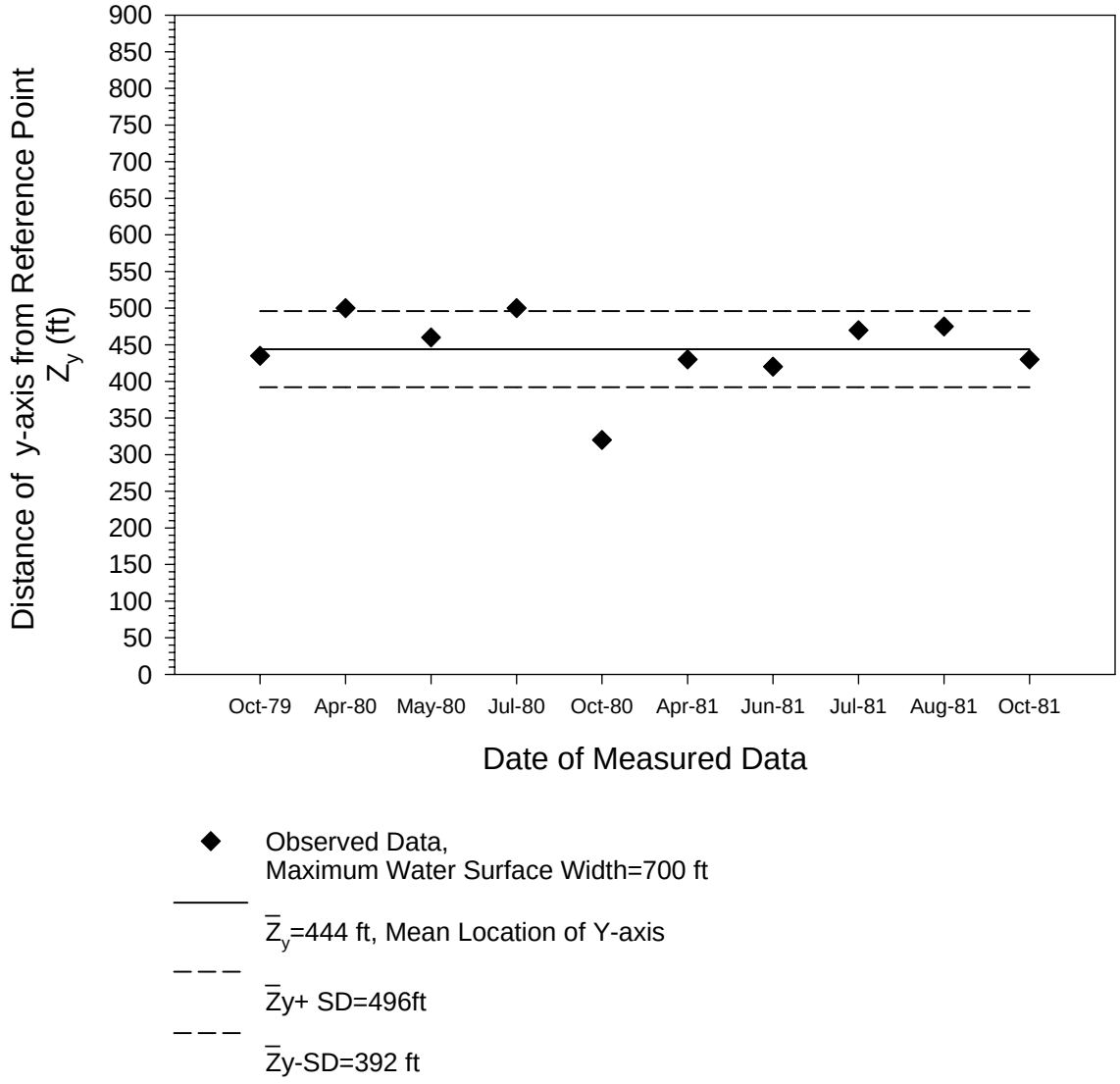

Figure 4-8 Location of y-axis, Missouri River at Sioux City

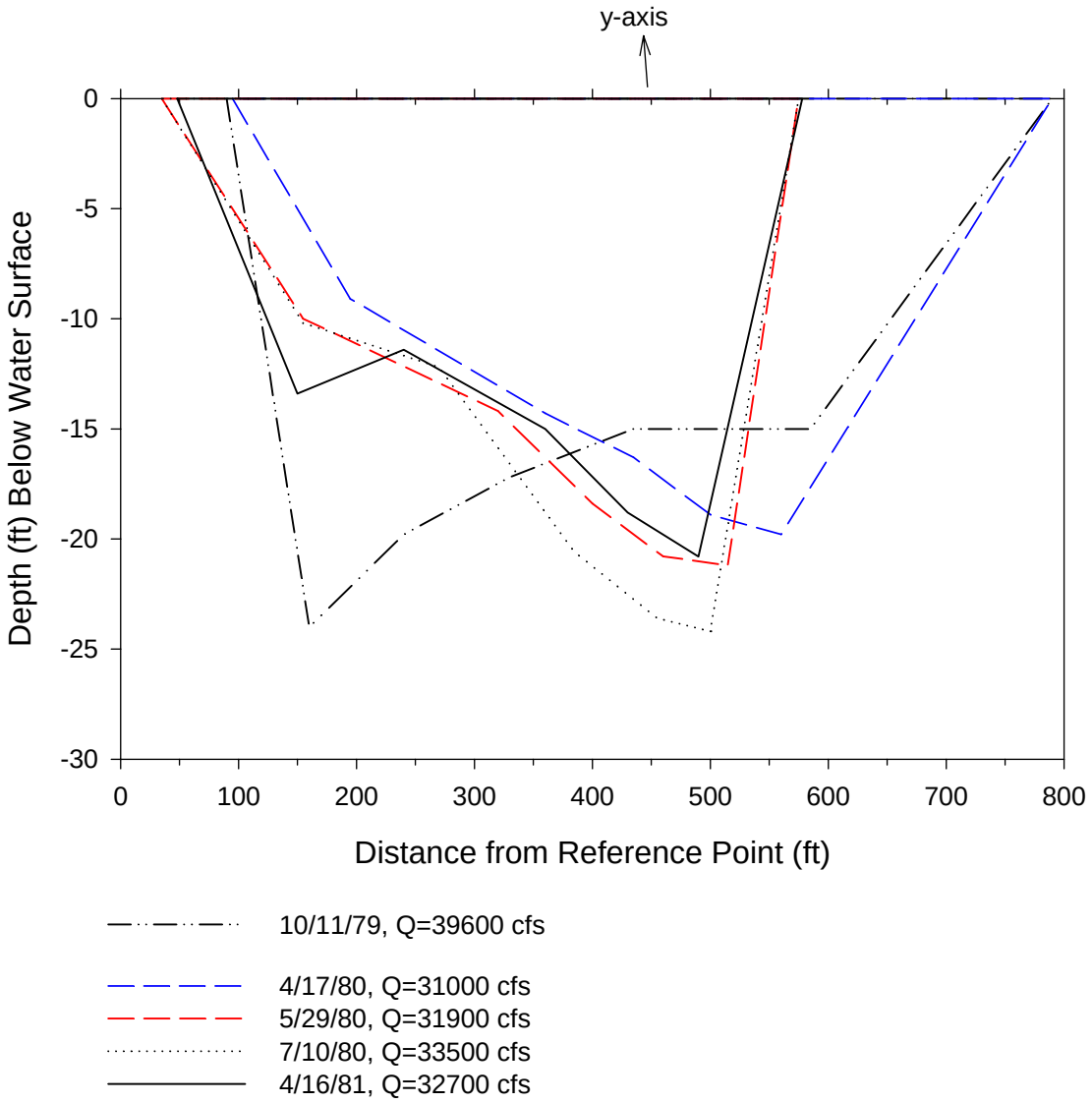

Figure 4-9 Channel Cross Section at Measured Verticals for Different Discharges, Missouri River at Sioux City

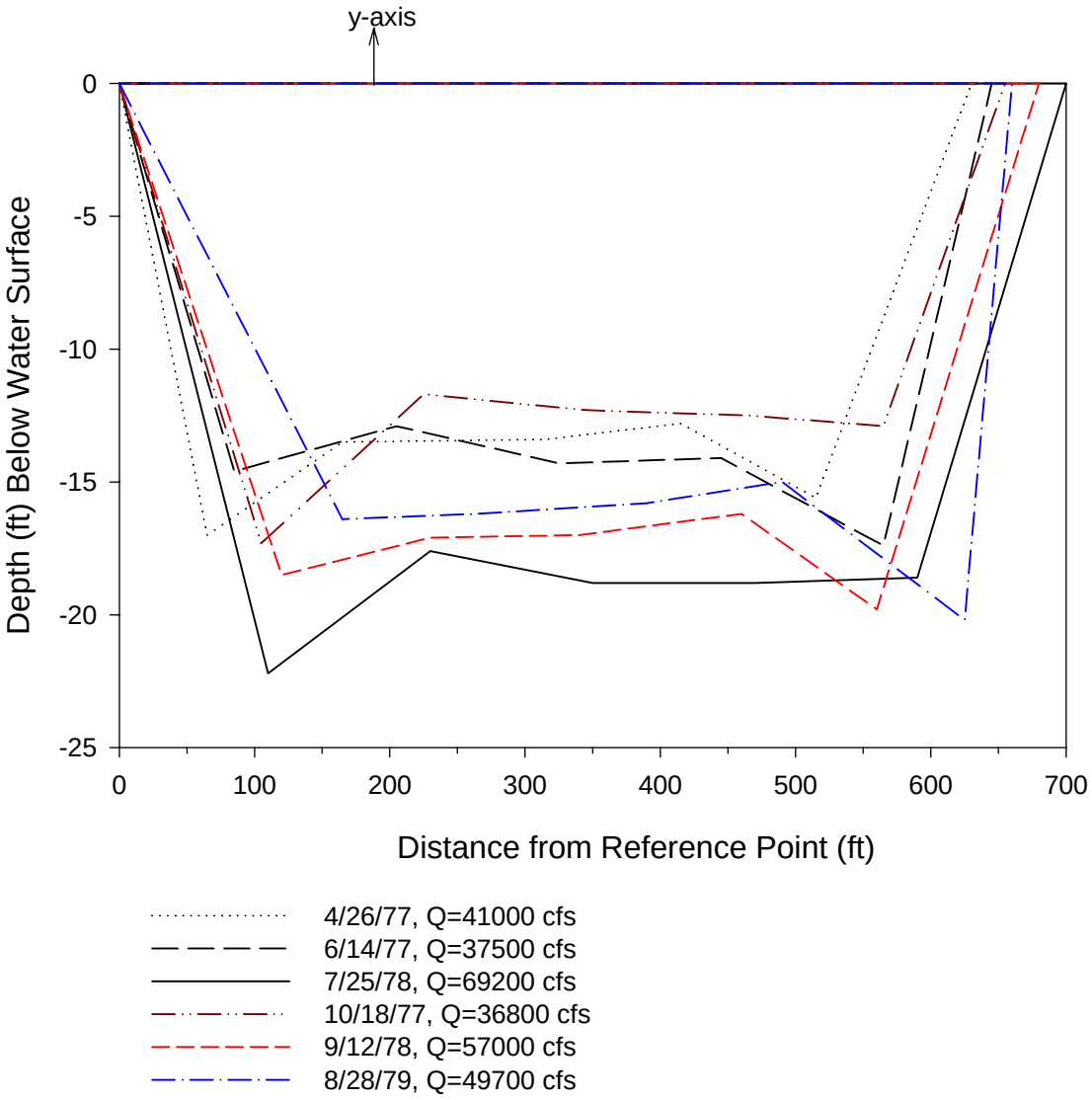

Figure 4-10 Channel Cross Section at Measured Verticals for Different Discharges, Missouri River at Nebraska City

4.3.3 Relation Between Mean and Maximum Velocities

The entropy parameter M of a channel section can be determined from the relation between the mean and maximum velocities. Chiu[1] developed a technique to determine the discharge from velocity profile on the y-axis in a channel section. The technique is an efficient way to estimate the discharge in streams and rivers during unsteady, high flow conditions.

Figures 4.11-4.15 show the relation between the mean and maximum velocities at a channel section. The slope of the regression line is ϕ, and M was computed using (4-24). M is the channel constant. For a specific channel section M is invariant with the discharge or water depth. To establish an equilibrium state and the corresponding M value, an erodible channel section adjusts the form and material, roughness, geometrical shape, slope, and alignment, under various values of discharge and water depth. A nonerodible or well-established channel section maintains the equilibrium state and the corresponding M and entropy by adjusting the velocity distribution through modifying the maximum velocity and h when the flow condition changes.

The location of y-axis at a channel section is stable and independent of the discharge and water depth [1]. Equation (4-24) is the slope of the $\overline{u}$ - u_{max} line.

It is desirable that the velocity data to be used include those collected as close to the water surface as possible so that maximum velocity and h determined may be accurate. However these data are often missing due to the difficulties in measurements near the water surface, or due to ignorance about the value of information contained in the maximum velocity. Without measurements near the water surface, the velocity data tend to indicate a continuously increasing trend, and often lead to overestimating the maximum and mean velocities.

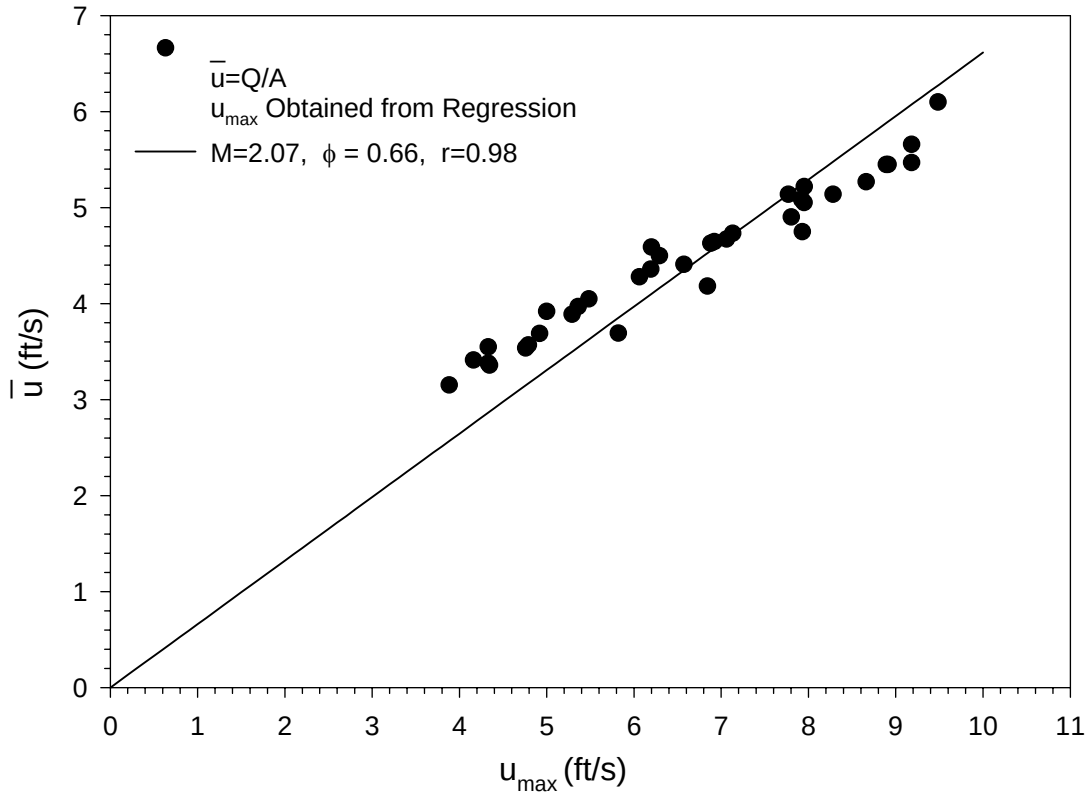

Figure 4-11 Relation between $\bar{u}$ and u_{max} Mississippi River at Union Point, 1994, 95 and 96

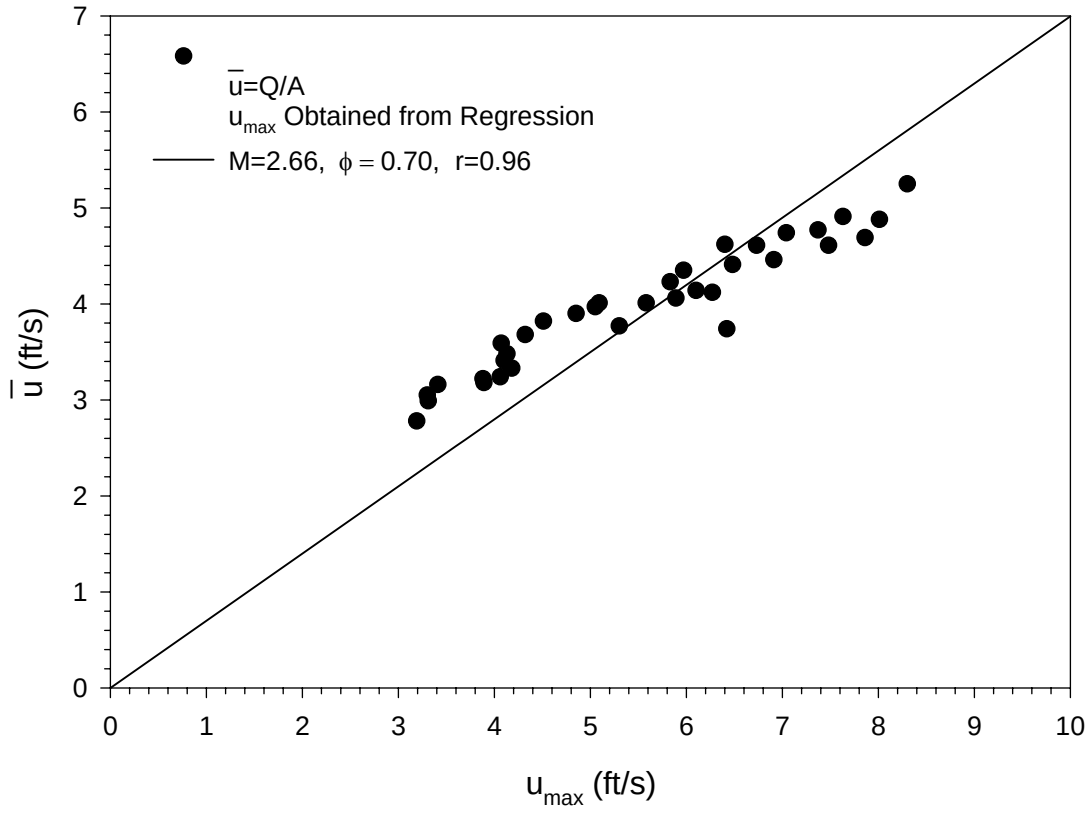

Figure 4-12 Relation between $\bar{u}$ and u_{max} Mississippi River at Tarbert,1995 and 1996

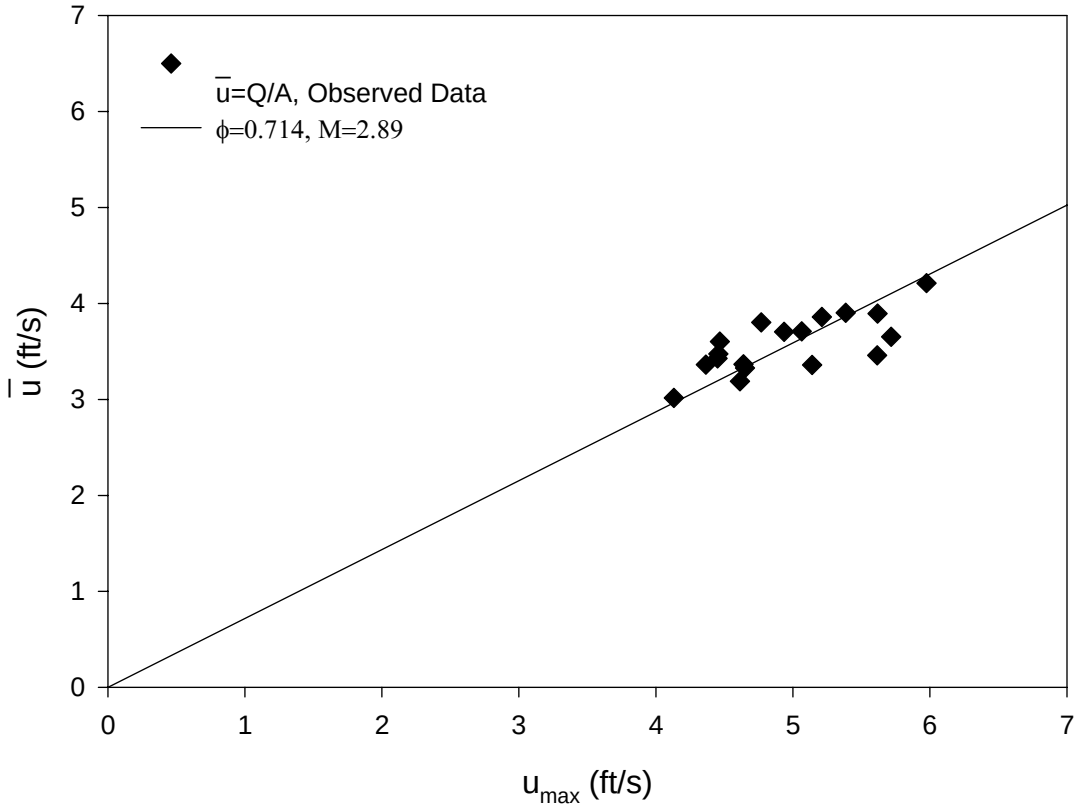

Figure 4-13 Relation between Mean and Maximum Velocities, Missouri River at Ponca, 10/26/1978 to 10/18/1979

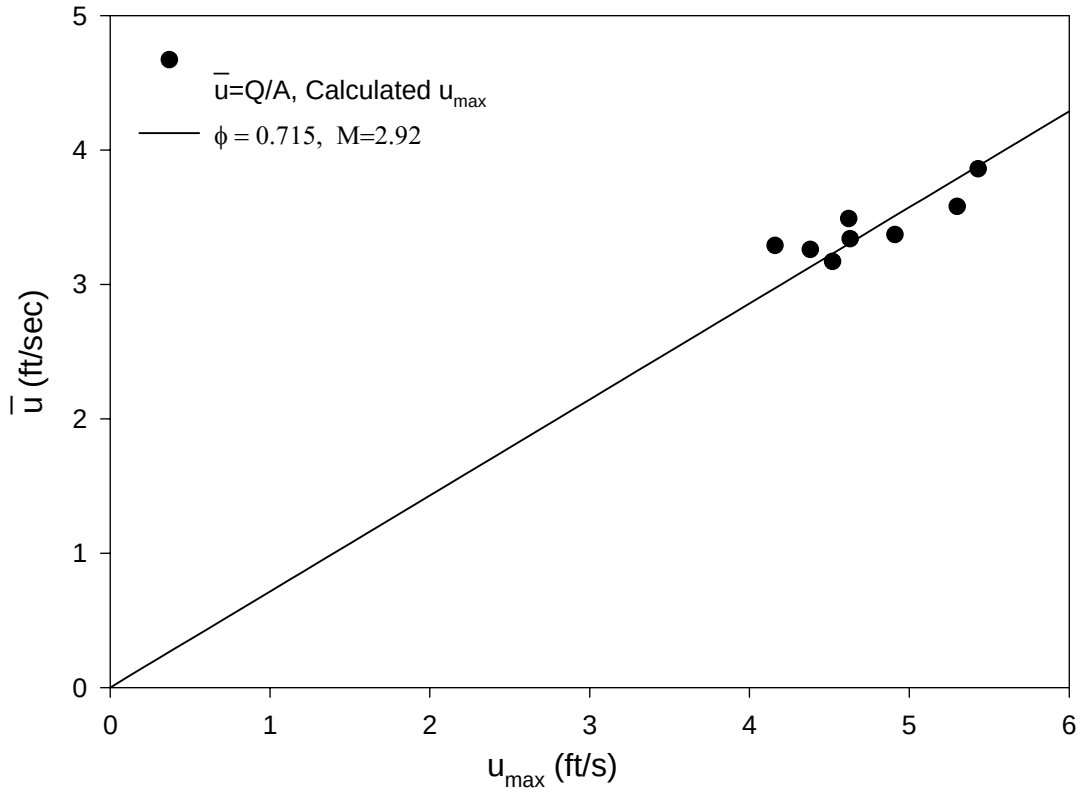

Figure 4-14 Relation between Mean and Maximum Velocities Missouri River at Gayville 4/22/1980 to 7/21/1981

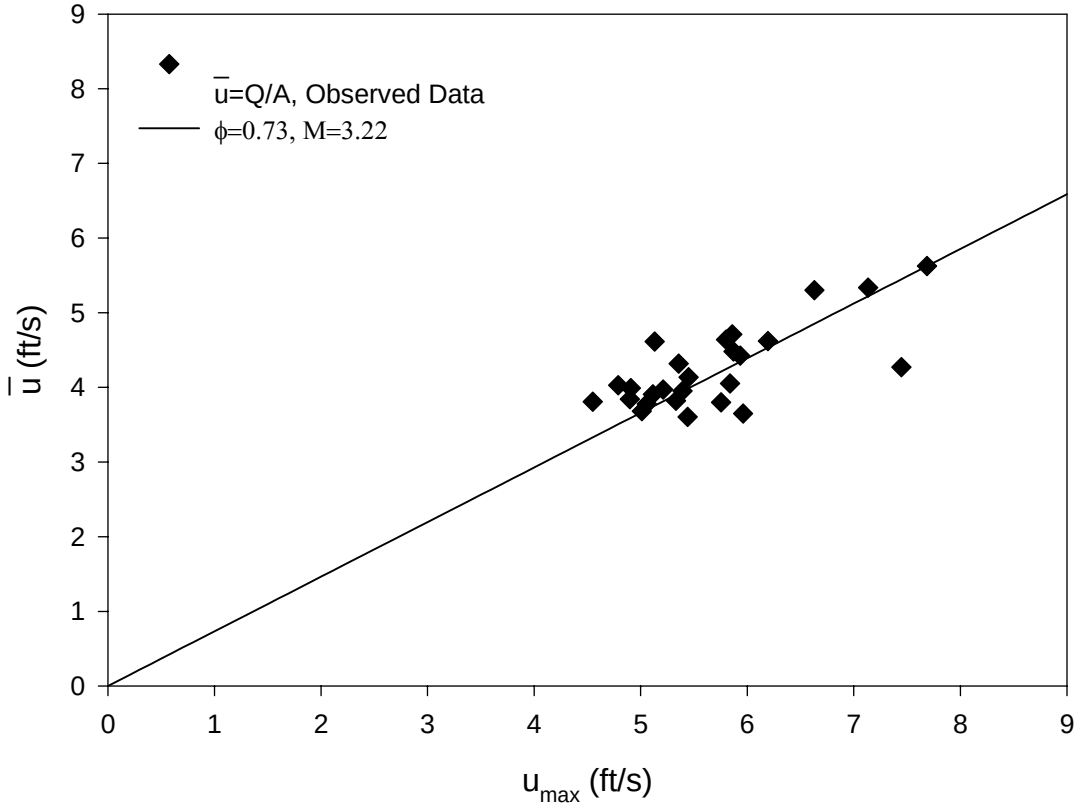

Figure 4-15 Relation between Mean and Maximum Velocities Missouri River at Omaha, 10/6/1976 to 7/15/1981

4.3.4 Parameter Estimation of Chiu's Velocity Distribution

The three parameters in Chiu's velocity distribution equation [1, 2], M, h, and u_{max}, can be determined by regression analysis on a set of velocity data at the verticals with maximum velocity in the cross section. The procedure is:

1. At the cross section of interest, determine the location of y-axis, which is the vertical with the maximum cross-sectional velocity, by plotting the isovel distribution. This research and prior studies have shown that the location of y-axis is stable over long period of time. Since a slight shift in the y-axis location has minimal effect on maximum velocity, the mean location of the y-axis can be used to estimate the maximum velocity.
2. Use the velocity distribution data along y-axis and apply regression analysis to solve for the M, h, and u_{max} values in Chiu's velocity distribution equation.
3. If the maximum velocity occurs on the water surface, $h \le 0$, y = D, and

$$\xi_{max} = \frac{D}{D-h} e^{(1-\frac{D}{D-h})} \tag{4-25}$$

then by substitution, the following velocity distribution is obtained, which is used in regression analysis

$$\frac{\xi}{\xi_{max}} = \frac{y}{D} e^{(\frac{D-y}{D-h})} \tag{4-26}$$

$$u = \frac{u_{max}}{M} \ln\left[1 + (e^{M} - 1)\frac{y}{D} e^{(\frac{D-y}{D-h})}\right] \tag{4-27}$$

4. When the maximum velocity is below the water surface, $h \succ 0$, $\xi_0 = 0$, and $\xi_{max} = 1$

$$u = \frac{u_{\max}}{M} \ln\left[1 + (e^{M} - 1)\xi\right] \tag{4-28}$$

The following equation is used in regression analysis

$$u = \frac{u_{\max}}{M} \ln\left[1 + (e^{M} - 1)\frac{y}{D-h} e^{(1-\frac{y}{D-h})}\right] \tag{4-29}$$

5. Compute the values of ϕ by linear regression for each of the velocity data sets using the relationship between $\bar{u}$ and $u_{\max}$. M is found from the Equation (4-24) in which

$\bar{u}$ = mean velocity of the cross section and is calculated as

$$\bar{u} = \frac{Q}{A} \tag{4-30}$$

The values of $u_{\max}$ are obtained by regression analysis in step 2.

6. Use the cross-sectional constant M in the Chiu's velocity distribution equation from step 4 and by regression compute $u_{\max}$ and h for the second time for the 5 or 6- point velocity data at each y-axis corresponding to a discharge.
7. For each cross section, plot the h/D versus $u_{\max}$ for each velocity dataset to estimate the mean of h/D, which is the cross-sectional constant. The values of h and $u_{\max}$, that are computed in step 6 are used to generate these plots (Figures 4.16 and 4.17).

Another method for finding h, was developed by Chiu and Tung [7]. The following equations show that by knowing M, the location of maximum velocity (h) below the surface at y-axis can be determined.

$$\frac{h}{D} = -0.2 \ln \frac{j(M)}{58.3} \tag{4-31}$$

$$j(M) = \frac{e^{M} - 1}{M\phi} \tag{4-32}$$

For wide channels

$$\xi = \frac{y}{D} \tag{4-33}$$

$\bar{u}$ = mean water velocity in the cross section; ϕ = section constant; A = cross-sectional area.

Table 4.1 is the summary of computed h/D and u_{max} related to Missouri River at Nebraska City. Figure 4.16 gives the average h/D and suggests that h/D does not change with u_{max} in a channel section. Figure 4.17 shows that h/D will increase when u_{max} increases.

Figure 4.18 is the Chiu's velocity distribution applied to the observed data on Missouri River at Omaha (4/26/1978). The figure depicts the location of maximum velocity below water surface.

Figure 4.19 compares logarithmic velocity distribution with Chiu's velocity distribution. It shows that the logarithmic equation can not compute the maximum velocity below water surface.

Figure 4.20 depicts the applicability of Chiu's velocity distribution near the channel bed and below water surface. It shows that Chiu's distribution becomes zero at the channel bed, but Prandtl-von Karman's distribution becomes zero at y=0.002 ft.

Table 4-1 h/D for Missouri River at Nebraska City, M=2.56

Date	Depth-D	h	h/D	u_{max}
4/26/1977	13.5	8.19	0.61	6.64
6/14/1977	12.9	7.72	0.6	6.09
8/2/1977	12.6	6.4	0.51	5.8
9/13/1977	11	6.09	0.55	5.85
10/18/1977	12.5	6.74	0.54	6.02
4/25/1978	15.8	6.71	0.42	7.54
7/25/1978	17.6	9.7	0.55	7.12
9/12/1978	17.1	10.55	0.62	6.72
10/24/1978	18.3	-0.69	-0.04	7.07
10/9/1979	13.7	8.42	0.61	6.12
8/28/1979	16.2	7.48	0.46	6.15

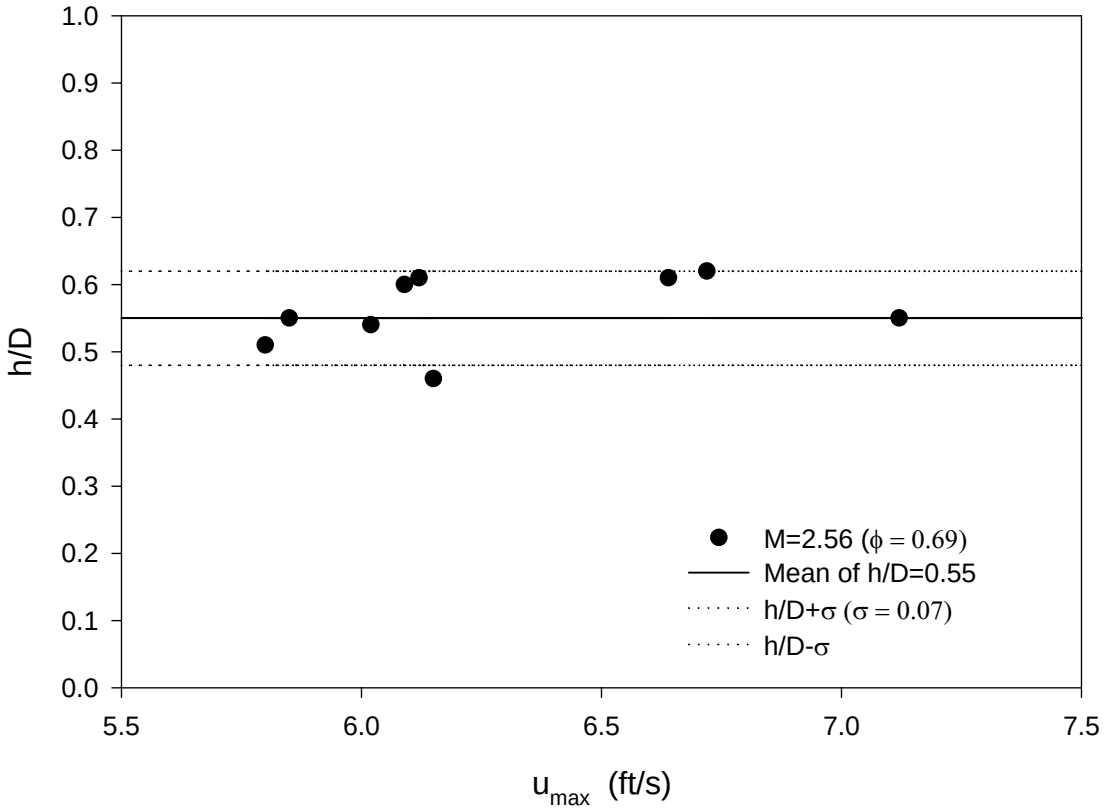

Figure 4-16 Relation between h/D and u_{max} Missouri River at Nebraska City

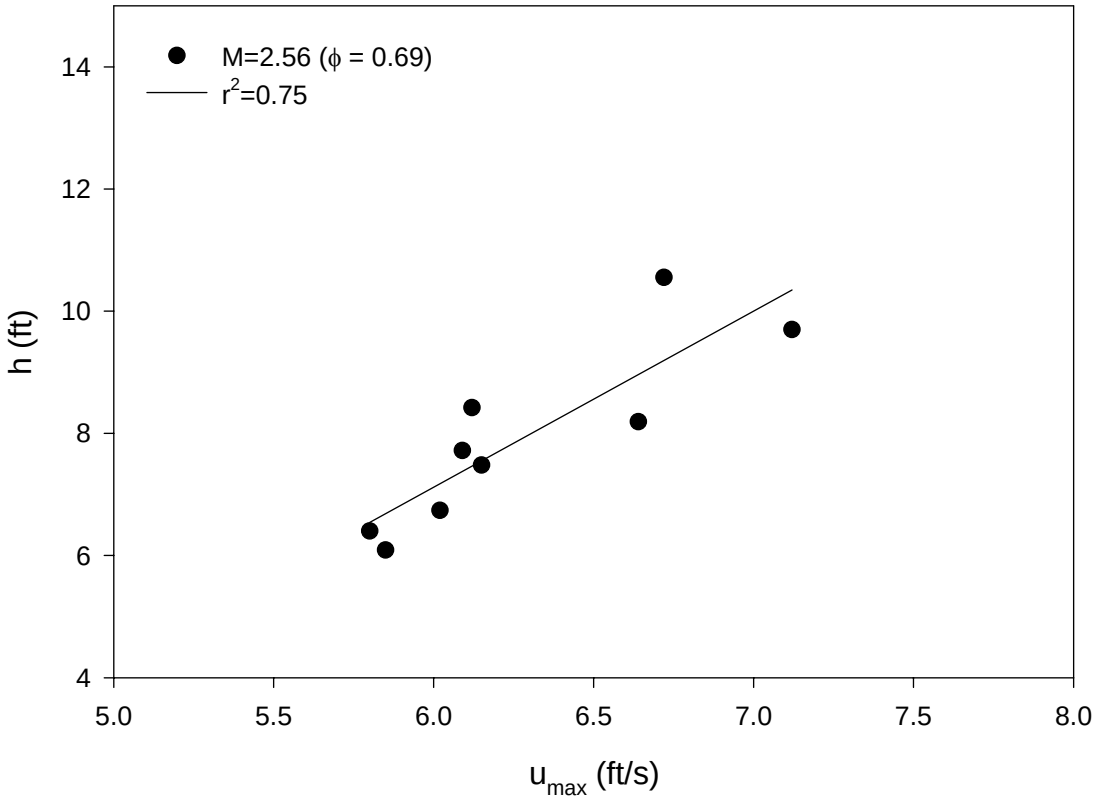

Figure 4-17 Relation between h and u_{max} Missouri River at Nebraska City

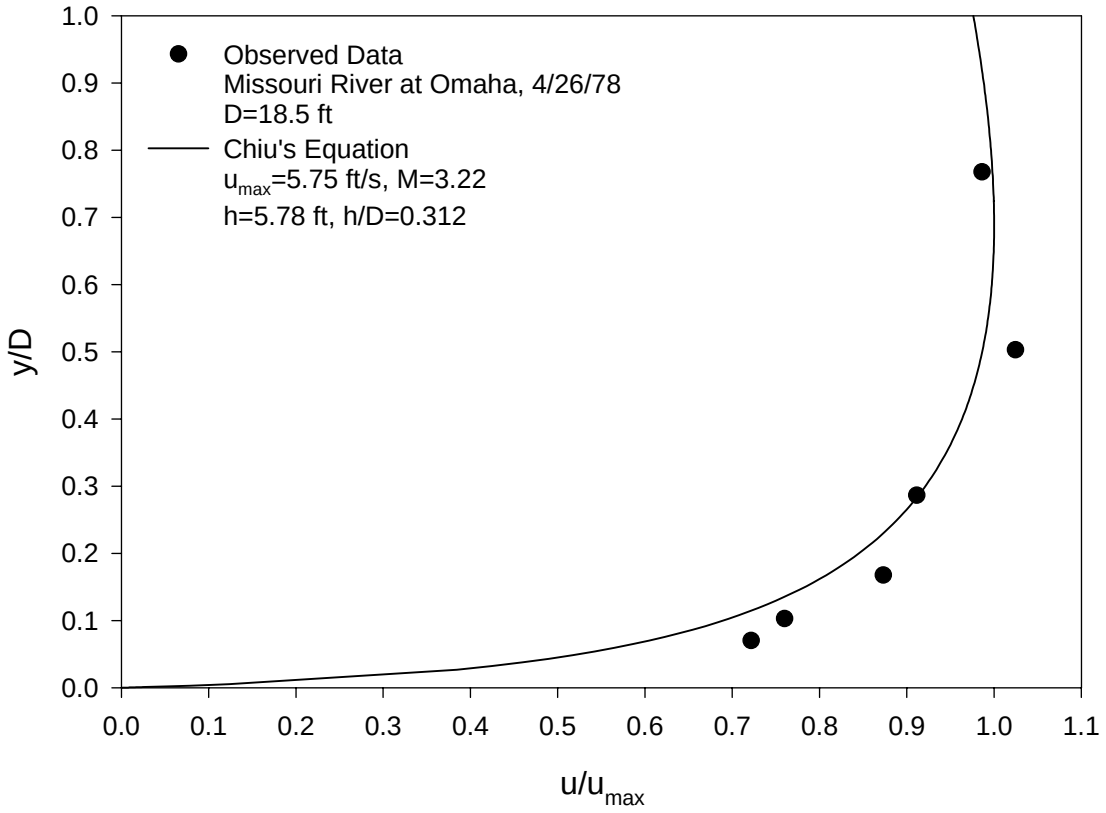

Figure 4-18 Velocity Distribution (Chiu's Equations)

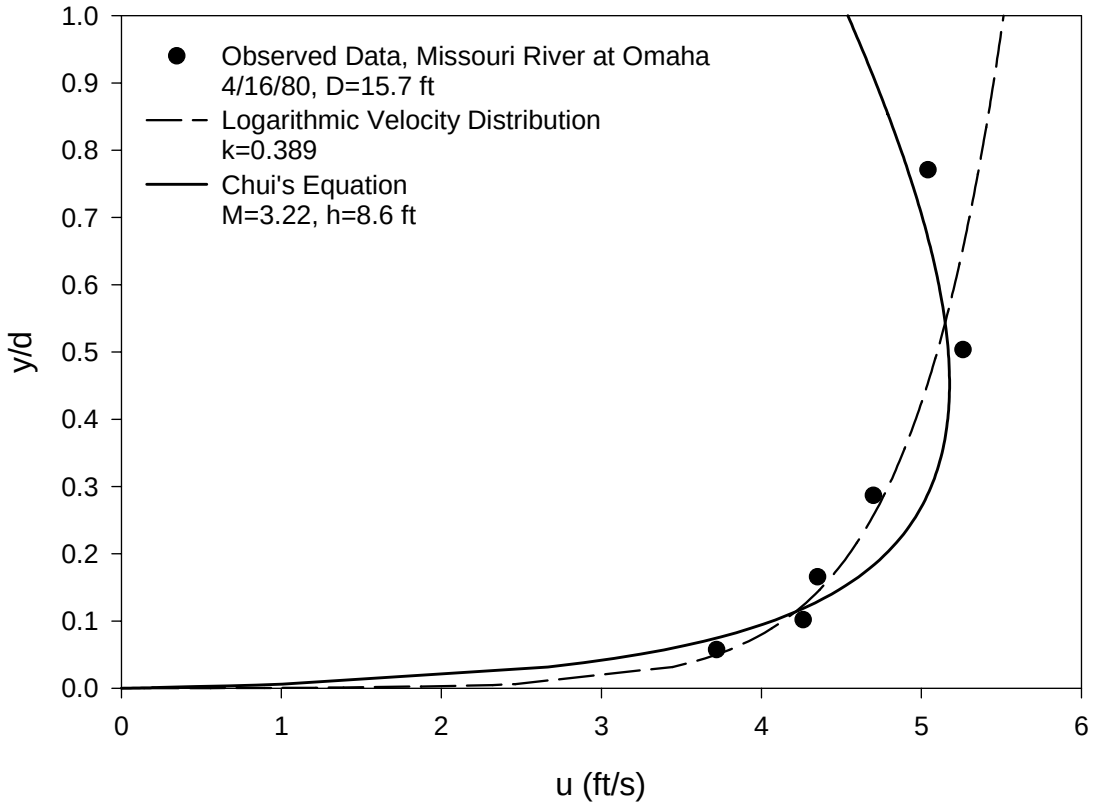

Figure 4-19 Comparison of Velocity Distributions

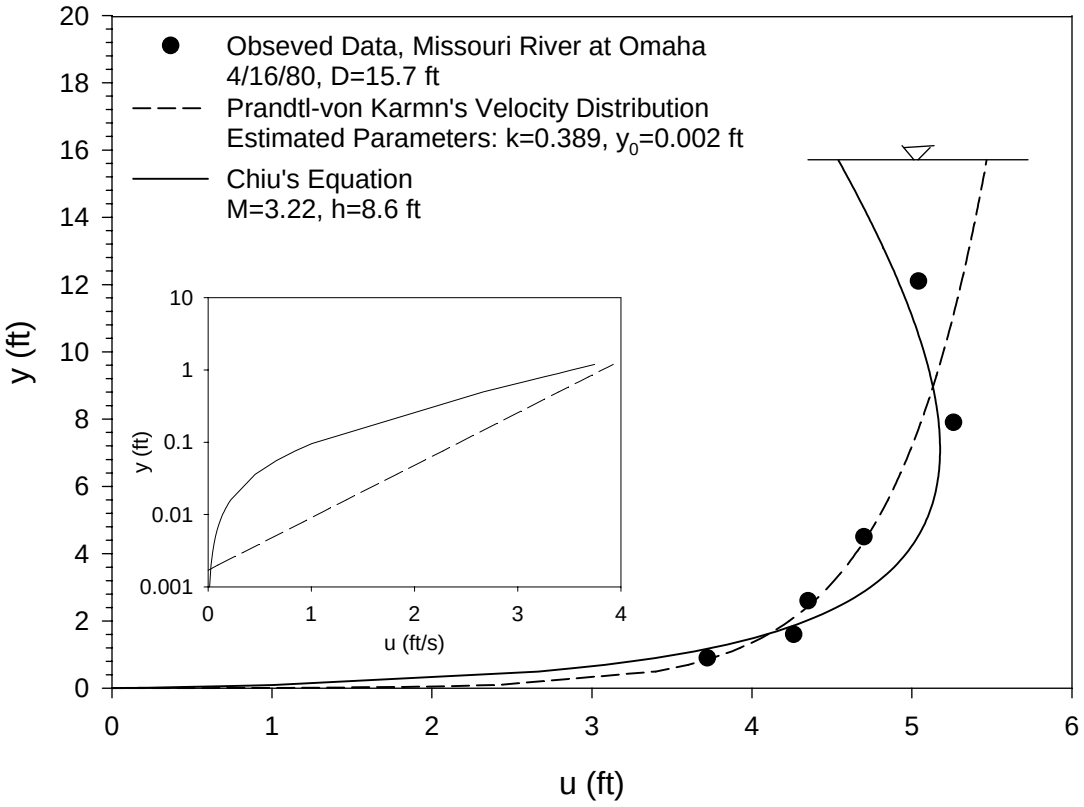

Figure 4-20 Applicability of Chiu's Velocity Distribution Near Bed and u_{max} below Water

5.0 ANALYSIS OF SEDIMENT SIZE DISTRIBUTION

Information on sediment movement and particle size distribution is needed in the design of dams, canals and other hydraulic structures. It is also required in determining the average sediment concentration.

In this thesis research, the median grain diameter (d_{50}) was calculated by using the sediment data at 5 or 6 points along the y-axis. Figure 5.1 shows the grain size distribution for the sediment sample taken on y- axis at a point 1.1 ft above the channel bed of the Missouri River at Omaha. The sample d_{50} is obtained from Figure 5.1. d_{50} at other five points along y-axis were determined by first plotting the figures similar to Figure 5.1 at each sample point. Figure 5.2 shows the distribution of d_{50} along the y-axis. Figure 5.3 shows the relation between d_{50} and y/D on y-axis in an 8-foot flume (McQuivey [19], 1973).

Table 5.1 shows the sediment size distribution and the calculated d_{50} of the Mississippi and Atchafalaya Rivers [27] (Lower Mississippi River Study). Tables 5.2 and 5.3 show d_{50} at 5 or 6 points along y-axis of the Missouri River at Ponca and Nebraska City. d_{50} of each sample along y-axis was calculated by plotting sediment size distribution data similar to Figures 5.1 and 5.2.

Table 5-1 Sediment Size Distribution, Mississippi River

	Percent Finer Than Indicated Sizes in mm											d_{50}	Sta. d_{50}
	1	0.5	0.25	0.125	0.0625	0.0442	0.0312	0.0221	0.0156	0.011	0.0075	mm	mm
Union Point													
2/6/1996	100	99.9	96.9	71	61.6	44.6	41.5	35	32			0.051	
2/27/1996	100	100	98.3	73.4	64.6	51.3	49.5	42	38			0.041	
3/12/1996	100	99.9	97.4	74.6	67.5	54.7	51	43	39			0.031	
4/2/1996	100	100	97.1	82.6	76.5	62.5	58	49.9	45			0.022	
5/7/1996	100	99.5	96	88.5	83.6	67	61	51	46			0.02	
5/21/1996	100	99.9	97	75.9	67.1	53.4	50.8	45	41			0.029	
6/11/1996	100	99.8	96.1	83	79.2	70.4	69.2	64	61			0.01	
6/25/1996	100	99.9	96.8	76.5	71.1	57.2	55	50	47			0.022	
8/6/1996	100	100	99.7	94.7	92.6	86.9	83.8						
10/8/1996	100	100	98.6	92.2	88.3	80.5	74						
12/3/1996	100	99.9	96.3	83.9	77	59.5	55.4						
12/17/1996	100	99.8	96.3	74.8	66.8	47.7	44.9						
Union Point													
1/24/1995	100	99.9	95.7	82.7	69.7	51.8	48	40.5	35.7	32.2		0.037	
2/7/1995	100	100	96.9	82.3	71.3	58.3	56.2	52.2	52.3	38.1		0.015	
3/7/1995	100	100	98.8	89.8	84.9	72.1	69.9	61	56	51		0.008	
3/28/1995	100	100	98.5	87	77.9	65.9	62.1	55	51	47.7		0.014	
4/11/1995	100	99.9	99.1	94.5	92.3	81.2	73.9	56	46	39		0.02	
4/25/1995	100	100	99.1	95.8	91.4	79.2	72.2	58.5	50			0.015	
5/9/1995	100	98.5	92.6	82.2	74.4	68.2	55.6	49				0.023	

Table 5.1 (continued)

6/6/1995	100	100	98.5	88.5	64.8	52.9	49.9	44.1			0.031	
6/20/1995	100	100	98.7	90.8	76	67.5	65.5	61.6	59.2	56	0.008	0.022
Range 362.2												
4/26/1991	100	99.7	97.4	85.6	82.8	72.8	70.4	63.7			0.008	
5/10/1991	100	100	99.9	95.5	93.4	87.7	85.5	80.7	76.9		0.004	
5/24/1991	100	100	99	88.9	83.7	73.9	71.6	65.5	61	57.1	0.007	
6/7/1991	100	99.8	97.5	90	87.5	81.4	78.9	71.8	67.5	63.4	0.005	
6/21/1991	100	99.9	99.3	96.5	94.9	88.9	85.2	77.7	72.7	68.5	0.004	
7/9/1991	100	99.7	97.9	96.9	94.6	93	90.9	83.3	78.2	75	0.003	
7/23/1991	100	100	96.8	94.3	93							
8/7/1991	100	99.1	98.5	96.6	94.6							
8/16/1991	100	98.5	98.2	97.1	96.2							
9/12/1991	100	100	99.2	94.1	92.9	73.3	65.5	49.3	40		0.025	
10/1/1991	100	100	100	100	99.5	96.5	91.2	74.1	63		0.01	
10/10/1991	100	99.9	99.6	99.2	98.7	90.5	83.9	70.3			0.009	
10/25/1991	100	100	99.9	99.7	98.3							0.007
11/6/1991	100	100	99.9	98.9	96.6							
11/22/1991	100	98.7	98	95.1	91.4							
12/6/1991	100	99.5	98.6	92.7	86.7							
12/18/1991	100	99.8	96.5	84	74.9							
Tarbert												
1/11/1995	100	100	99.6	95	91.1	81.8	75.5	61.4	53.8	48	0.012	
1/26/1995	100	100	97	88	74	56	52	45			0.03	
2/9/1995	100	100	99	86.9	77.5	67	64	56	52	48	0.012	
2/23/1995	100	100	99.5	93.7	85.6	78.7	73.8	62.7	56	51	0.01	

Table 5.1 (continued)

3/9/1995	100	100	99.5	95	89.1	74.6	67	54	46	40		0.017
3/22/2009	100	99.9	97.7	87.4	76.4	62.7	58	51	48	45	40	0.02
4/6/2009	100	100	99.2	95.9	89.3	78.6	74	66	60	56.9	51.6	0.007
5/4/1995	100	99.9	99.3	95.9	88.5	69	63	52	47	43		0.019
5/17/1995	100	99.9	99.2	93.5	83.6	71.9	66	54.9	49	45		0.04
6/1/1995	100	99.7	98	88.3	74.2	51	47	39	35	32		0.007
6/15/1995	100	100	98.7	92.1	86.5	81	78	71	66	62		0.004
6/29/1995	100	100	97.9	87.7	75.5	64.5	61.9	56	52	50		0.011
7/12/1995	100	100	100	99.2	96.1	93.2	88.9	78.8	73	68	62	0.004
8/3/1995	100	100	99.9	98.7	94.2	87	82	68	61	56	50	0.008
8/31/1995	100	100	99.5	98.3	94.8	88	87.4	74	68	62	51	0.007
9/14/1995	100	100	99.7	98.5	97.2	93.6	86	71	62	55	46	0.008
9/26/1995	100	100	100	99.3	98	96	93	78	71	65	57	0.007
2/1/1996	100	100	98.3	84.6	75.1	48	45	38	34	31		0.05
2/15/1996	100	100	98.3	81	71.4	63	59	51	47	44		0.02
3/14/1996	100	99.9	97.8	80.9	76.2	65	62	56	52	48		0.01
3/28/1996	100	100	98.6	83.7	78.8	70	66	56	50	45		0.015
4/11/1996	100	99.9	96.6	78.9	73	55.9	53	46	41			0.026
4/25/1996	100	100	99.8	95.3	93.5	81	75.7	65	59	54	49	0.008
5/22/1996	100	99.8	96.7	75.5	67	56	53	47	44	41		0.03
6/6/2009	100	99.9	97.1	74.9	69.5	57	55	48.7	45	42		0.023
6/19/2009	100	100	97.2	79.9	76.7	64	63	57	54	52	46	0.01
7/18/1996	100	100	99.8	97.9	95	92	88	75	67	62	54	0.007
8/1/1996	100	99.6	98.3	93	87.1	75.7	69	59	49	44		0.016
10/10/1996	100	100	99.8	96.3	91.7	84	77	61	54			0.01

Table 5.1 (continued)

11/21/1996	100	99.9	98.7	88.8	82.4	65	60	50	44			0.022	
12/5/1996	100	100	98.1	88.8	82.9	66	62	53	48			0.017	
12/19/1996	100	100	97.9	85	78.2	65	61	52	47			0.018	
12/30/1996	100	100	95.9	78.6	71.7	57	54	47	42			0.026	0.012
Atchafalaya													
River													
1/5/1994	100	100	99.9	90.9	83.6	64	59.7	51.1	48			0.02	
1/19/1994	100	100	99.4	90.9	81.1	68.8	63.1	50	45			0.022	
2/2/1994	100	100	99.3	95.7	62.5	54.8	43.8	26.8				0.035	
2/16/1994	100	99.5	95	71.2	44.2	33.7	32.2	28.9				0.07	
3/2/1994	100	100	96.3	81.3	66	57	53	46	41			0.03	
3/16/1994	100	99.8	94	75.1	54.2	34.7	32	27	25			0.05	
3/30/1994	100	99.8	91.2	64.2	51.5	47	44.7	40	37.7	34		0.059	
4/13/1994	100	100	93.6	72.3	57.2	50.7	48	43	42			0.043	
5/2/1994	100	99.9	93.1	62.1	44.8	30.4	29	25.9	24.9			0.08	
5/18/1994	100	100	96.3	78.4	72.5	65.7	63	57.9	54.9	51		0.01	
6/15/1994	100	100	100	98.5	96.3	91	86	77	72	66		0.008	
6/27/1994	100	100	99.3	97.1	95.1	93	90	83.7	79	75		0.007	
7/13/1994	100	100	99.9	99.6	97.7								
7/28/1994	100	100	99.8	98.4	93	96	91	76	70	67	53	0.007	
8/17/1994	100	100	100	99.4	94.6	96	94.4	79.7	73	71	57	0.006	
10/5/1994	100	100	100	99.8	96	99	95	81	73	72	55	0.007	
11/9/1994	100	100	99.8	98.3	88.8	78	74	64	59	55	50	0.008	
12/21/1994	100	100	99.4	96.5	75.3	58	53	43	37			0.03	
12/28/1994	100	100	98.7	90.2	63.5	50.8	46.7	39				0.044	0.026

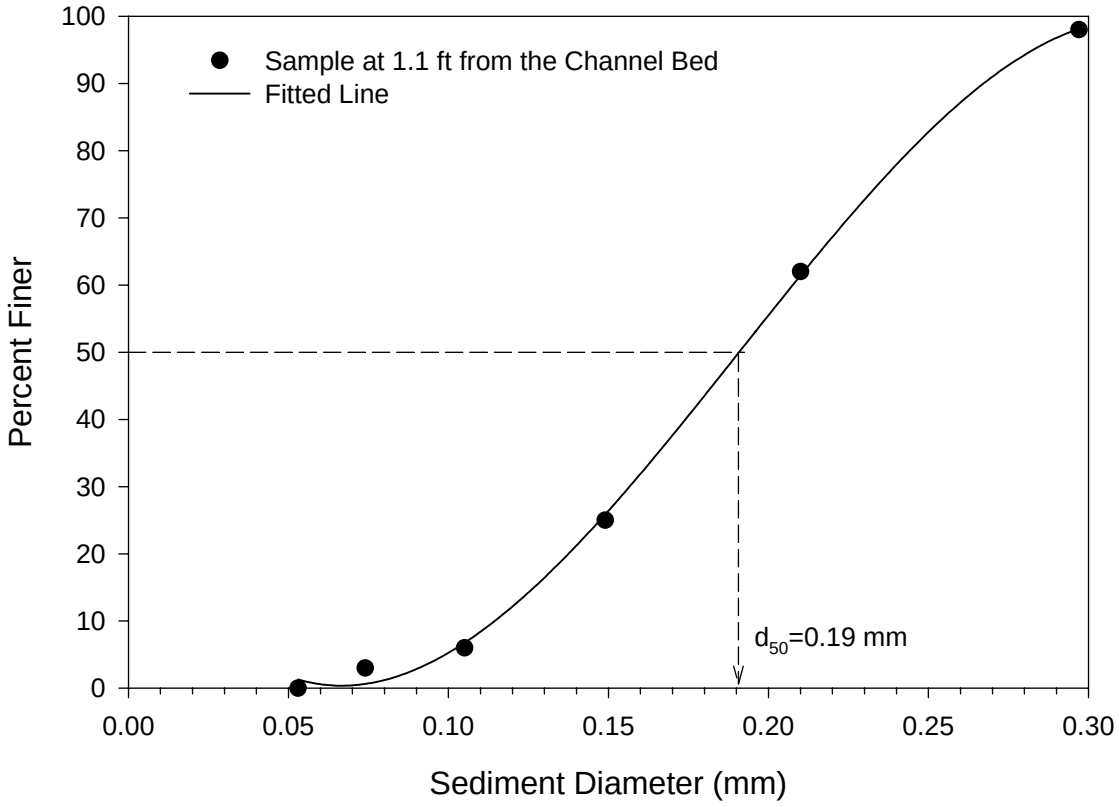

Figure 5-1 Determining Sample d_{50} on y-axis, from Grain Size Distribution, Missouri River at Omaha, D=18.4 ft, 0/16/1976

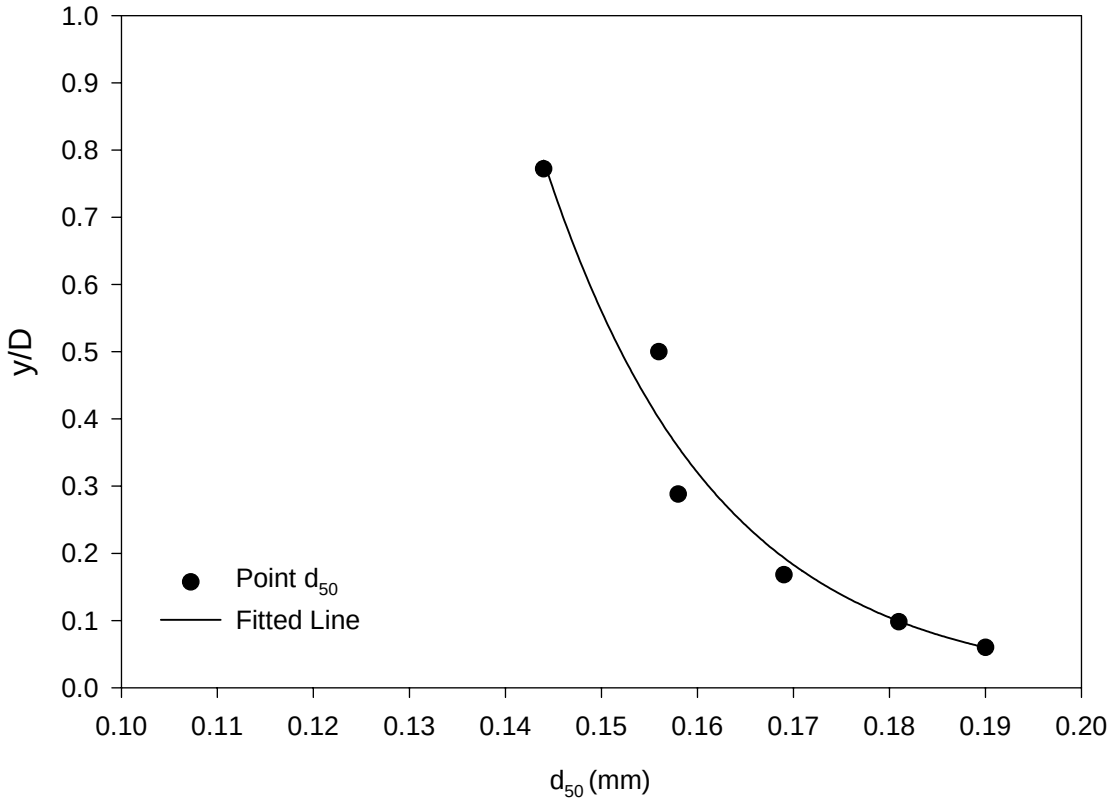

Figure 5-2 Distribution of Sample d_{50} on y-axis, Omaha Station, D=18.4 ft, 10/16/1976

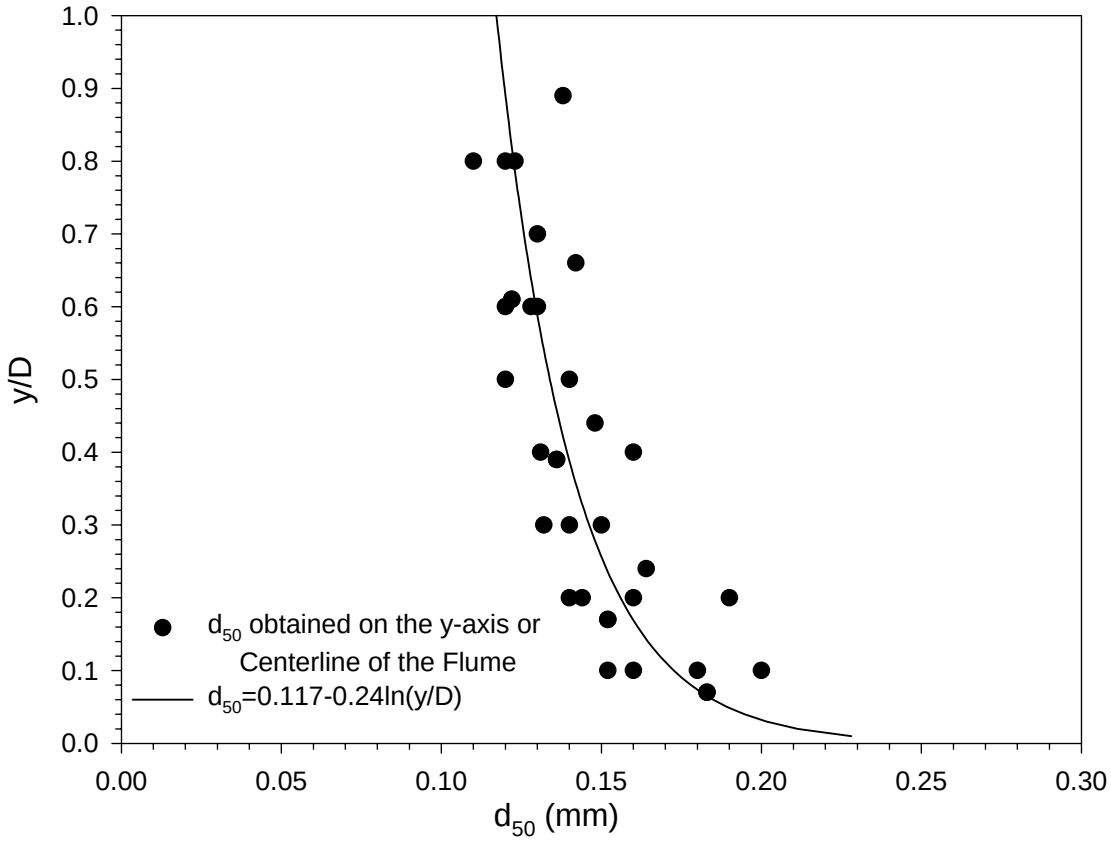

Figure 5-3 Relation between d_{50} and y/D, 8-foot Wide Flume
(Data from R.S. McQuivey, 1973)

Table 5-2 d_{50} along y-axis, Missouri River at Ponca Station

Q=53100 cfs		Q=52200 cfs		Q=54000 cfs		Q=41700 cfs	
10/26/1978		9/20/1978		7/27/1978		6/22/1978	
D=21.9 ft		D=20.9 ft		D=17.1 ft		D=18.2 ft	
d_{50}	y/D	d_{50}	y/D	d_{50}	y/D	d_{50}	y/D
0.191	0.041	0.21	0.053	0.308	0.058	0.158	0.769
0.18	0.05	0.185	0.105	0.305	0.099	0.126	0.5
0.187	0.091	0.19	0.172	0.219	0.17	0.128	0.286
0.188	0.16	0.17	0.287	0.207	0.287	0.138	0.165
0.178	0.279	0.159	0.502	0.139	0.497	0.16	0.099
0.17	0.498	0.153	0.77	0.122	0.766	0.16	0.06
0.154	0.767						
Q=35000 cfs		Q=31000 cfs		Q=33500 cfs		Q=32700 cfs	
8/4/1977		4/28/1977		6/16/1977		4/23/1981	
D=18.1 ft		D=15.5 ft		D=12.9 ft		D=11 ft	
d_{50}	y/D	d_{50}	y/D	d_{50}	y/D	d_{50}	y/D
0.197	0.061	0.183	0.065	0.192	0.062	0.151	0.745
0.188	0.099	0.176	0.103	0.21	0.101	0.179	0.445
0.166	0.166	0.181	0.174	0.178	0.163	0.213	0.209
0.156	0.282	0.163	0.29	0.168	0.287	0.219	0.073
0.134	0.503	0.172	0.503	0.136	0.535	0.327	0
0.179	0.768	0.161	0.768	0.123	0.767		
Q=32500 cfs		Q=31800 cfs		Q=32500 cfs		Q=36300 cfs	
10/20/1977		6/11/1981		8/21/1980		7/17/1980	

Table 5.2 (continued)

D= 12.2 ft		D=11.7 ft		D=12.2 ft		D=8.2 ft	
d_{50}	y/D	d_{50}	y/D	d_{50}	y/D	d_{50}	y/D
0.204	0.098	0.148	0.769	0.137	0.77	0.139	0.768
0.2	0.164	0.147	0.504	0.122	0.451	0.183	0.5
0.19	0.287	0.158	0.291	0.139	0.287	0.223	0.28
0.176	0.5	0.158	0.171	0.155	0.164	0.235	0.171
0.163	0.77	0.205	0.111	0.15	0.098	0.246	0.098
Q=29800 cfs		Q=29800 cfs		Q=38400 cfs		Q=31000 cfs	
4/27/1978		4/24/1980		10/18/1979		9/15/1977	
D=9.9 ft		D=14.8 ft		D=19.4 ft		D=14.8 ft	
d_{50}	y/D	d_{50}	y/D	d_{50}	y/D	d_{50}	y/D
0.149	0.768	0.164	0.77	0.151	0.768	0.203	0.061
0.179	0.495	0.149	0.5	0.173	0.5	0.198	0.101
0.21	0.293	0.18	0.284	0.202	0.284	0.193	0.169
0.248	0.172	0.194	0.169	0.228	0.165	0.164	0.284
0.277	0.101	0.284	0.101	0.221	0.098	0.159	0.5
						0.125	0.77

Table 5-3 d_{50} along y-axis, Missouri River at Nebraska City

Q=42000 cfs		Q=41000 cfs		Q=37500 cfs		Q=38500 cfs	
10/5/1976		4/26/1977		6/14/1977		8/2/1977	
D=13.4 ft		D=13.5 ft		D=12.9 ft		D=12.6 ft	
d_{50}	y/D	d_{50}	y/D	d_{50}	y/D	d_{50}	y/D
0.153	0.067	0.164	0.067	0.182	0.07	0.159	0.103
0.154	0.097	0.161	0.104	0.176	0.101	0.158	0.167
0.157	0.164	0.172	0.17	0.169	0.163	0.146	0.286
0.159	0.284	0.174	0.289	0.165	0.287	0.149	0.5
0.162	0.5	0.163	0.504	0.163	0.504	0.115	0.77
0.165	0.769	0.153	0.77	0.168	0.767		
Q=38000 cfs		Q=36800 cfs		Q=51000 cfs		Q=69200 cfs	
9/13/1977		10/18/1977		4/25/1978		7/25/1978	
D=11.0 ft		D=12.5 ft		D=15.8 ft		D=17.6 ft	
d_{50}	y/D	d_{50}	y/D	d_{50}	y/D	d_{50}	y/D
0.178	0.1	0.18	0.096	0.183	0.057	0.219	0.057
0.174	0.164	0.179	0.168	0.177	0.101	0.218	0.102
0.173	0.282	0.176	0.28	0.169	0.165	0.185	0.165
0.159	0.5	0.164	0.496	0.164	0.285	0.194	0.284
0.137	0.773	0.147	0.768	0.145	0.5	0.183	0.5
				0.142	0.766	0.177	0.767
Q=57000 cfs		Q=60500 cfs		Q=44900 cfs		49700 cfs	

Table 5.3 (continued)

9/12/1978		10/24/1978		10/9/1979		8/28/1979	
D= 17.1 ft		D=18.3 ft		D=13.7		D=16.2 ft	
d_{50}	y/D	d_{50}	y/D	d_{50}	y/D	d_{50}	y/D
0.224	0.041	0.237	0.06	0.158	0.051	0.143	0.062
0.223	0.099	0.214	0.098	0.163	0.095	0.159	0.099
0.203	0.17	0.212	0.164	0.174	0.161	0.167	0.167
0.196	0.292	0.201	0.284	0.188	0.277	0.175	0.284
0.173	0.772	0.186	0.497	0.198	0.496	0.172	0.5
		0.206	0.765	0.194	0.766	0.18	0.772

6.0 MATHEMATICAL MODELS OF SEDIMENT DISTRIBUTION

6.1 CONVENTIONAL MODLE-ROUSE EQUATION

The concentration profile C(y) is calculated by knowing the diffusion concept for suspended sediment [31, 32]. In steady uniform flow, this leads to a balance between the downward settling of sediment due to gravity and upward diffusion associated with turbulent fluctuations

$$v_s C + \varepsilon_s \frac{dC}{dy} = 0 \tag{6-1}$$

$$\frac{dC}{C} = -\frac{v_s}{\varepsilon_s} dy \tag{6-2}$$

Where v_s = settling velocity; and ε_s = diffusion coefficient for suspended sediment, which is normally taken to be proportional to the eddy viscosity of the flow ε .

$$\varepsilon_s = \beta \varepsilon_m \tag{6-3}$$

Where β = momentum correction factor and ε_m = diffusion coefficient for momentum transfer.

$$\tau = \rho \varepsilon_m \frac{du}{dy} = \tau_0 \left(1 - \frac{y}{D}\right) \tag{6-4}$$

$$\frac{\tau}{\tau_0} = 1 - \frac{y}{D} \tag{6-5}$$

$$\varepsilon_m = \frac{\tau_0}{\rho}(1 - \frac{y}{D})(\frac{du}{dy})^{-1} = u_*^{\,2} \frac{\tau}{\tau_0}(\frac{du}{dy})^{-1} \tag{6-6}$$

where ρ = fluid density; $\frac{du}{dy}$ = velocity gradient; u_* = shear velocity; and τ and τ_0 = shear stress at y and y = 0, respectively. Therefore, solution of (6-1) gives

$$\frac{C}{C_0} = \exp\left[-\frac{v_s}{\beta u_*^{\,2}} \int_0^Y \left(\frac{\tau}{\tau_0}\right)^{-1} \frac{du}{dy} dy \right] \tag{6-7}$$

where $C_0 = C$ at y = 0.

Mathematical models of distribution of sediment concentration may be derived by substituting velocity distributions in Equation (6-7). The well-known Rouse equation is derived when Prandtl-von Karman logarithmic equation is used. The shear stress distribution, equation (6-5) was used in deriving Rouse equation.

$$\frac{C}{C_a} = \left[\frac{a}{D-a} \frac{D-y}{y} \right]^z \tag{6-8}$$

$$z = \frac{v_s}{kU_*\beta} \tag{6-9}$$

C = concentration of suspended sediment; C_a = a reference concentration at a distance a above the bed; y = vertical coordinate, measured upward from the bottom; D = water depth, and z= Rouse number.

The conventional method of computation of sediment load is to substitute the logarithmic or power velocity distribution and the Rouse concentration profile in the following integral [8,11, 32]:

$$q_s = \int_a^D Cu dy = \overline{C}_i q \tag{6-10}$$

q_s = sediment discharge per unit width; q = water discharge per unit width; a = two times the sediment diameter at the bed according to Einstein [32]; $\overline{C}_i$ = average concentration per unit width.

When Prandtl-von Karman universal velocity equation is used in derivation of Rouse equation, sediment concentration cannot be determined within a distance "a" from the channel bed.

6.1.1 Parameter Estimation

In order to estimate parameters of Rouse equation, A and B in the following equation must be calculated first by regression [10, 11, 18].

$$C = A\left[\frac{D-y}{y}\right]^B \tag{6-11}$$

in which

$$A = C_a\left[\frac{a}{D-a}\right]^B \tag{6-12}$$

$$B = \frac{v_s}{ku_*} \tag{6-13}$$

To calculate the Rouse parameters z and C_0, the following assumptions are made: $\beta = 1$, and a = 0.05D.

6.2 CHIU'S MATHEMATICAL MODEL OF DISTRIBUTION OF SEDIMENT CONCENTRATION

The velocity and sediment concentration profiles for the y-axis are defined by Chiu's velocity and sediment concentration equations [2], which estimate sediment concentration from the channel bed (y = 0) to the water surface (y= D).

1. If maximum velocity occurs on the water surface, $h \le 0$, y = D, then, Equations (4-25), (4-26), and (4- 27) are used. In this case, the shear stress and velocity distribution are represented by Equations (6-5) and (4-10) with $\xi = \frac{y}{D}$ respectively, therefore, (6-7) gives the following equation:

$$\frac{C}{C_0} = \left[\frac{1 - \frac{y}{D}}{1 + (e^M - 1)\frac{y}{D}} \right]^{\lambda'} \tag{6-14}$$

in which C_0 is C at y = 0 and y = D at C = 0

$$\lambda' = \frac{v_s u_{\max}(1 - e^{-M})}{\beta u_*^{\,2} M} = \frac{v_s \bar{u}(1 - e^{-M})}{\beta u_*^{\,2} M \phi} = \lambda G \tag{6-15}$$

where

$$G = \frac{1 - e^{-M}}{M\phi} \tag{6-16}$$

and

$$\lambda = \frac{v_s \bar{u}}{\beta u_*^{\,2}} = \theta \frac{\phi M (2 + e^M)}{6(e^M - 1)} \tag{6-17}$$

Equation (6-14) is applicable at the channel bed but Rouse equation is not although both equations appear to be similar [2].

2. If maximum velocity occur below water surface, h>0, $\xi_{\max} = 1$, $\xi_0 = 0$, then, Equations (4-28) and (4-29) are used.

Shear stress distribution compatible with the velocity distribution with ξ given by (4-11) is expressed in the following power series form:

$$\frac{\tau}{\tau_0} = \frac{h}{D}\left(1 - \frac{y}{D-h}\right) + \left(1 - \frac{h}{D}\right)\left(1 - \frac{y}{D-h}\right)^2 \tag{6-18}$$

which satisfies the boundary conditions that $\tau = \tau_0$ at y = 0; $\tau = 0$ at y = h-D where $u = u_{\max}$ and also at y = D (water surface). As $\frac{h}{D}$ approaches negative infinity, Equation (6-18) becomes (6-5).

Equation (4-29) with $\frac{du}{dy}$ given by (6-19)

$$\frac{du}{dy} = \frac{\bar{u}}{\phi M \xi_{\max}}(e^M - 1)\left\{h_\xi\left[1 + (e^M - 1)\frac{\xi}{\xi_{\max}}\right]\right\}^{-1} \tag{6-19}$$

gives

$$\frac{C}{C_0} = \exp\left[-\lambda' I\left(\frac{y}{D}, \frac{h}{D}, M\right)\right] \tag{6-20}$$

$$\frac{C}{C_0} = e^{\left[-\lambda' I\left(\frac{y}{D}, \frac{h}{D}, M\right)\right]} \tag{6-21}$$

$$I = \frac{e^M}{\xi_{\max}} \int_0^Y h_\xi^{-1}\left[1 + (e^M - 1)\frac{\xi}{\xi_{\max}}\right]^{-1} \left(\frac{\tau}{\tau_0}\right)^{-1} dy \tag{6-22}$$

$$h_\xi = (D-h)\left[\left(1 - \frac{y}{D-h}\right)e^{\left(1 - \frac{y}{D-h}\right)}\right]^{-1} \tag{6-23}$$

$$I = \frac{e^M}{\xi_{\max}} \int_0^Y \left[\frac{D-h-y}{(D-h)^2} e^{(1-\frac{y}{D-h})} \right] \left[1 + (e^M - 1)\frac{y}{D} e^{(\frac{D-y}{D-h})} \right]^{-1} \left[\frac{h}{D}(1-\frac{y}{D-h}) + (1-\frac{h}{D})(1-\frac{y}{D-h})^2 \right]^{-1} dy \quad (6\text{-}24)$$

Figures 6.1 and 6.2 compare Chiu's sediment distribution with Rouse equation near the channel bed. They show that Chiu's sediment distribution estimates the sediment concentration from the water surface to the channel bed, while Rouse equation is not applicable within a distance "a" from the channel bed. Figure 6.3 depicts Chiu's sediment distribution model applied to a sediment data with the grain diameters (d=0.062 and 0.254 mm). It shows that for d=0.062 mm, the distribution of sediment concentration is uniform along y-axis.

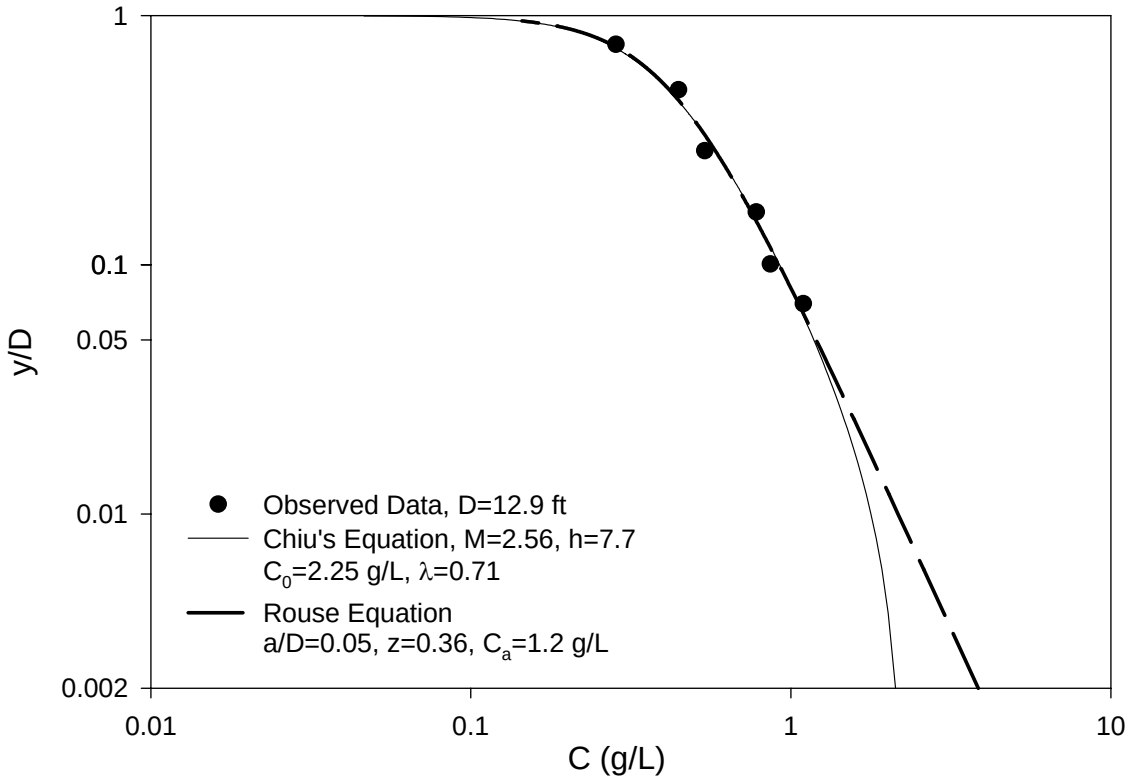

Figure 6-1 Comparison of Sediment Distribution Models; Missouri River at Nebraska City, 6/14/1977

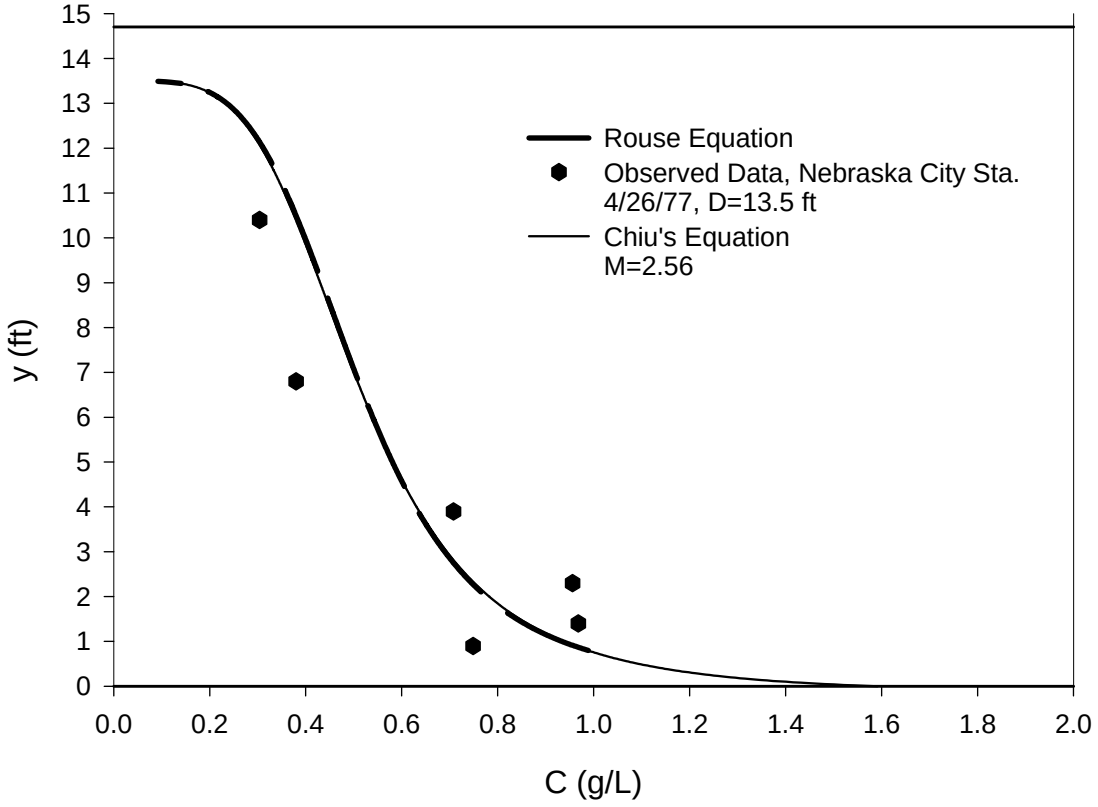

Figure 6-2 Comparison of Sediment Distribution Models

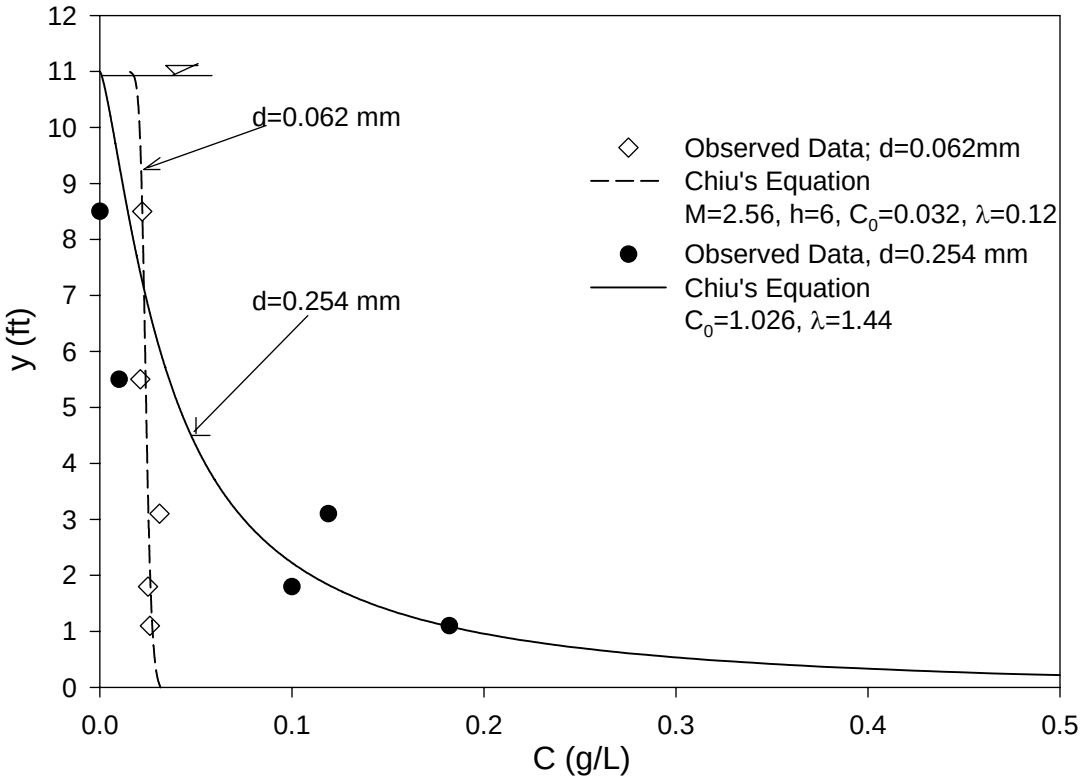

Figure 6-3 Distribution of Sediment Concentration for two Sediment Diameters, Missouri River at Nebraska City, 9/13/1977

6.2.1 Parameter Estimation

To use the sediment distribution equations the parameters C_0 and λ must be calculated by regression method as explained in the following steps:

Apply the Equations (6-14) or (6-21) to sediment data at 5 or 6 points on y-axis, and find the parameters C_0 and λ'

1. Find λ from the equation

$$\lambda = \frac{\lambda'}{G} \tag{6-15}$$

2. θ and β are calculated from the following equations, having M and λ.

$$\theta = \frac{v_s D}{\varepsilon_s} = 6\frac{v_s \bar{u}}{\beta {u_*}^2}\frac{e^M - 1}{\phi M(2+e^M)} = \lambda\frac{6(e^M-1)}{\phi M(2+e^M)} \tag{6-17}$$

A mathematical equation [2] (Cheng 1997) for settling velocity is used to calculate λ.

$$\frac{v_s d}{\nu} = (\sqrt{25+1.2{d_*}^2}-5)^{1.5} \tag{6-25}$$

where d = particle diameter; ν = kinematics viscosity of the fluid; and

$$d_* = \left(\frac{(\rho_s-\rho)g}{\rho\nu^2}\right)^{\frac{1}{3}} d \tag{6-26}$$

where ρ_s = density of sediment.

The coefficient β that relates ε_s to ε_m is about unity, varying little with sediment concentration, and is constant along a vertical. It also tends to vary with sediment size and it is impossible to be calculated accurately. Therefore, by probabilistic approach Chiu presented the method of calculation as follows:

$$\theta = \frac{v_s D}{\varepsilon_s} = 6\frac{v_s \bar{u}}{\beta u_*^{\,2}} \frac{e^M - 1}{\phi M (2 + e^M)} = \lambda \frac{6(e^M - 1)}{\phi M (2 + e^M)} \tag{6-17}$$

θ is the only unknown parameter in the above equation that can be calculated.

θ is fairly invariant with sediment concentration but increases with sediment size. A practical procedure of determining β, is to obtain θ first, then substitute it into (6-17). Since M at a channel section is constant, the value of λ and λ' can be obtained by (6-17) and (6-15) respectively.

Tables 6.1 and 6.2 present the summary of discharge, d_{50}, λ and θ of Missouri River at four monitoring stations. The values of λ and θ were computed using Equations (6-15) and (6-17) respectively.

Figures 6.4, 6.5, and 6.6 show Chiu's distribution of sediment concentration applied to sediment data on y-axis of Missouri River at Nebraska City and Omaha. Parameters C_0 and λ' were estimated by regression method and λ from Equation (6-15).

Figure 6.7 shows there is a good agreement between the measured and computed mean concentration using Chiu's equations on y-axis.

Figures 6.8 and 6.9 present the transverse distribution of mean sediment concentration and mean velocity (measured) on each vertical in the Missouri River at Nebraska City. These figures show that the maximum sediment concentration and maximum velocity occur on y-axis.

Table 6-1 Hydraulic Data, Missouri River

Missouri River at	Date of Sediment Measurement M-D-Y	Water discharge cfs	Total Depth D ft	Vertical d_{50} mm	λ	θ
Sioux City	10/7/1976	36500	11.4	0.177	0.86	1.53
	10/11/1979	39600	15	0.181	1.76	3.03
	4/17/1980	31000	18.9	0.197	1.53	2.62
	5/29/1980	31900	20.8	0.162	1.54	2.64
	7/10/1980	33500	24.2	0.184	2.03	3.49
	8/28/1980	33700	12	0.144	0.85	1.45
	10/16/1980	36600	17.2	0.17	0.54	0.92
	4/16/1981	32700	18.8	0.188	1.55	2.65
	6/4/1981	32100	18.8	0.168	1.19	2.04
	7/16/1981	33400	17.2	0.227	1.69	2.9
	8/27/1981	33400	16.6	0.246	3.57	6.13
	10/15/1981	35100	13.6	0.224	1.04	1.78
Gayville	7/21/1981	35300	16.4	0.187	1.24	3.05
	6/9/1981	32200	15.7	0.174	1.35	3.31
	4/21/1981	33900	12.9	0.258	1.56	3.83
	10/7/1980	37600	20	0.21	1.39	3.41
	8/19/1980	32300	15.7	0.143	1.96	4.81
	7/15/1980	36600	13.7	0.199	1.65	4.04
	6/3/1980	28500	12.8	0.177	1.24	3.03

Table 6.1 (continued)

	4/22/1980	31400	15.4	0.166	1.73	4.25
Nebraska City	10/5/1976	42000	13.4	0.158	0.27	0.72
	4/26/1977	41000	13.5	0.164	0.61	1.64
	6/14/1977	37500	12.9	0.169	0.89	2.41
	8/2/1977	38500	12.6	0.149	0.96	2.6
	9/13/1977	38000	11	0.173	0.87	2.35
	10/18/1977	36800	12.5	0.176	1	2.69
	4/25/1978	51000	15.8	0.167	1.43	3.87
	7/25/1978	69200	17.6	0.19	0.85	2.31
	9/12/1978	57000	17.1	0.203	1.6	4.33
	10/24/1978	60500	18.3	0.209	2.01	5.41
	10/9/1979	44900	13.7	0.181	1.72	4.66
	8/28/1979	49700	16.2	0.169	0.96	2.6

Table 6-2 Hydraulic Data, Missouri River at Omaha

Missouri River at	Date of Sediment Measurement M-D-Y	Water discharge cfs	Total Depth D ft	Vertical d_{50} mm	λ	θ
Omaha	10/6/1976	38000	18.4	0.164	1.59	3.59
	4/27/1977	31500	13.2	0.149	0.72	1.63
	6/15/1977	34500	15.5	0.15	0.47	1.07
	7/26/1978	63300	13.1	0.187	1.28	2.88
	8/3/1977	34500	20	0.167	1.17	2.64
	9/14/1977	34500	16.6	0.15	1.46	3.38
	10/19/1977	33000	15.1	0.171	1.34	3.03
	4/26/1978	34500	18.5	0.145	1.07	2.24
	6/21/1978	47200	21.4	0.155	1.89	4.28
	10/25/1978	58100	19	0.173	1.76	3.99
	9/12/1978	54800	19.8	0.172	1.04	2.35
	4/30/1979	43100	12.8	0.186	1.43	3.53
	6/6/1979	46400	20.2	0.164	1.34	3.03
	7/18/1979	43000	18.1	0.19	1.38	3.12
	8/29/1979	43900	16	0.177	1.56	3.53
	4/16/1980	34700	15.7	0.182	0.73	1.66
	10/10/1979	41200	17.5	0.163	0.87	1.97
	5/30/1980	32900	17.4	0.181	1.90	2.65
	8/26/1980	34100	17.4	0.181	1.85	4.29
	7/9/1980	32800	19	0.153	1.57	3.56

Table 6.2 (continued)

10/15/1980	37100	16.2	0.175	1.48	3.34
4/15/1981	35700	13.6	0.179	0.99	2.23
6/3/1981	31700	17.2	0.167	0.99	2.24
10/14/1981	32900	14.2	0.176	1.51	3.37
8/26/1981	33800	16.6	0.187	1.16	2.69
7/15/1981	33300	16.2	0.187	1.58	3.66

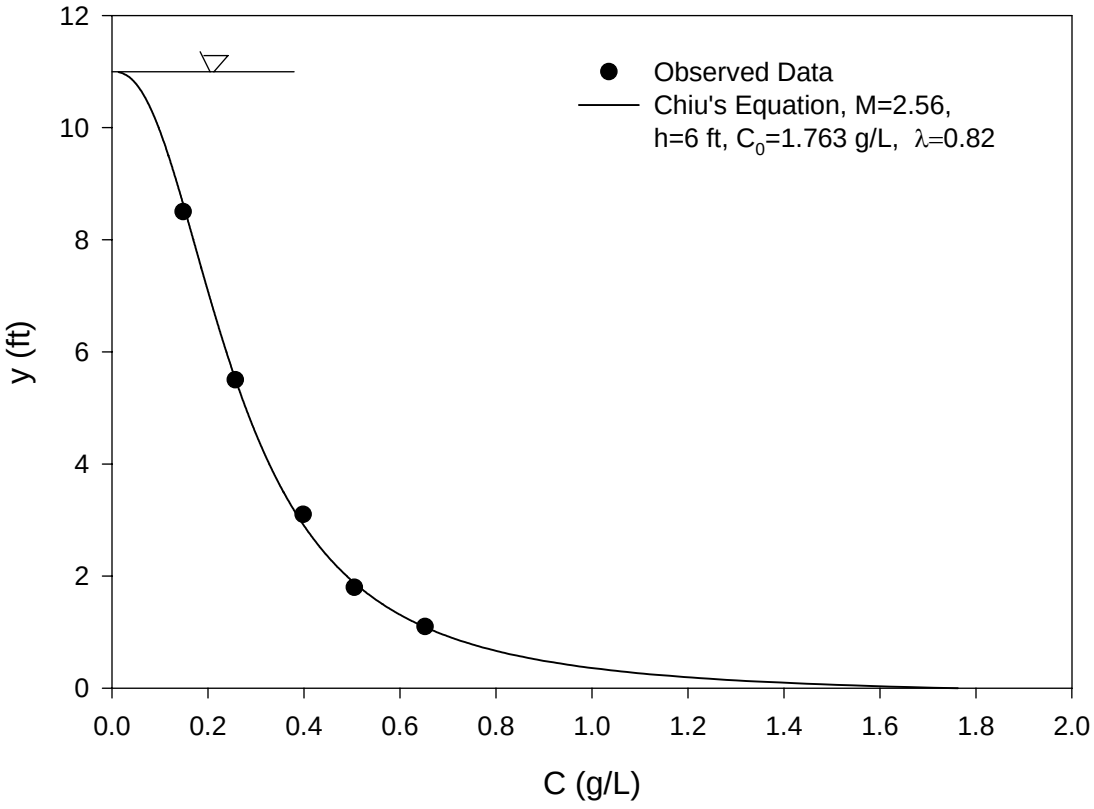

Figure 6-4 Chiu's Distribution of Sediment Concentration, Missouri River at Nebraska City, D=11.0 ft, 9/13/1977

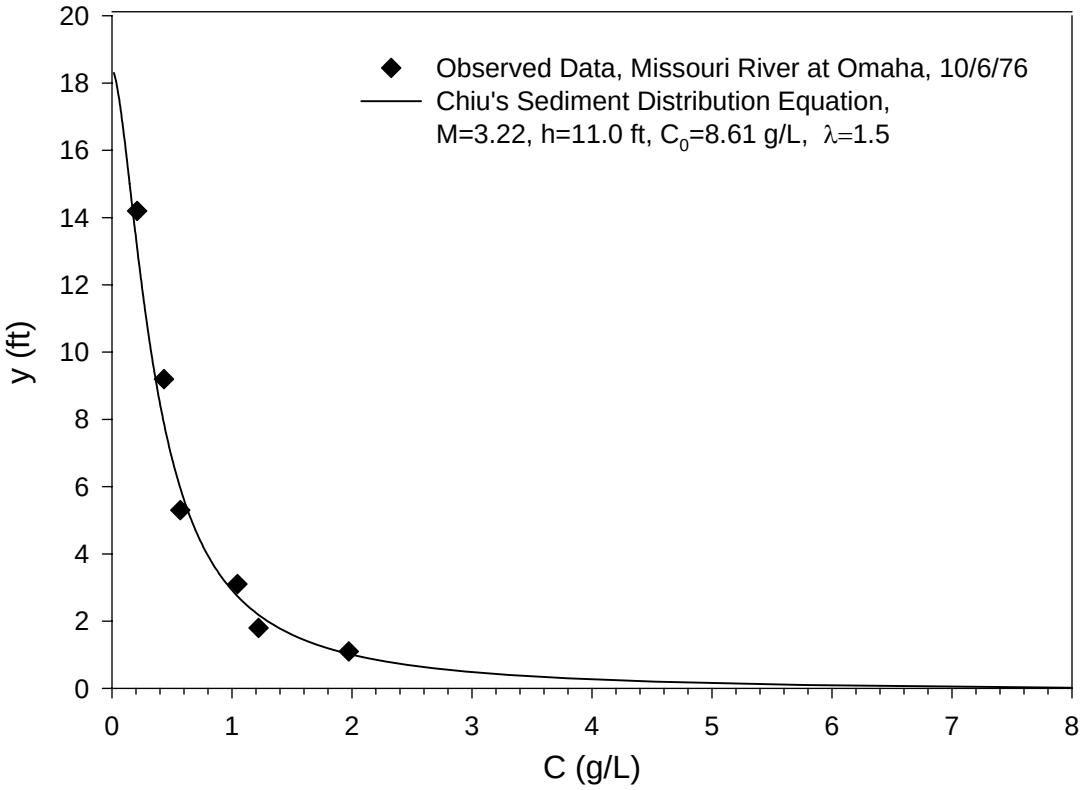

Figure 6-5 Chiu's Distribution of Sediment Concentration, Missouri River at Omaha, D=18.4 ft, 10/6/1976

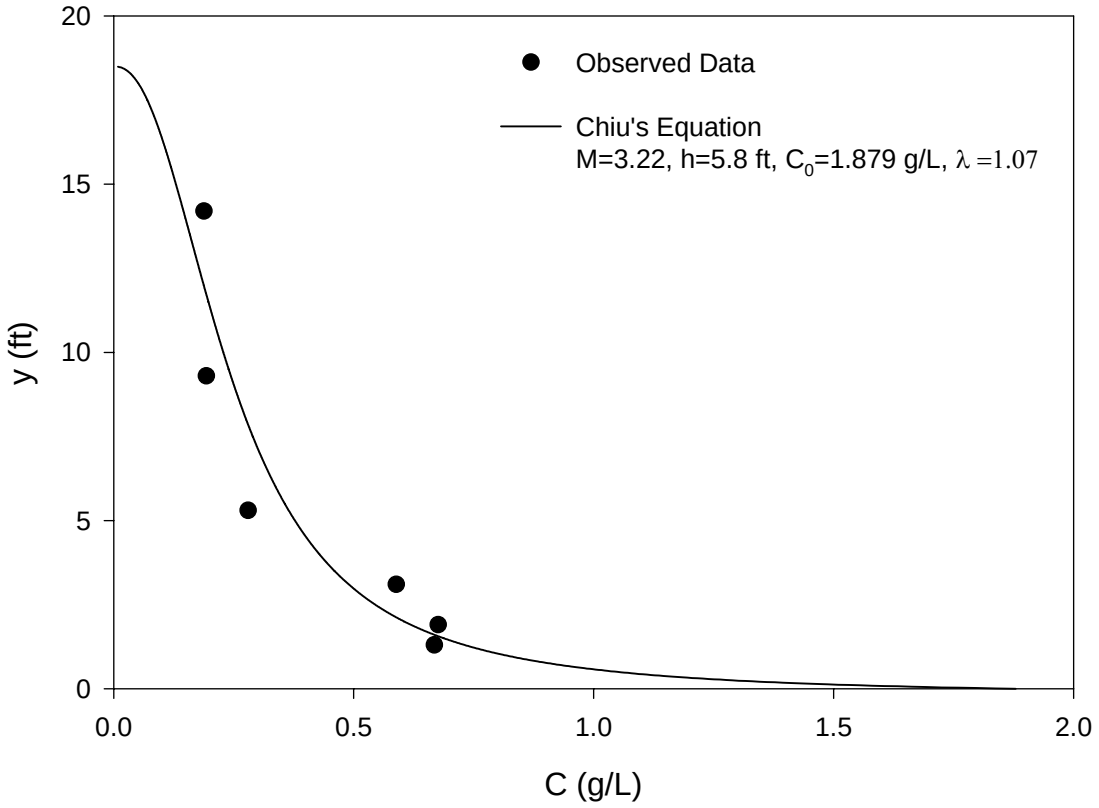

Figure 6-6 Chiu's Distribution of Sediment Concentration, Missouri River at Omaha, D=18.5, 4/26/1978

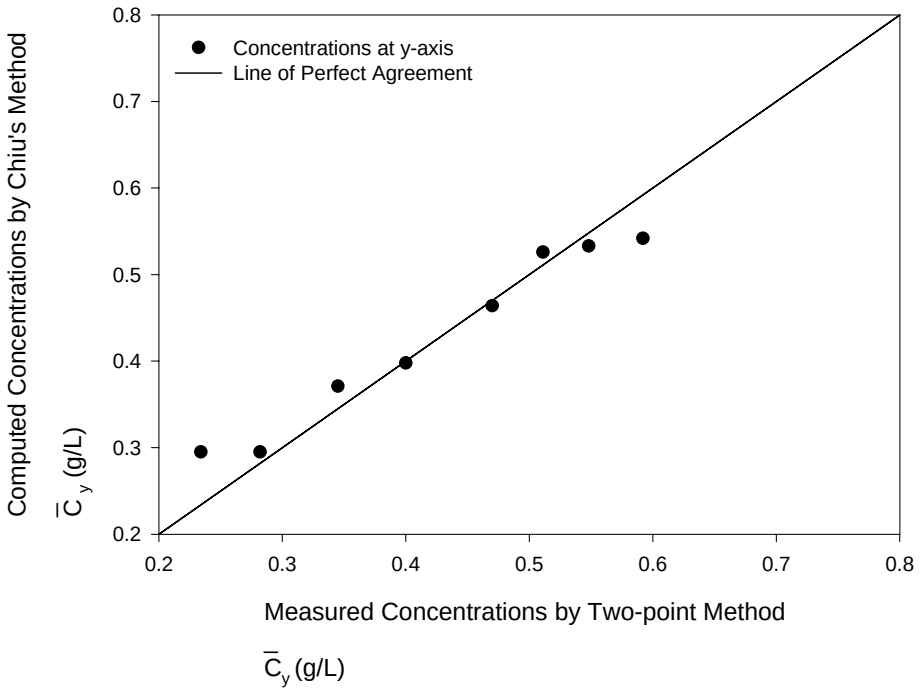

Figure 6-7 Comparing the Computed and Measured Mean Concentration on y-axis, Missouri River at Nebraska City

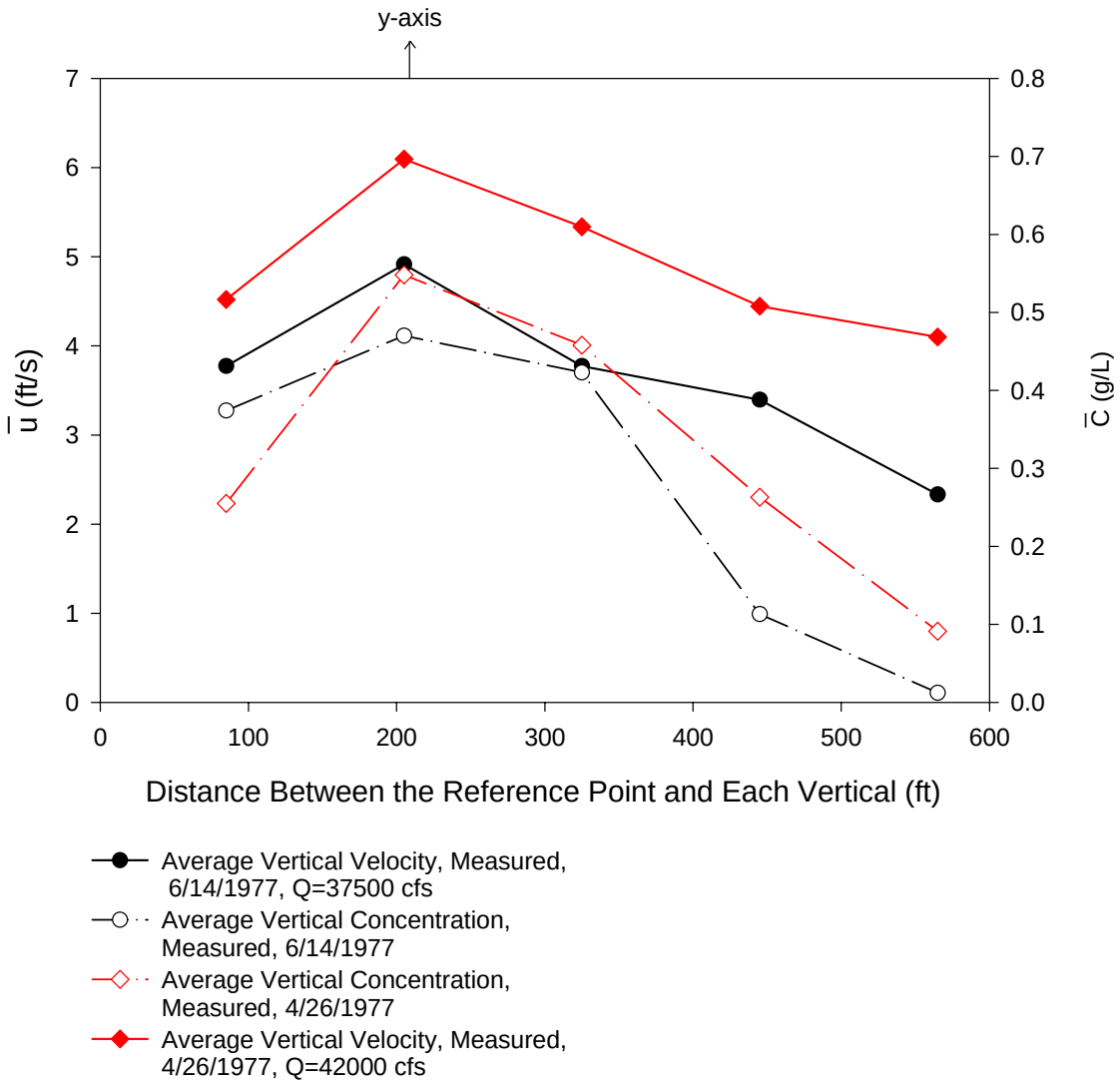

Figure 6-8 Transverse Distribution of Average Sediment Concentration and Velocity, Missouri River at Nebraska City

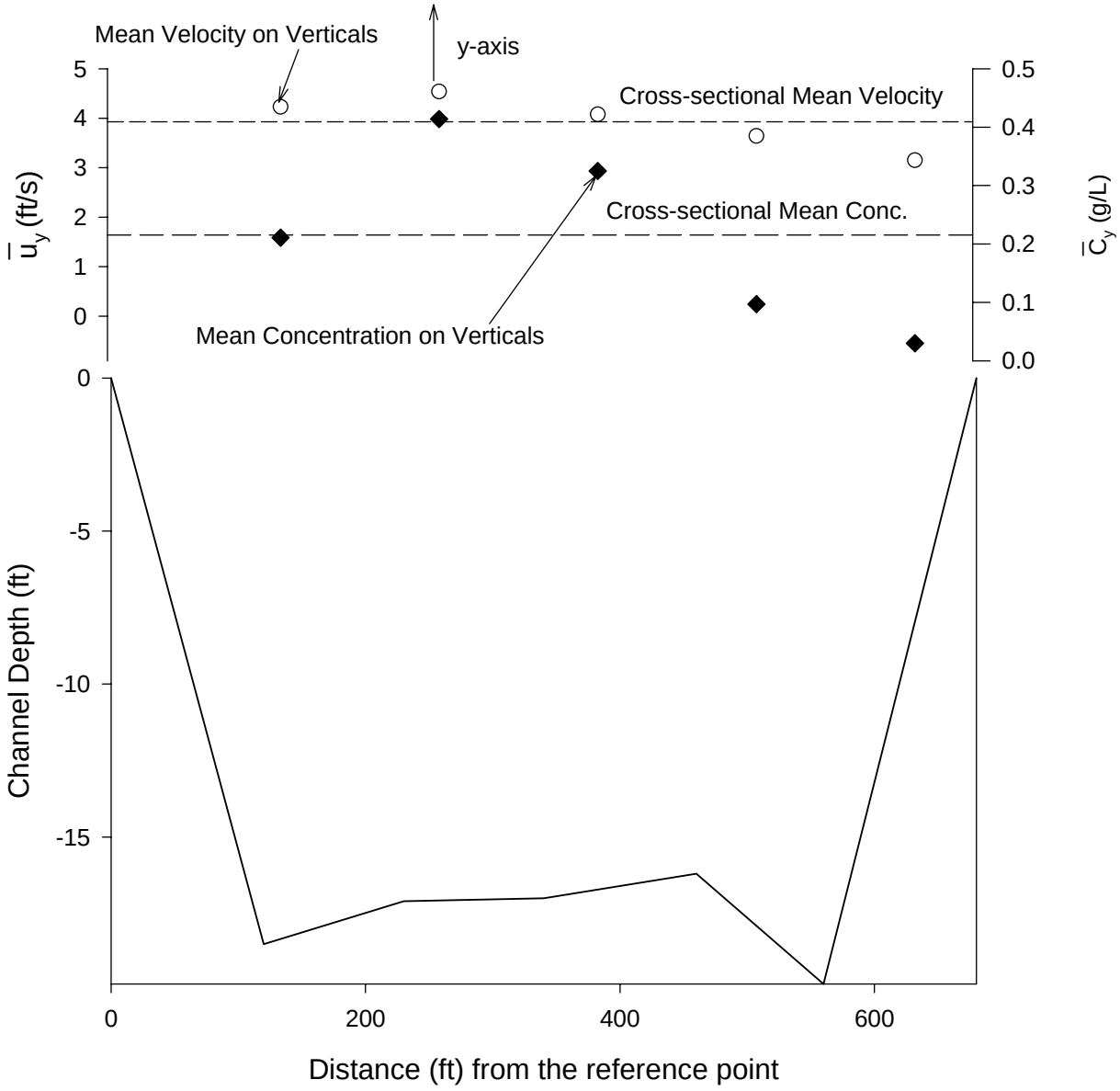

Figure 6-9 Distribution of Average Concentration and Velocity (Measured) across the Channel of Missouri River at Nebraska City

7.0 CALCULATION OF THE CROSS-SECTIONAL MEAN CONCENTRATION BY THE EFFICIENT METHOD

7.1 CORRELATION BETWEEN THE CROSS-SECTIONAL MEAN CONCENTRATION AND THE MEAN CONCENTRATION ON EACH VERTICAL

Figures 7.1 to 7.6 show the correlation between cross-sectional mean concentration and the mean concentration on each vertical across the channel sections of different rivers. These figures demonstrate that the correlation is highest on y-axis and decreases toward the channel banks. Therefore, it provides a basis for collecting the data on y-axis.

The mean concentration on each vertical ($\overline{C_i}$, i =1..5) was obtained by averaging the sediment concentration measured at two-tenths and eight-tenths of water depth on each vertical using Equation (2-10). The cross-sectional mean concentration ($\overline{C_x}$) was calculated using the Equation (2-8). A study of Figures 7.1 to 7.6 revealed that the river sections with coarser d_{50} such as Missouri River have lower r^2 than the river sections with finer d_{50} such as Mississippi River. It is obvious that in channel sections with coarse particles, the transverse distribution is not uniform. According to L.Yuqian [22] appreciable errors would be expected in the concentration of coarse sediment if only a limited number of verticals were adopted.

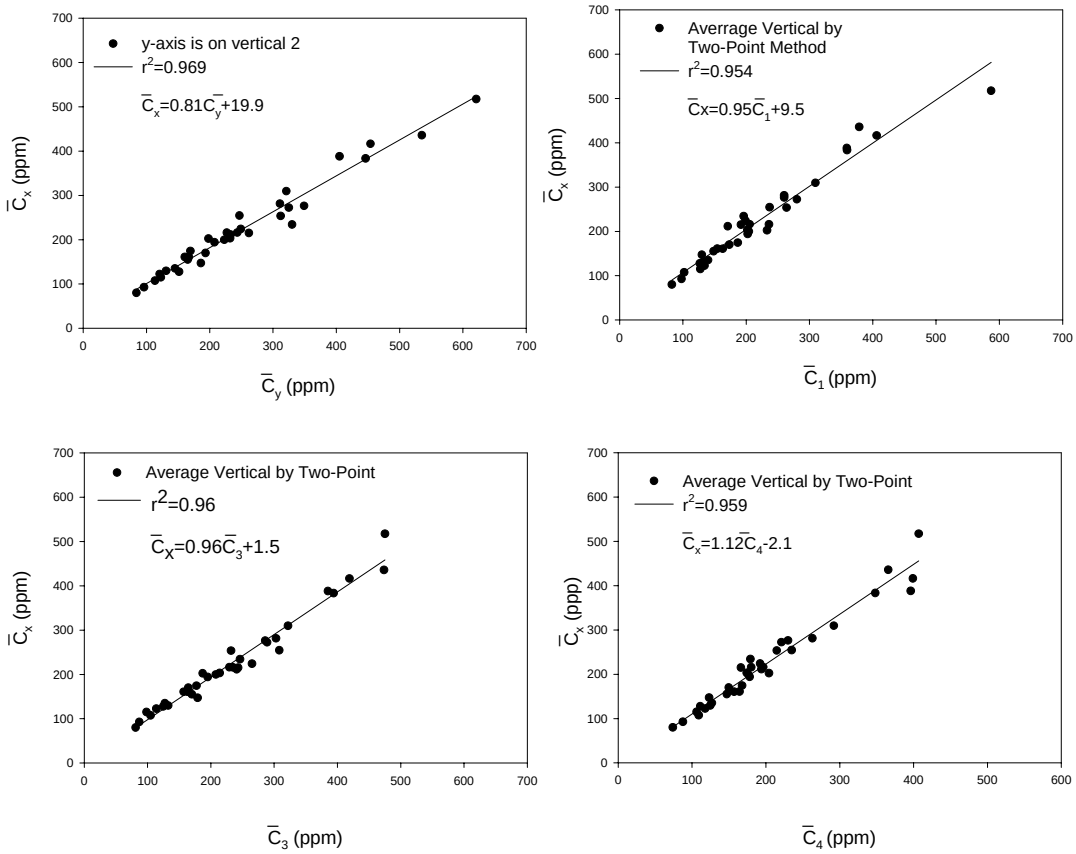

Figure 7-1 Correlation between Mean Concentration on each Vertical and Cross-sectional Mean Concentration (All Sizes), Mississippi River at Tarbert, 1995 and 96

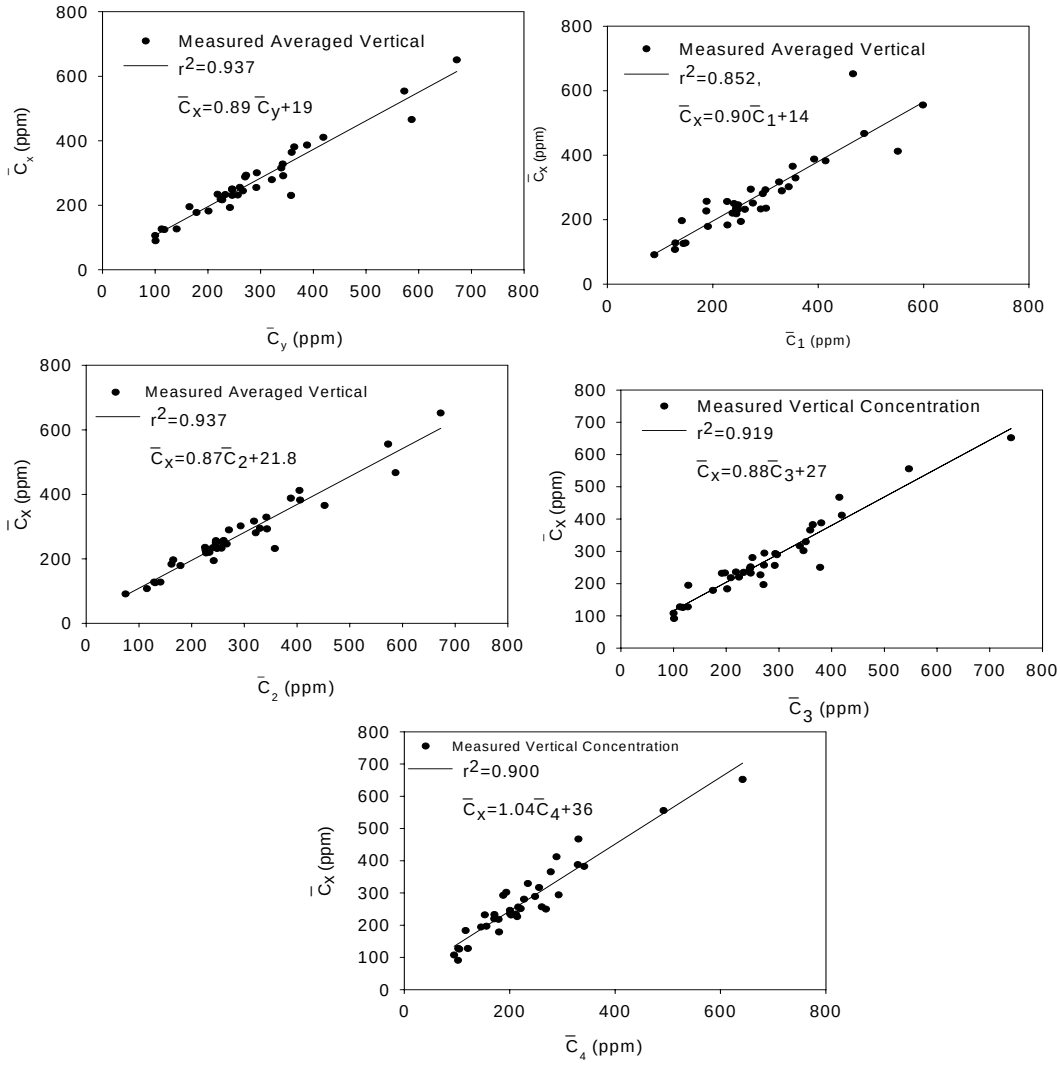

Figure 7-2 Correlation between Mean Concentration on each Vertical and Cross-sectional Mean Concentration, Mississippi River at Union Point, 1994, 95 and 96

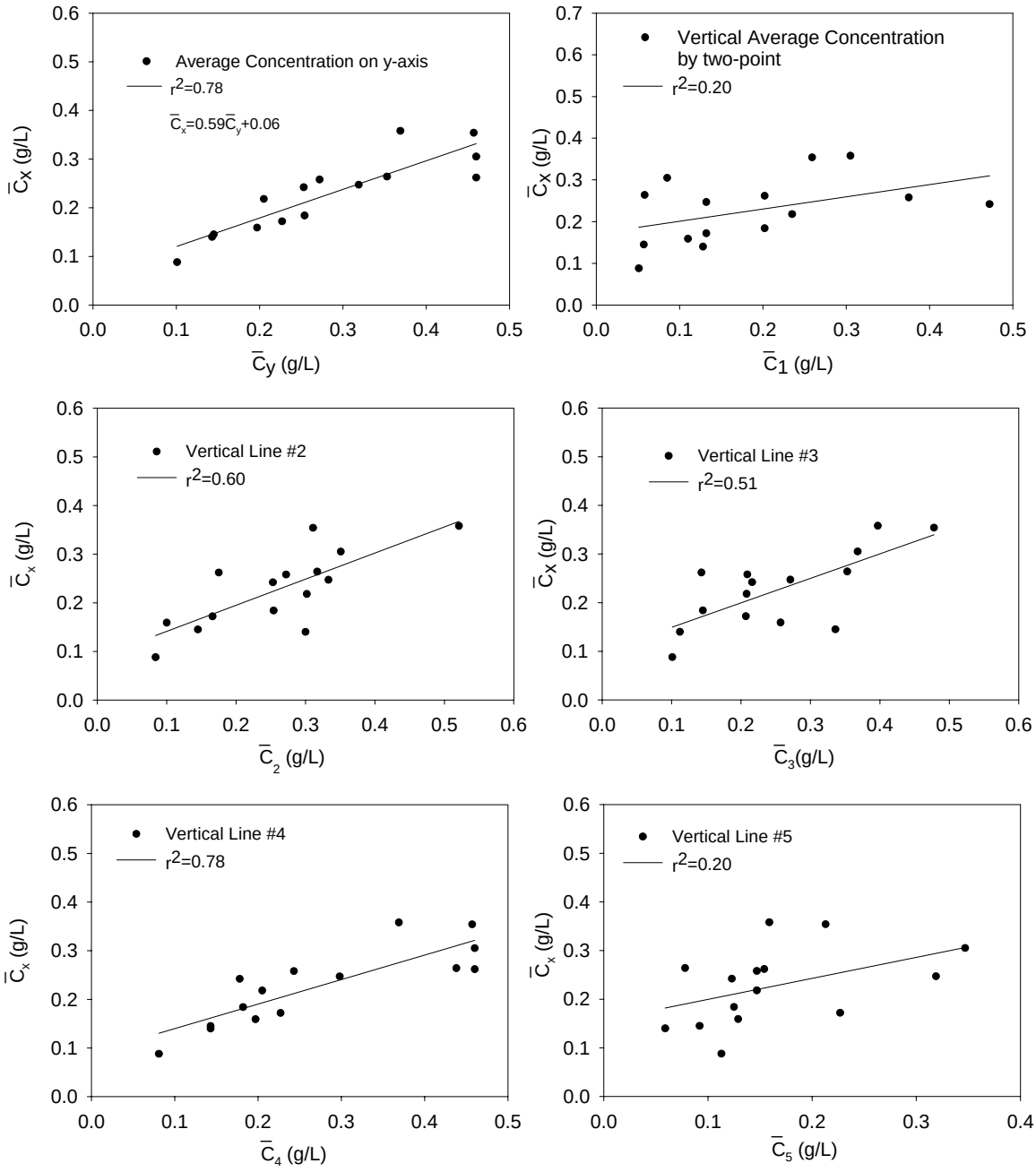

Figure 7-3 Correlation between Mean Concentration on each Vertical and Cross-sectional Mean Concentration, Missouri River at Ponca, 1979-81

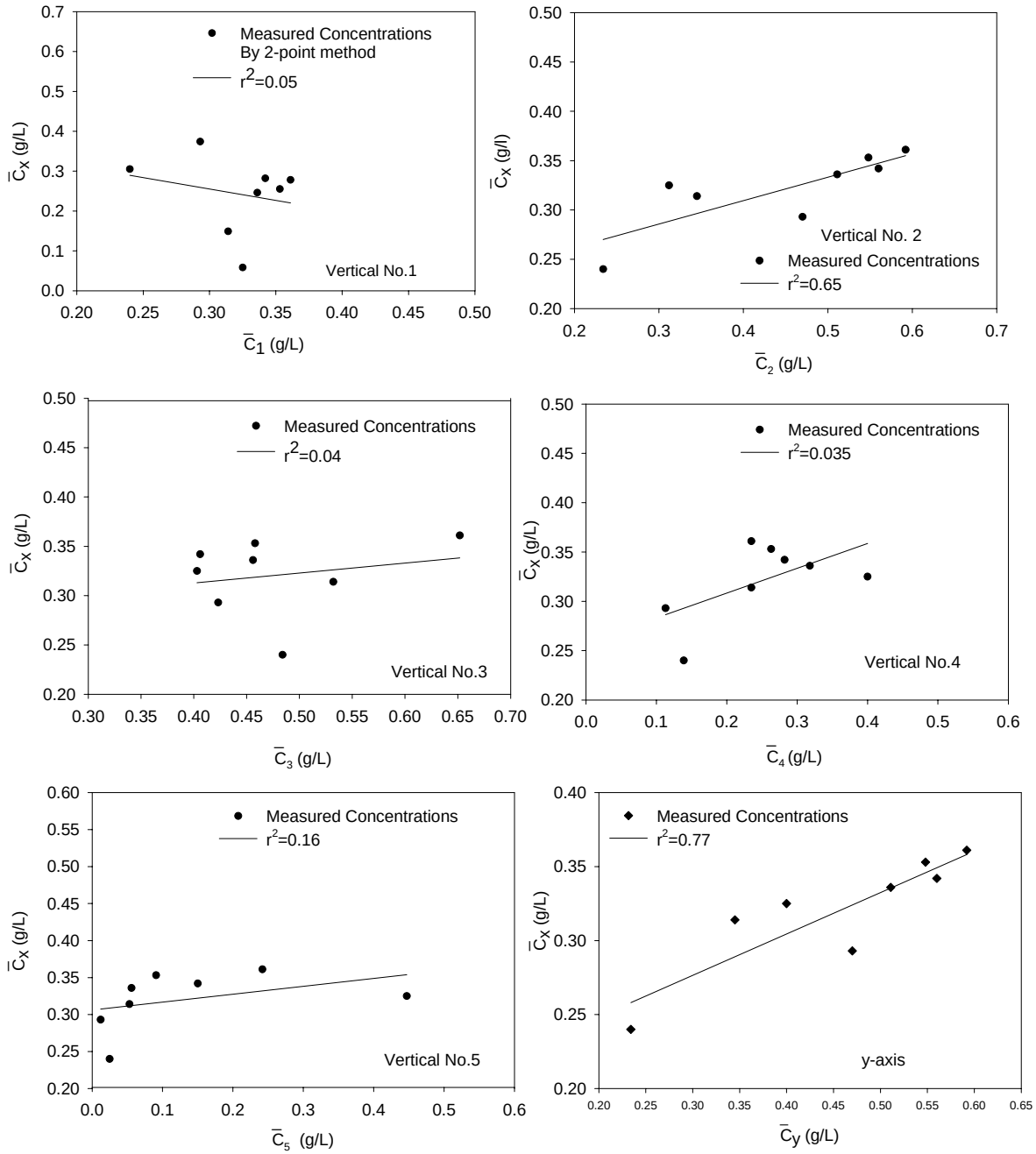

Figure 7-4 Correlation between Mean Concentration on each Vertical and Cross-sectional Mean Concentration, Missouri River at Nebraska City 1977-81

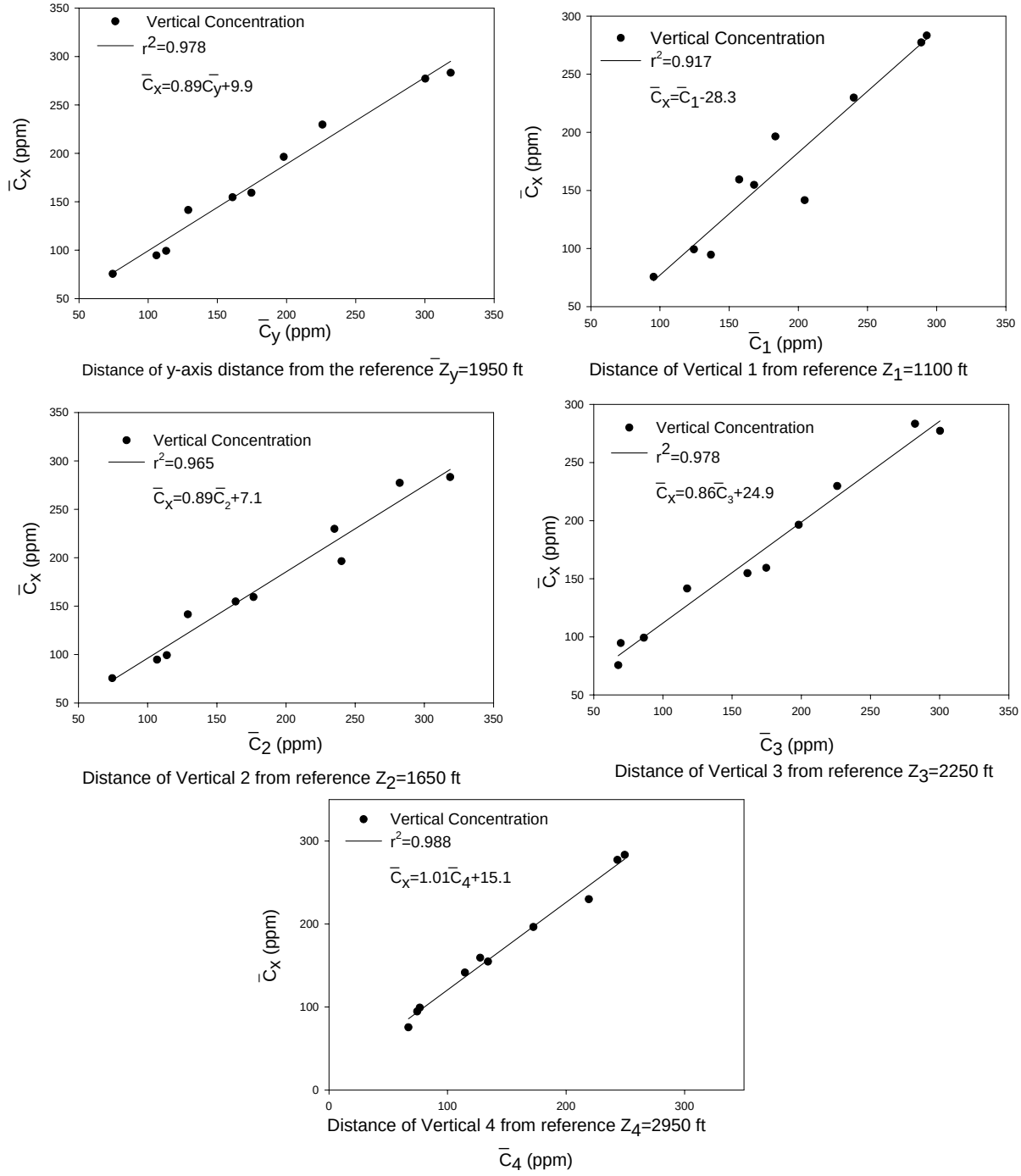

Figure 7-5 Correlation between Mean Concentration on each Vertical and Cross-sectional Mean Concentration, Mississippi River at Range 362.2

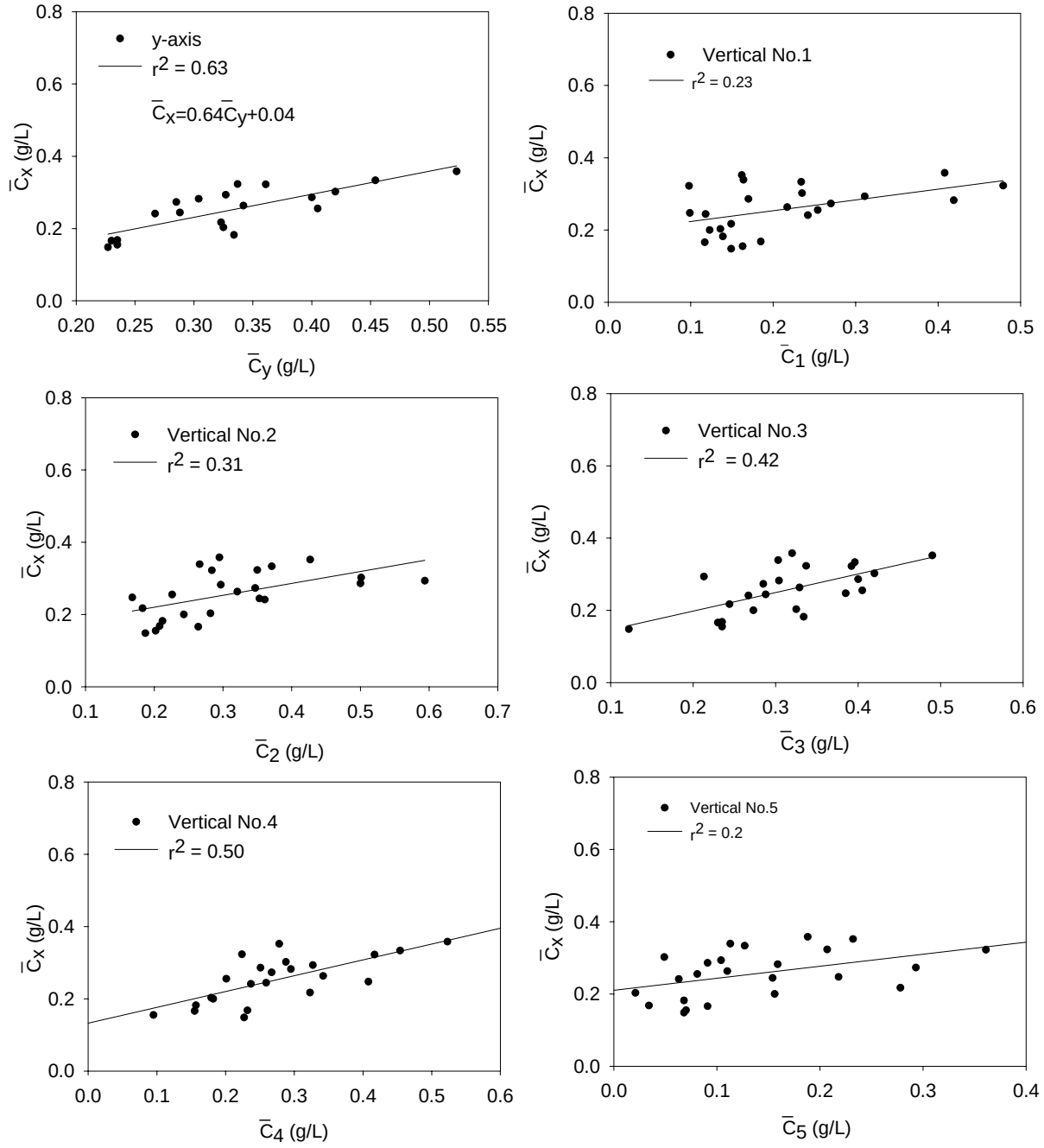

Figure 7-6 Correlation between Mean Concentration on each Vertical and Cross-sectional Mean Concentration, Missouri River at Omaha, 1976-81

7.2 CORRELATION BETWEEN CROSS-SECTIONAL MEAN CONCENTRATION AND MEAN CONCENTRATION ON Y-AXIS

The ratio of cross-sectional mean concentration ($\overline{C}_x$) to mean concentration on y-axis ($\overline{C}_y$) is defined $\psi = \frac{\overline{C}_x}{\overline{C}_y}$. This coefficient was calculated for each sediment size (d) and median size (d_{50}) on y-axis. The ψ value representative of each station was determined by regression.

The ψ values obtained from the plots of $\overline{C}_x$ against $\overline{C}_y$ were used in developing the relation between M and ψ. Figures 7.7 to 7.15 show the correlation between cross-sectional mean concentration and the concentration on y-axis. These figures show ψ and r^2 decrease as sediment size (d=average of each size class) increases. Also, ψ found to be higher for channel sections with finer d_{50}.

The suspended sediment of Mississippi River consists predominantly of particles finer than 0.06 mm, as opposed to the Missouri and Niobrara Rivers, which contain coarser particles (0.13-0.19 mm). It was found that the Mississippi River (Figures 7.7, 7.8, and 7.11) has higher r^2 between $\overline{C}_x$ and $\overline{C}_y$ than Missouri River.

Figure 7.14 shows strong correlation between the cross-sectional mean concentration and mean concentration on y-axis of Sacramento River at station 37.85. The suspended sediment of the Sacramento River [17] consists of predominantly fine sediment with d_{50} of smaller than 0.06 mm.

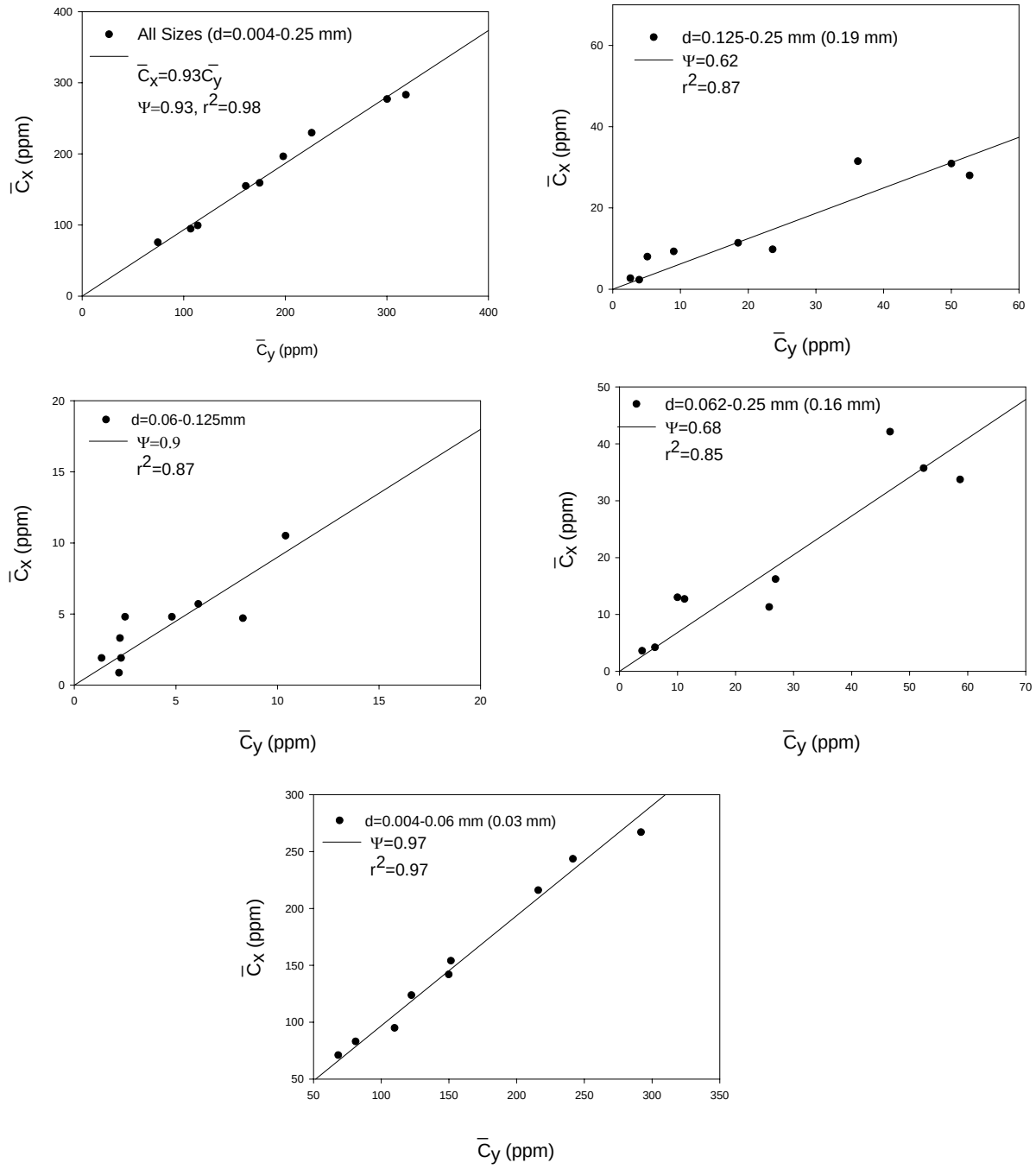

Figure 7-7 Relation between Mean Concentration on y-axis and Cross-sectional Mean Concentration for various sediment diameters, Mississippi River at Range 362.2, 1991 (M=2.67)

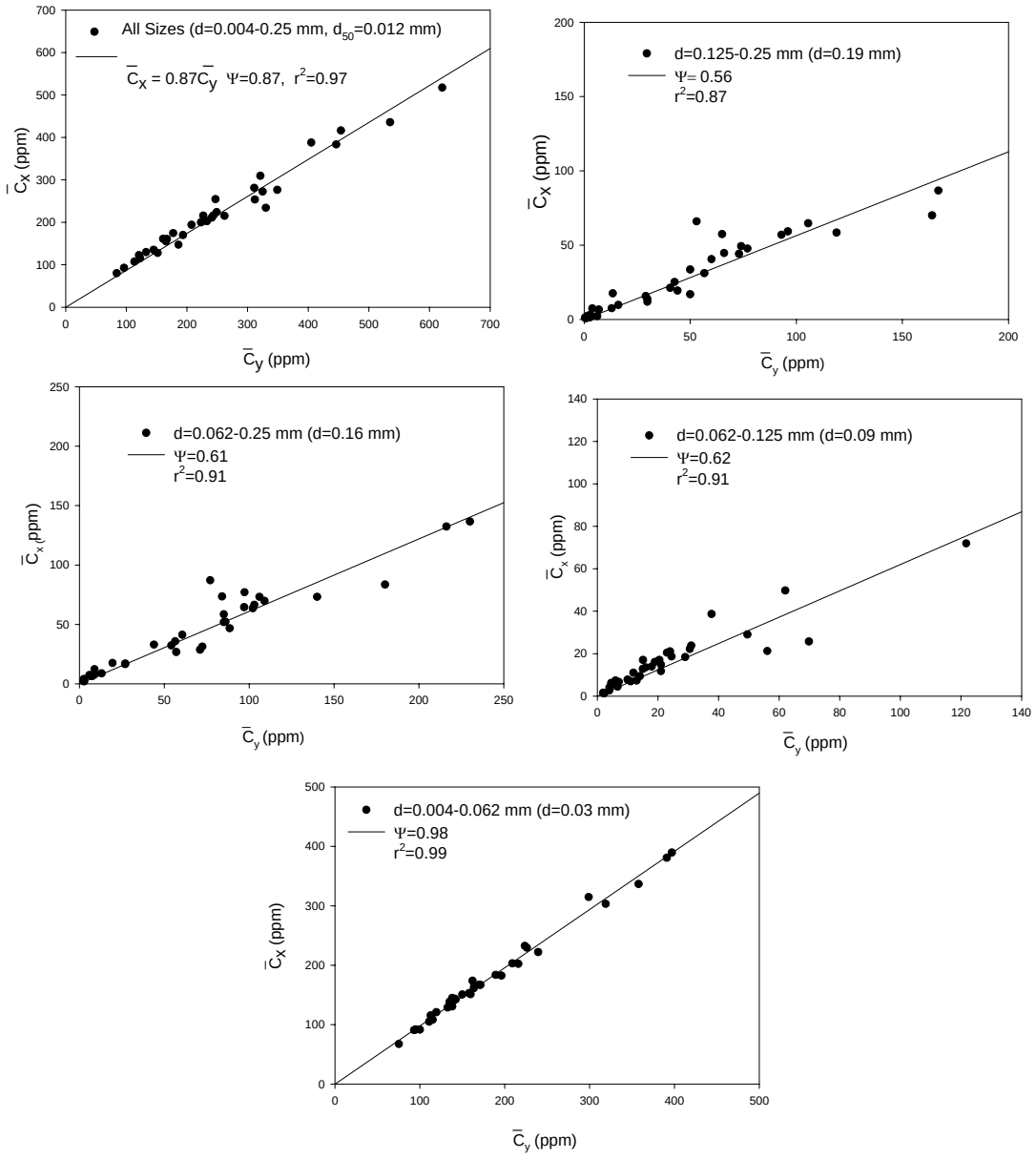

Figure 7-8 Relation between Mean Concentration on y-axis and Cross- sectional Mean Concentration for various sediment diameters, Mississippi River at Tarbert 1995-96 (M=2.65)

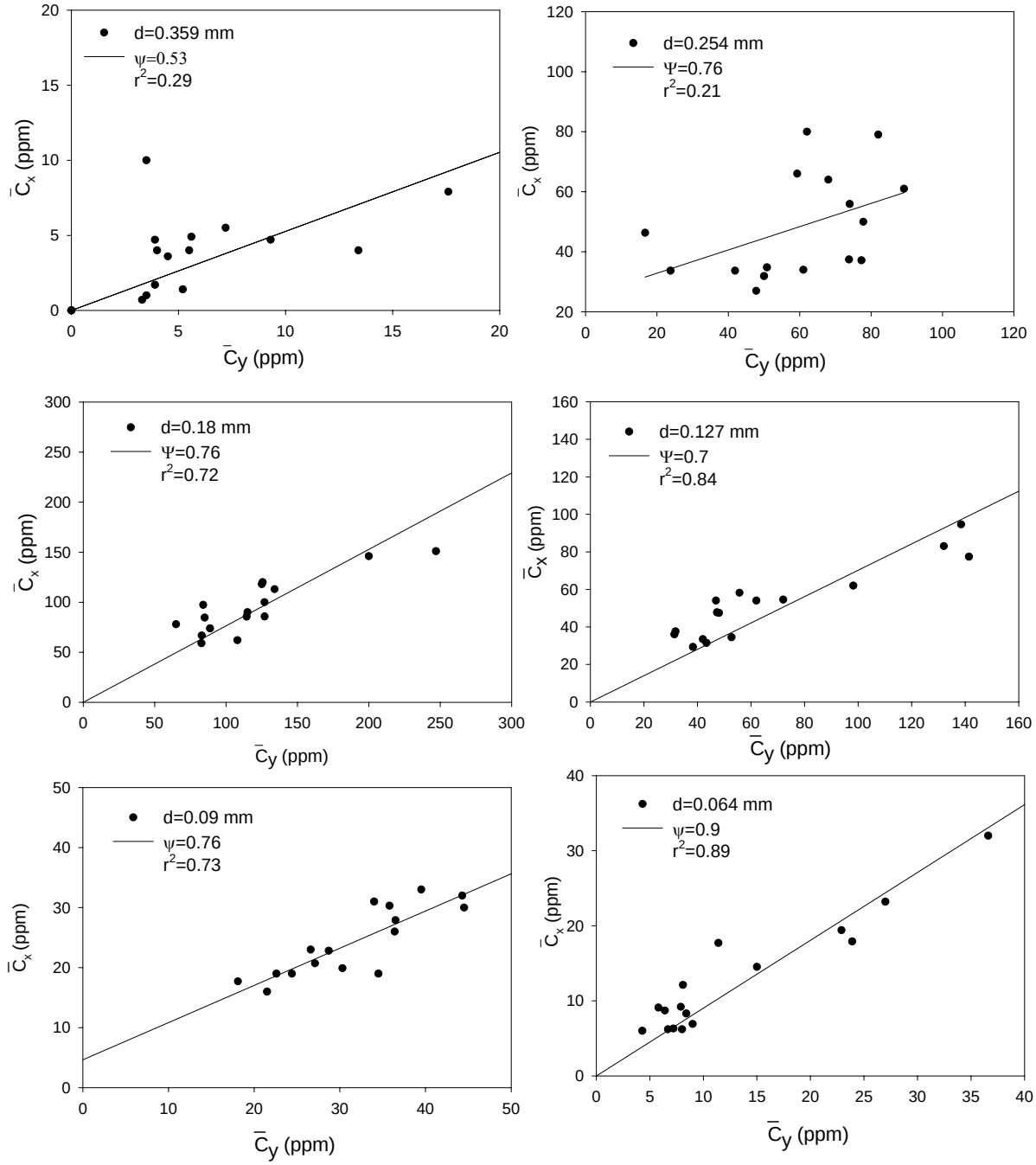

Figure 7-9 Relation between Mean Concentration on y-axis and Cross-sectional Mean Concentration for various Sediment Diameters, Missouri River at Omaha (M=3.22)

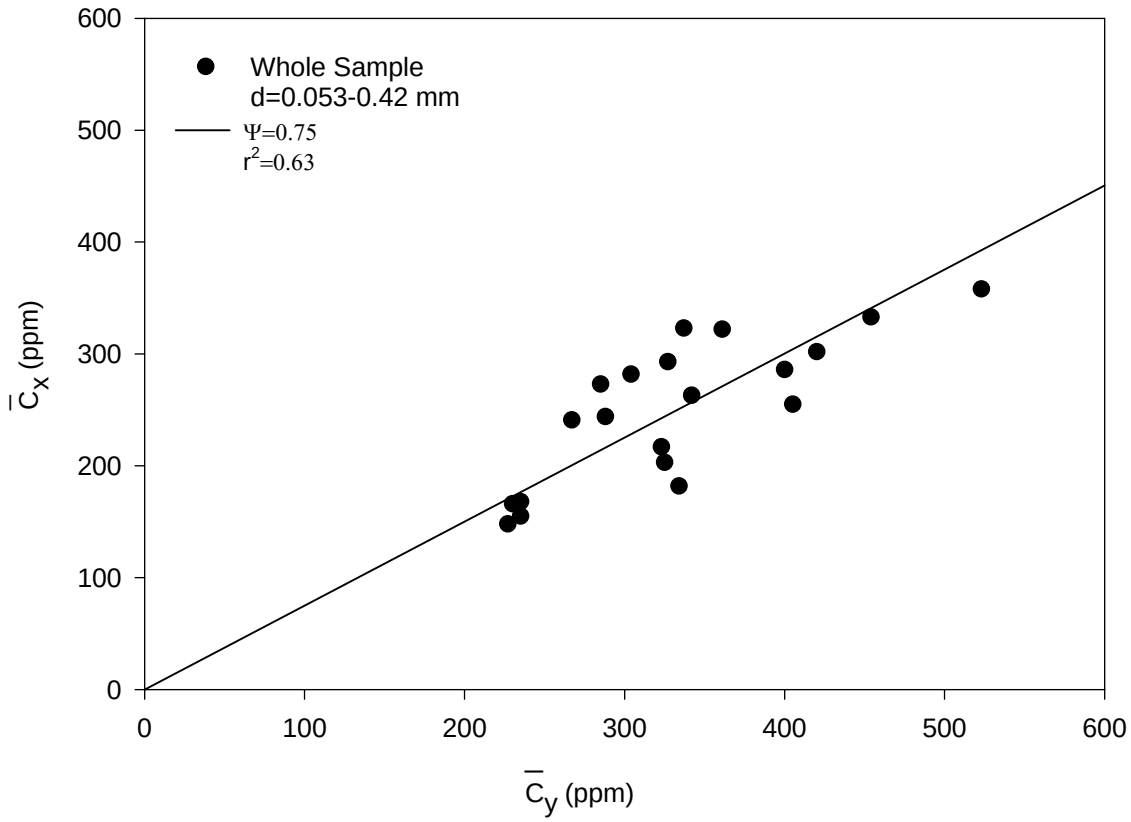

Figure 7-10 Relation between Mean Concentration on y-axis and Cross-sectional Mean Concentration for All Sizes Missouri River at Omaha (M=3.22)

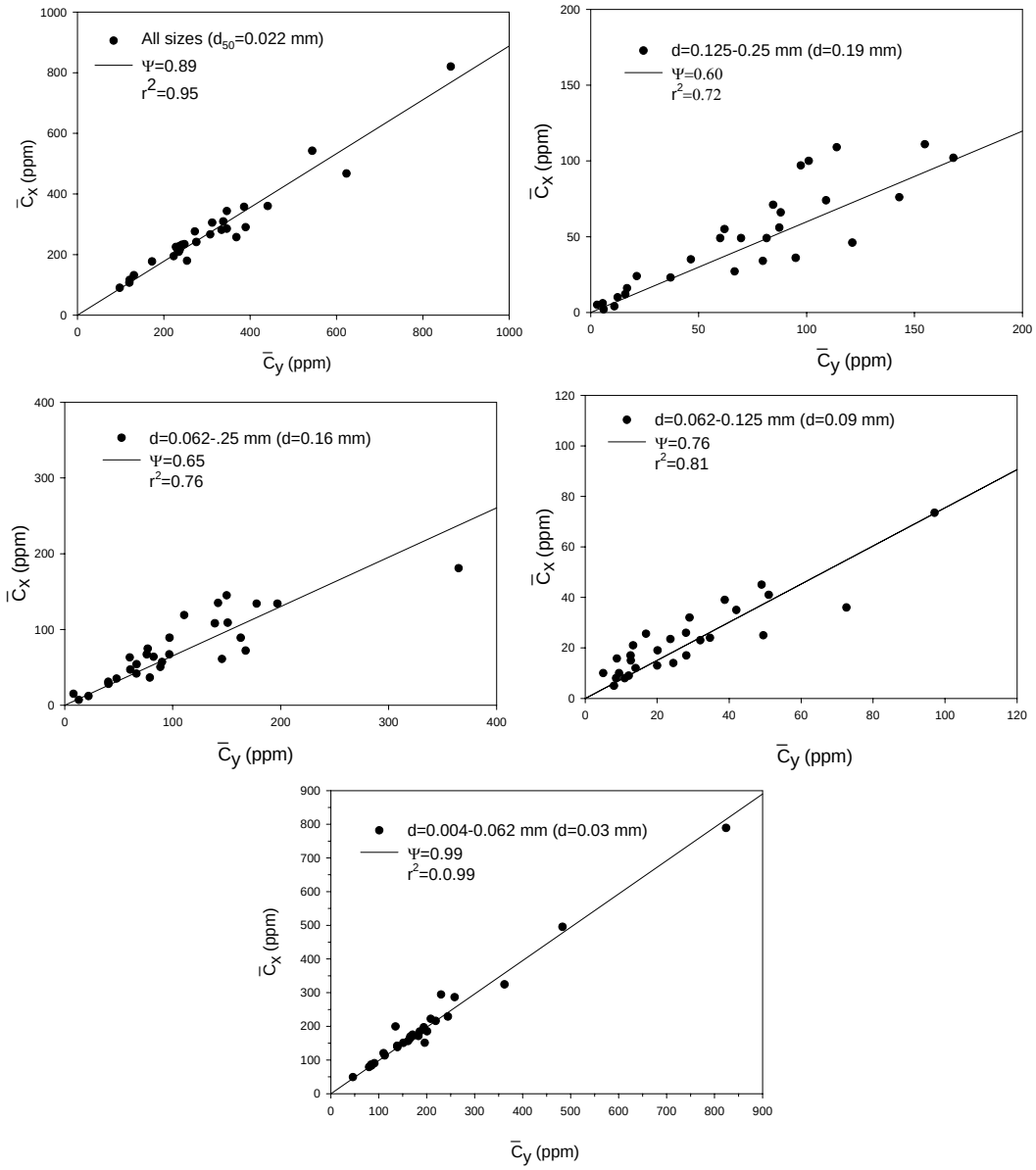

Figure 7-11 Relation between Mean Concentration on y-axis and Cross-sectional Mean Concentration for various Sediment Diameters, Mississippi River at Union Point, 1994, 95 and 96 (M=2.07)

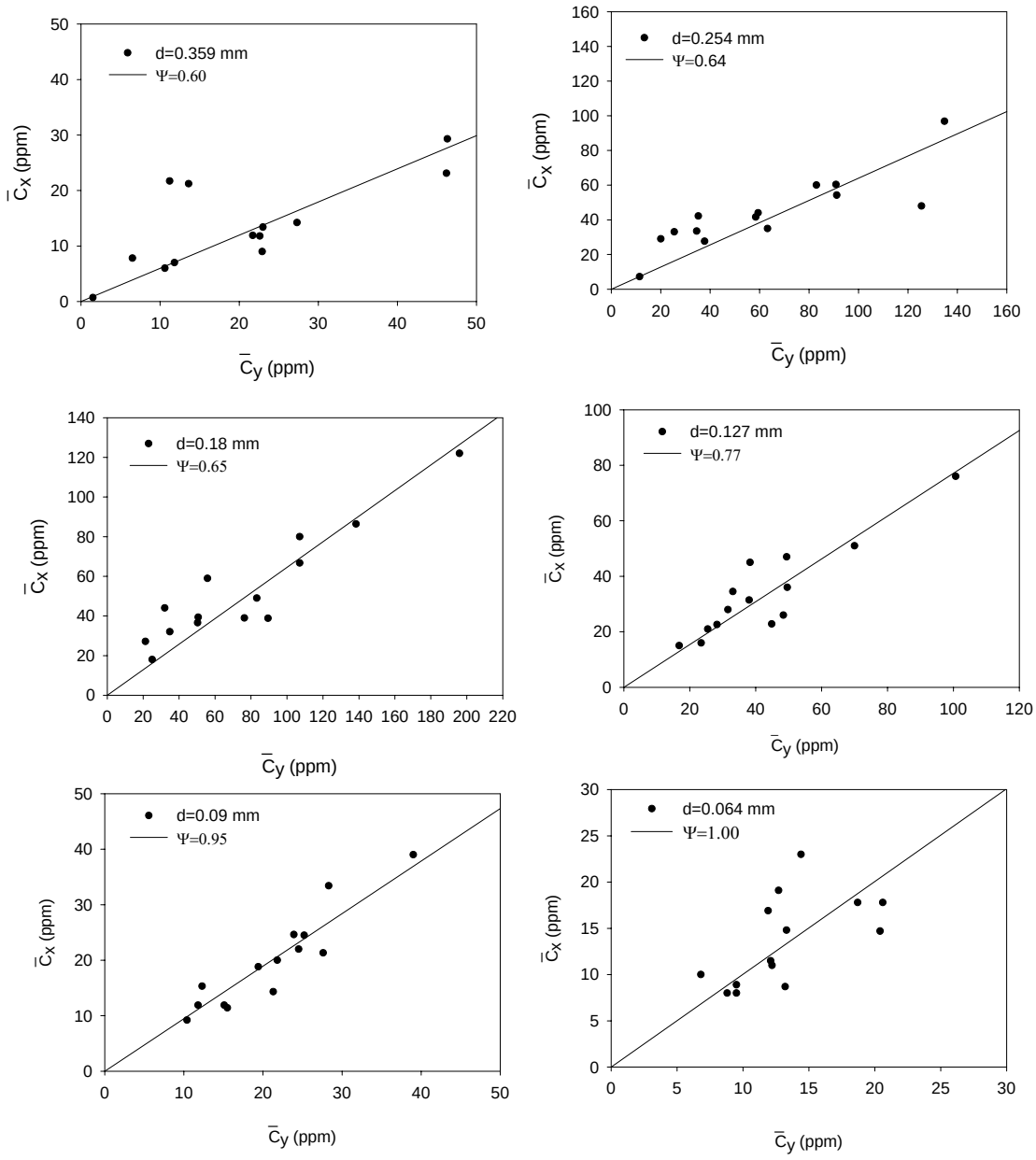

Figure 7-12 Relation between Mean Concentration on y-axis and Cross –sectional Mean Concentration for various Sediment Diameters, Missouri River at Ponca (M=2.89)

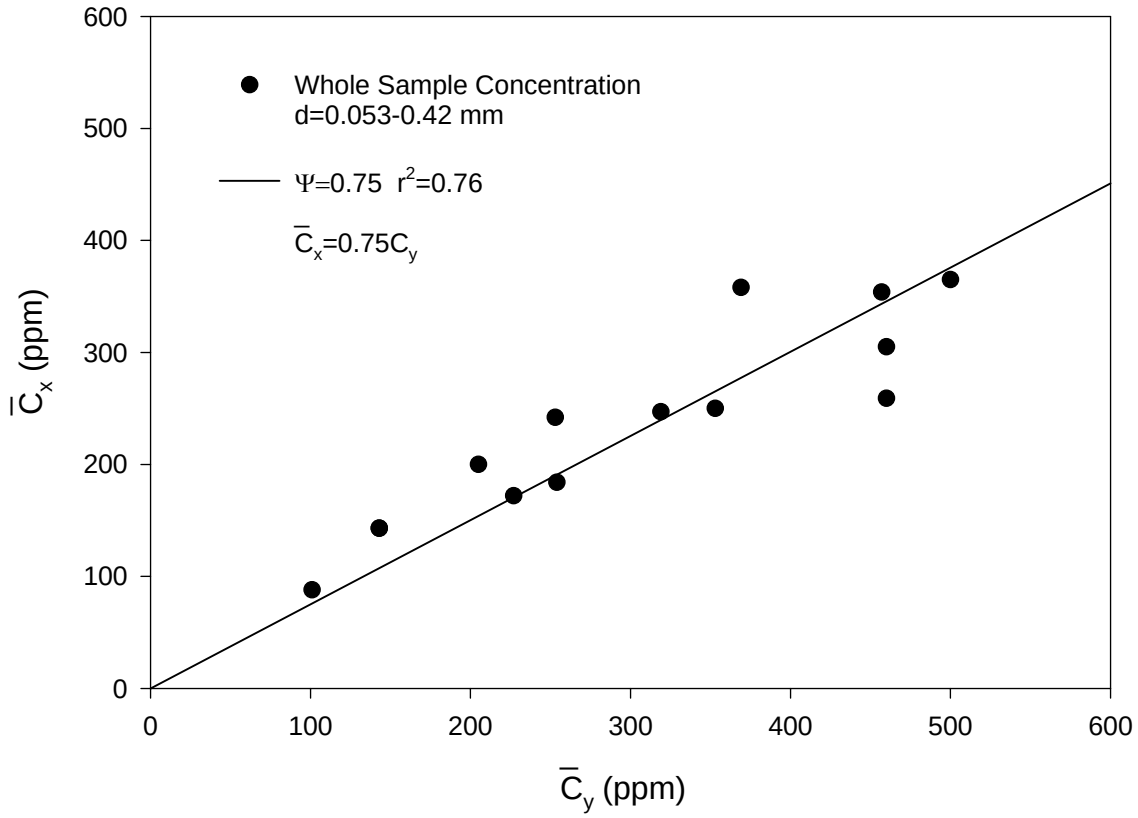

Figure 7-13 Relation between Mean Concentration on y-axis and Cross-sectional Mean Concentration for All Sizes Missouri River at Ponca (M=2.89)

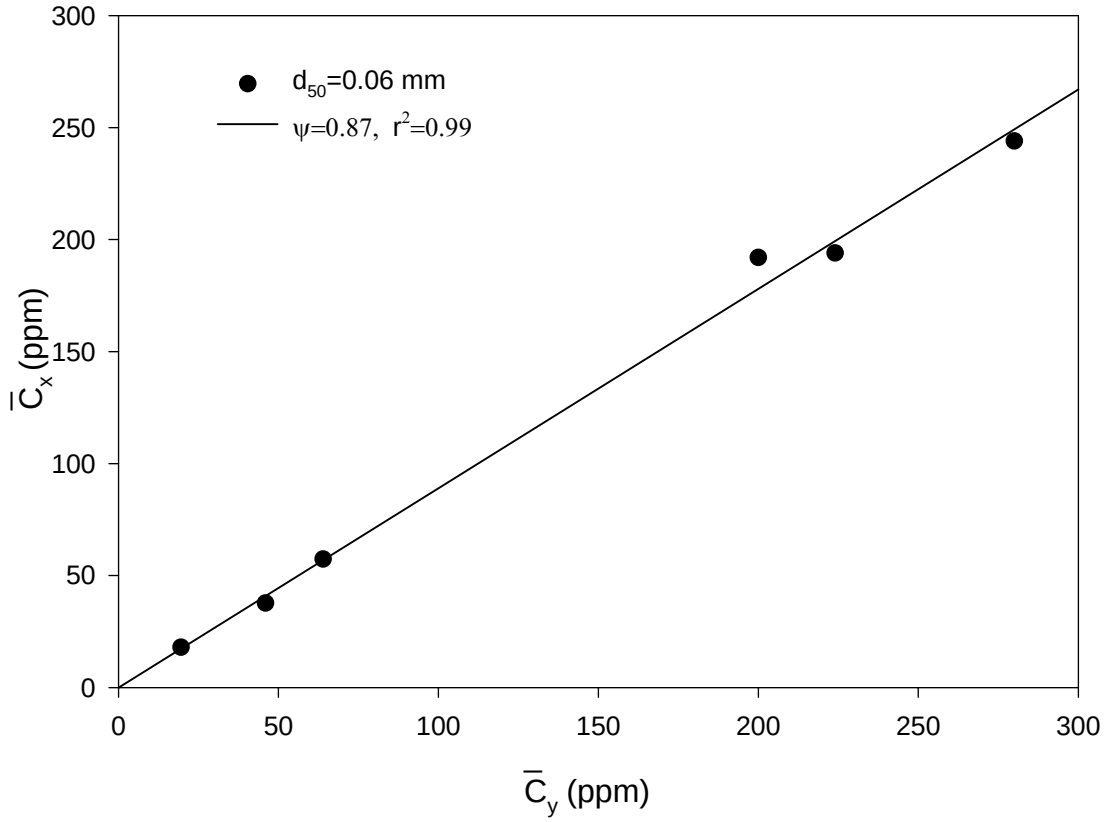

Figure 7-14 Relation between Mean Concentration on y-axis and Cross –sectional Mean Concentration for All Sizes Sacramento River at Station 37.85 (M=1.6)

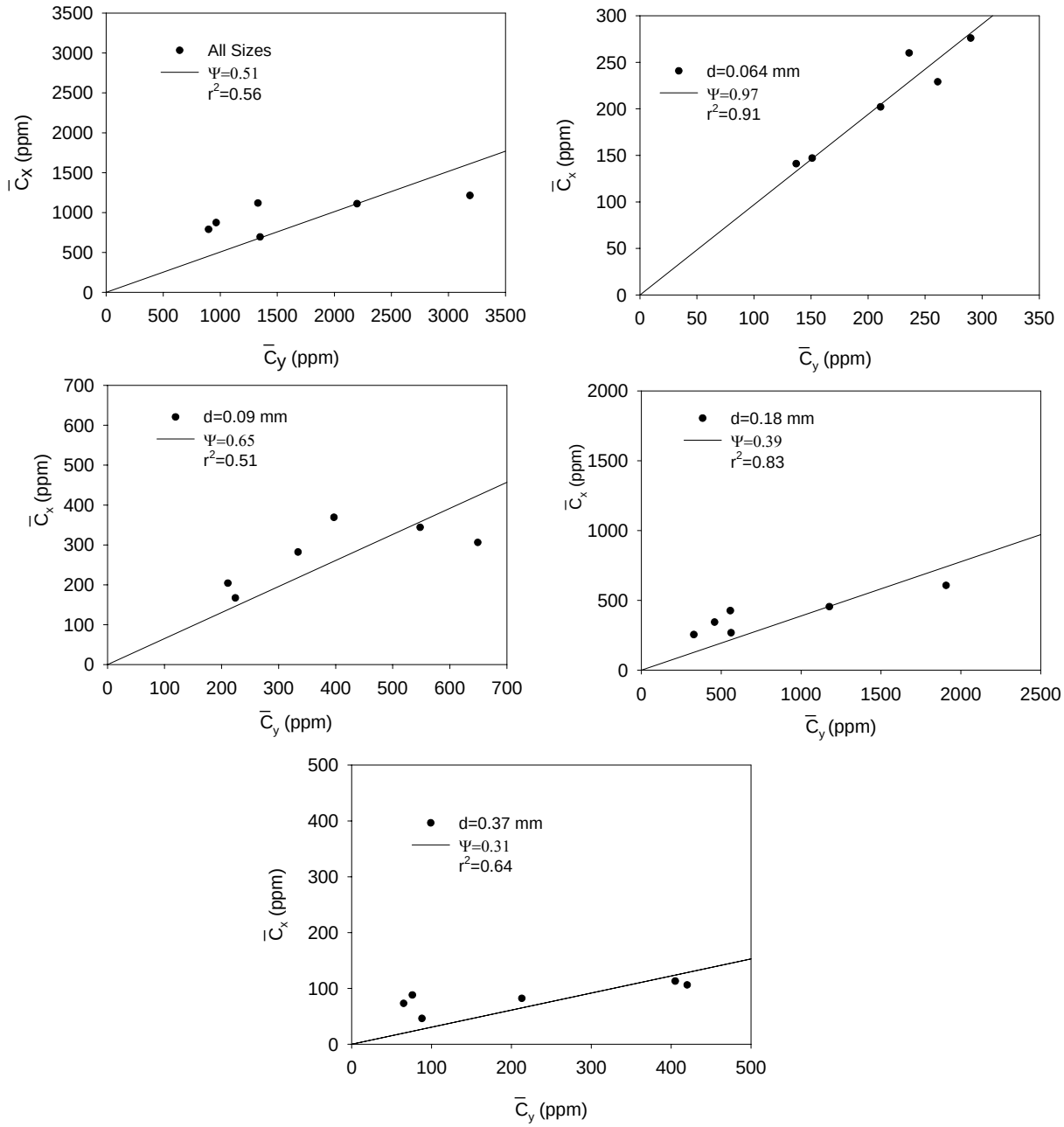

Figure 7-15 Relation between Mean Concentration on y-axis and Cross-sectional Mean Concentration for Various Sediment Diameters, Niobrara River Near Cody at Gaging Station (M=1.73)

7.2.1 Relation of r^2 to Sediment Diameter and Location of Verticals

The coefficient of determination (r^2) of $\overline{C}_x$-$\overline{C}_y$ relation is higher for fine sediment particles (d_{50}<0.062 mm). It means that in these streams, the sediment particles are uniformly distributed, and $\overline{C}_y$ is a good predictor of $\overline{C}_x$. The distribution of sediment concentration in channel sections, with coarse sediment particles (d_{50}>0.062 mm) is not uniform and r^2 is lower.

Figure 7.16 depicts the location of measured verticals relative to y-axis on Mississippi River at Tarbert. Vertical 2 is coincident with y-axis (Figure 4.4). B_j (j=1, 2) = the distance between y-axis and the channel banks, and z_3/B_2 = the ratio of the distance between vertical 3 and y-axis, to the distance between y- axis to the channel bank.

Figures 7.17, 7.19, 7.21, and 7.23 show the relation of r^2 (of ψ) to the sediment diameter on y-axis. These figures show that when sediment diameter increases, r^2 (of ψ) decreases. Figures 7.18, 7.20, 7.22 and 7.24 show the relation of r^2 (of ψ) to the location of each vertical relative to y-axis. These figures show that the correlation between $\overline{C}_x$ and $\overline{C}_y$ is higher on y-axis than other verticals. Also, the verticals closer to y-axis have higher values of r^2.

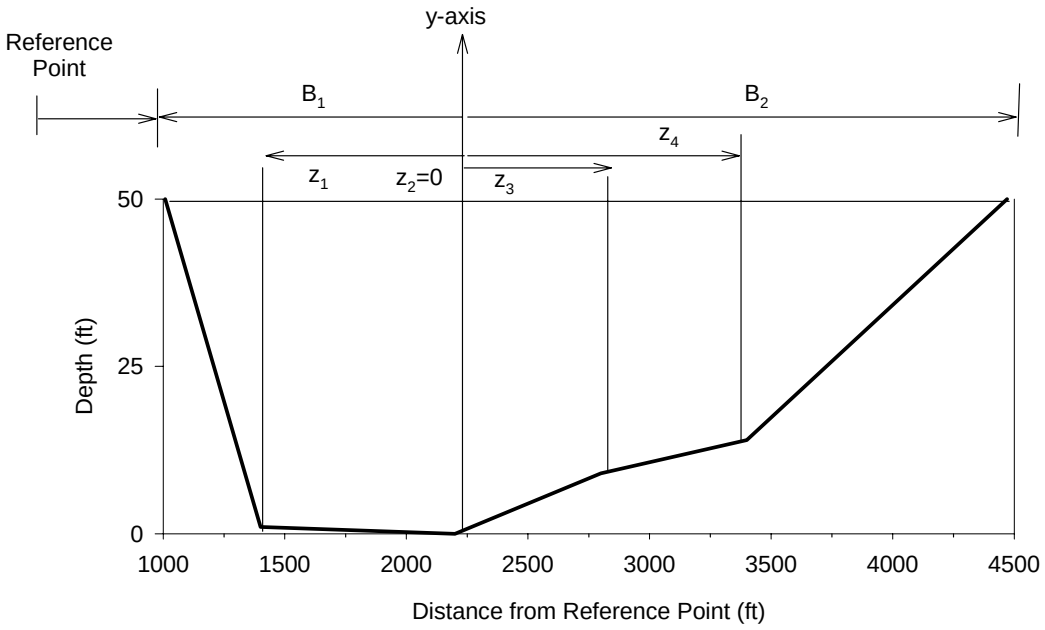

Figure 7-16 Location of Measured Verticals Relative to y-axis, Mississippi River at Tarbert

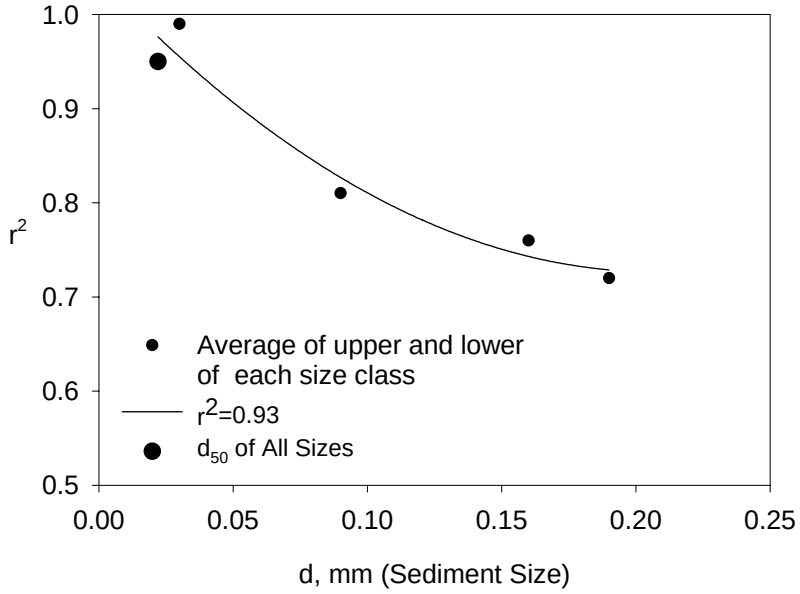

Figure 7-17 Relation of r^2 (of ψ) to Sediment Diameter on y-axis Mississippi River at Union Point, 1994, 95 and 96

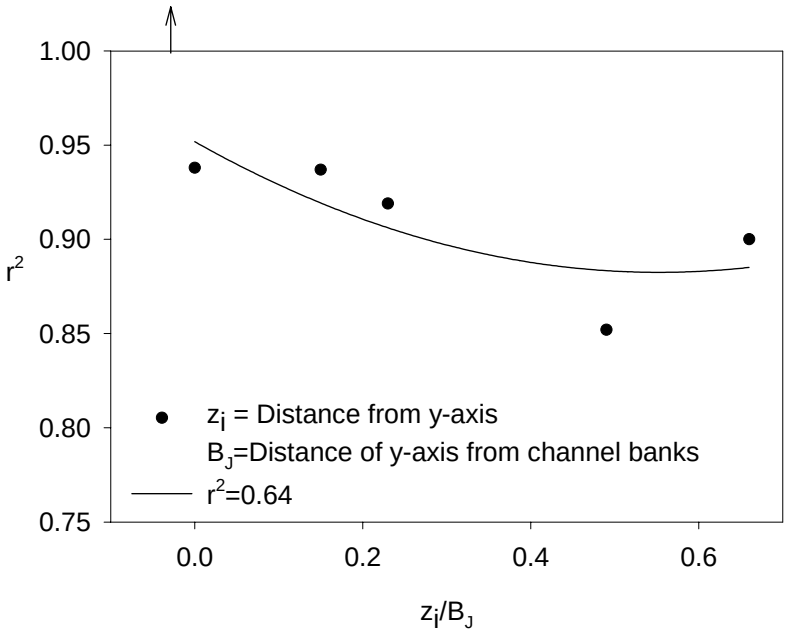

Figure 7-18 Relation of r^2 (of ψ) to the Location of Verticals (Relative to y-axis) Mississippi River at Union Point, 1994, 95 and 96

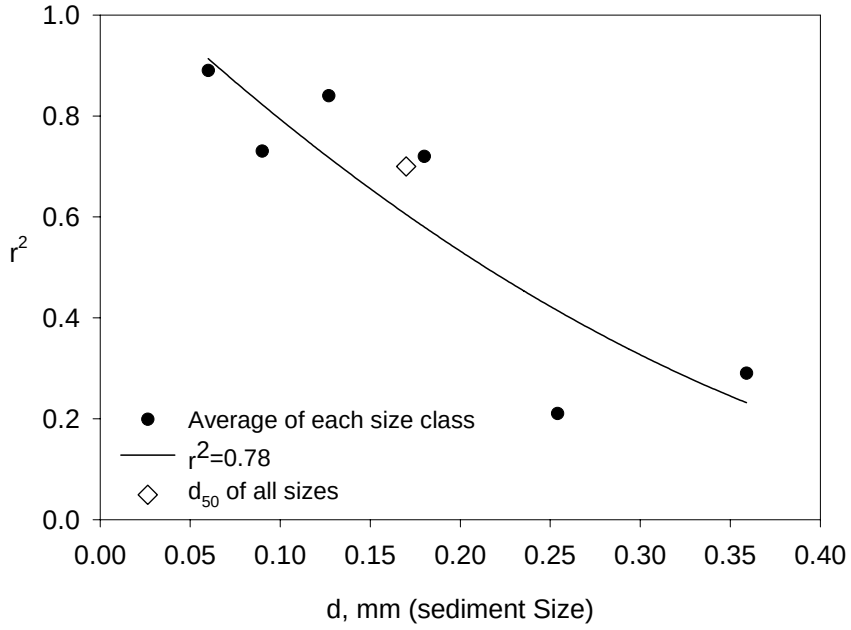

Figure 7-19 Relation of r^2 (of ψ) to Sediment Diameter on y-axis Missouri River at Omaha 1976-81

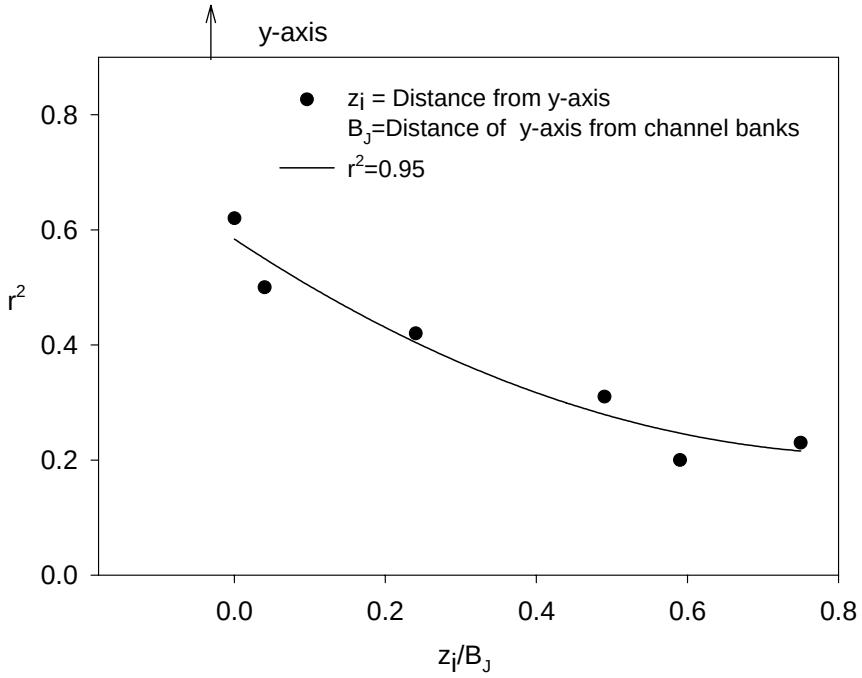

Figure 7-20 Relation of r^2 (of ψ) to the Location of Verticals Missouri River at Omaha 1976-81

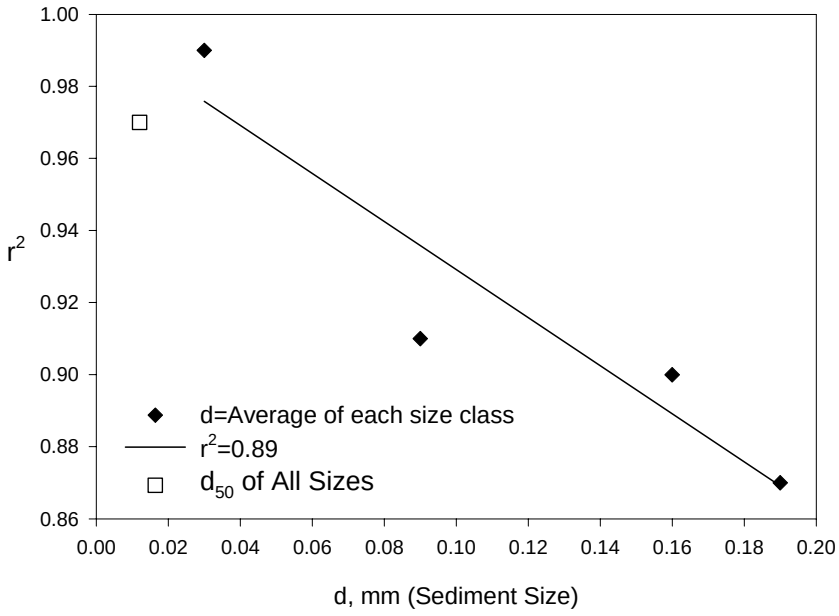

Figure 7-21 Relation of r^2 (of ψ) to Sediment Diameter on y-axis Mississippi River at Tarbert, 1995-96

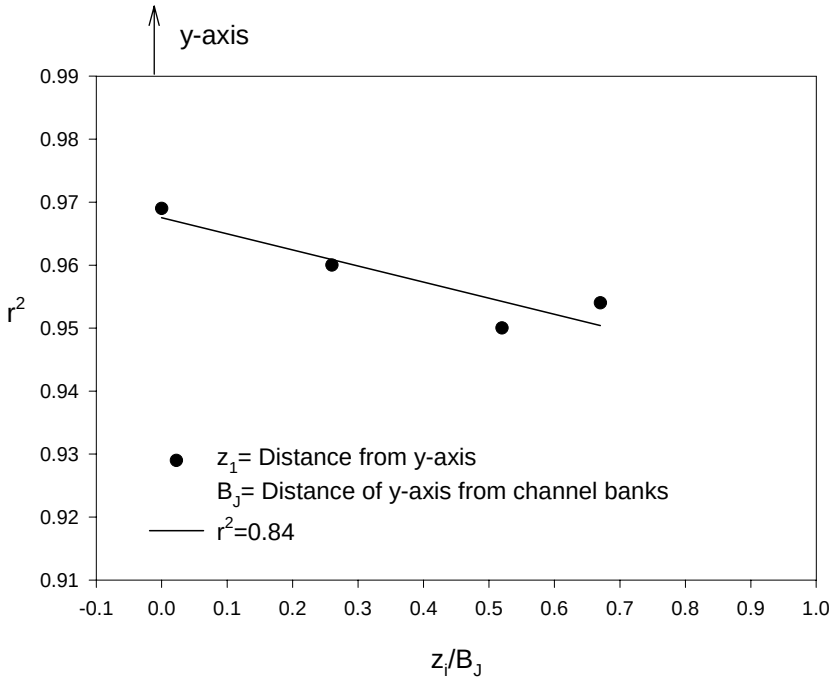

Figure 7-22 Relation of r^2 (of ψ) to Location of Verticals, Mississippi River at Tarbert, 1995-96

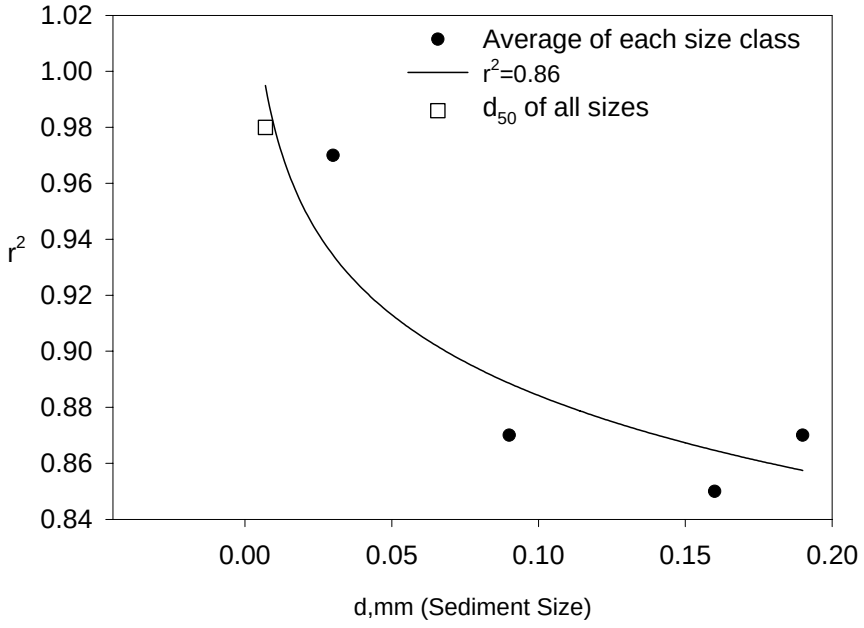

Figure 7-23 Relation of r^2 (of ψ) to Sediment Diameter on y-axis, Mississippi River at Range 362.2, 1991

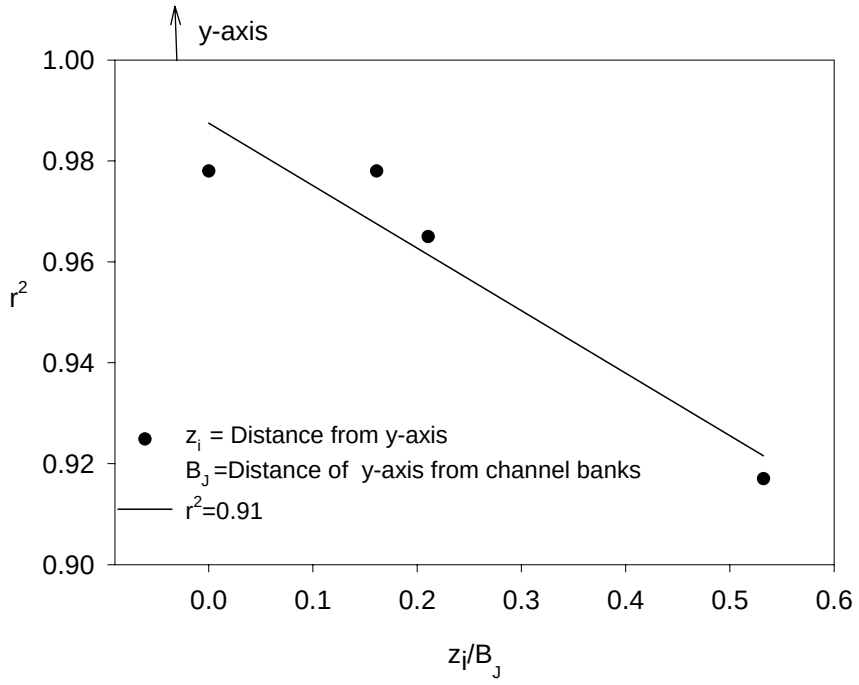

Figure 7-24 Relation of r^2 (of ψ) to Location of Verticals (Relative to y-axis) Mississippi River at Range 362.2, 1991

7.2.2 Relation of ψ to Q and d_{50}

Data analysis on different rivers in this research indicate that ψ is not sensitive to changes in water discharge and $d_{50,}$ but it decreases as sediment diameter (average of each size class) increases at a station. Figures 7.25 to7.29 show that ψ has poor relation with Q and d_{50}. Figure 7.30 shows as sediment diameter (d, not d_{50}) increases for a channel section, ψ and r^2 will decrease. r^2 is defined as the coefficient of determination between cross-sectional mean concentration and mean concentration on y-axis as indicated on Figures 7.7 to 7.15.

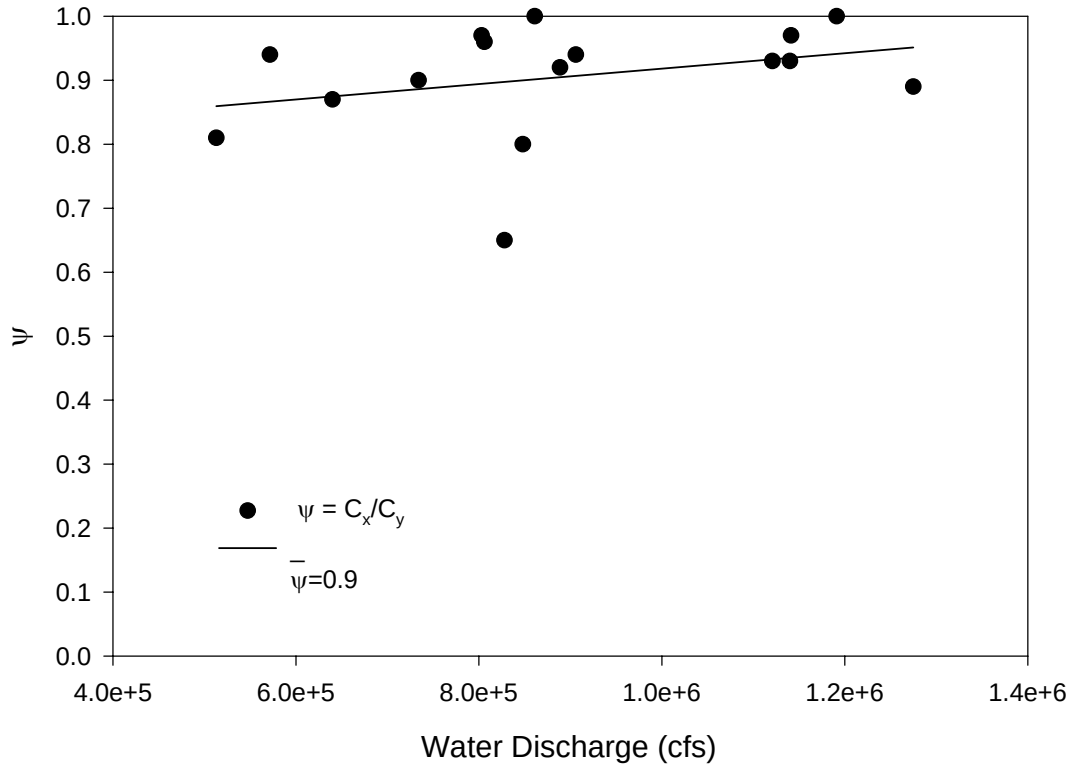

Figure 7-25 Relation between ψ and Discharge, Mississippi River at Union Point, 1995-96

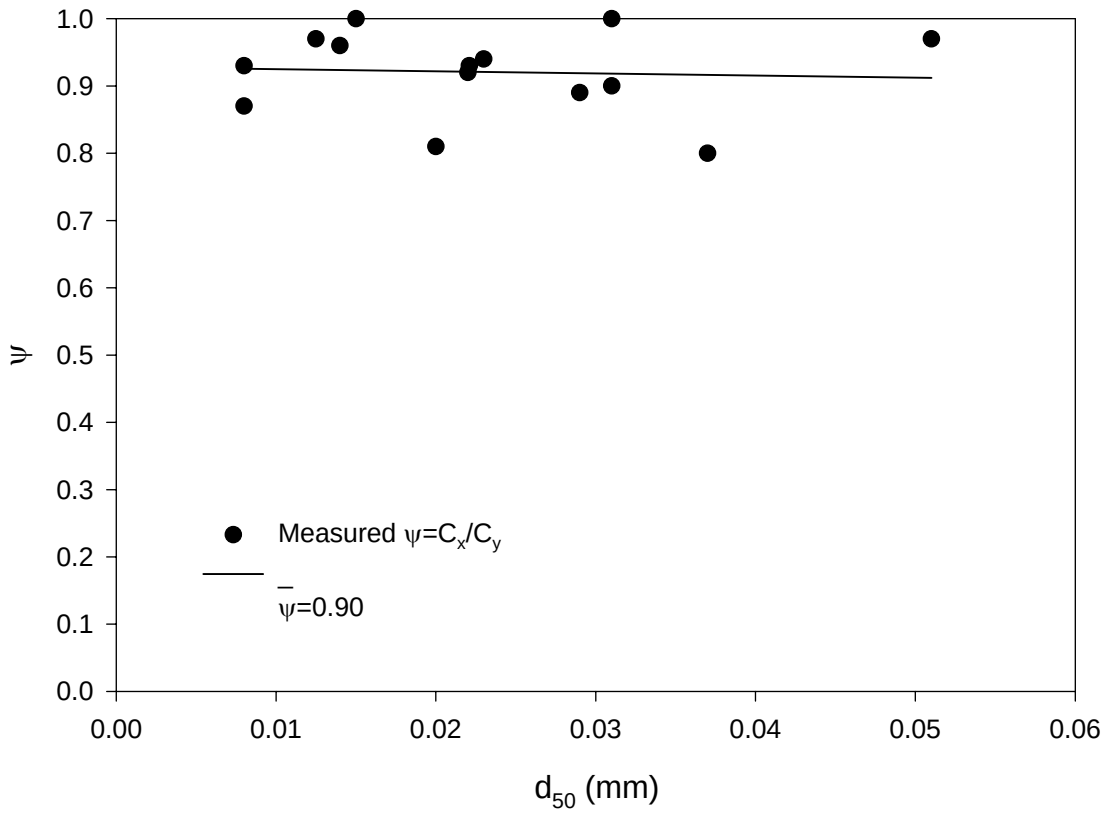

Figure 7-26 Relation between ψ and d_{50} on y-axis, Mississippi River at Union Point, 1995-96

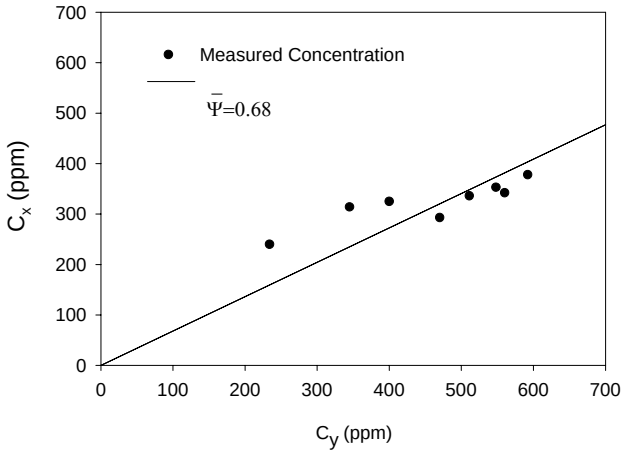

a) Relation Between Mean Cross-sectional Concentration and and Mean Concentration on y-axis

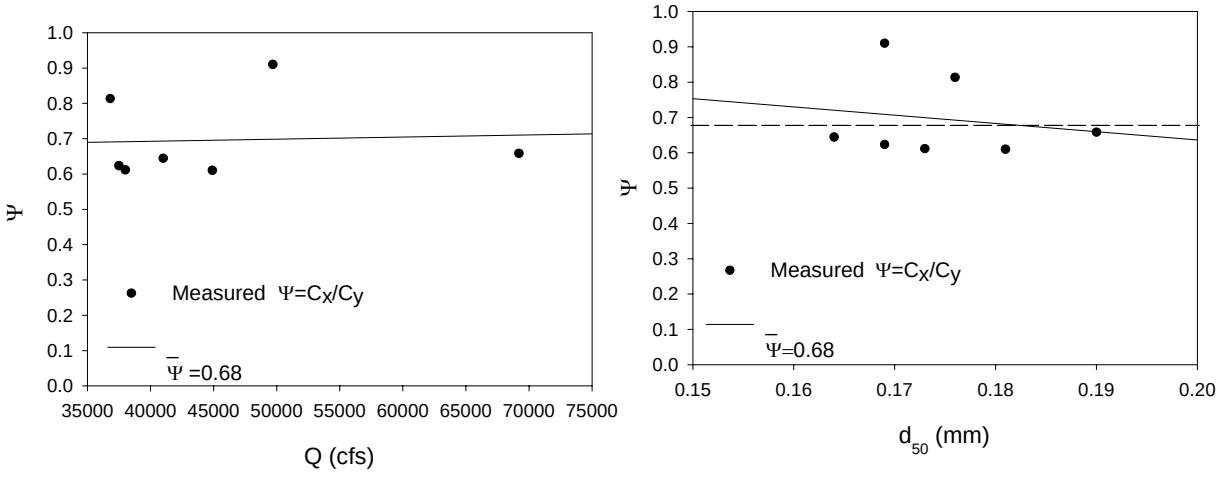

b) Relation Between Ψ and Q

c) Relation Between Ψ and d_{50}

Figure 7-27 Relation of ψ to d_{50} and Discharge, Missouri River at Nebraska City

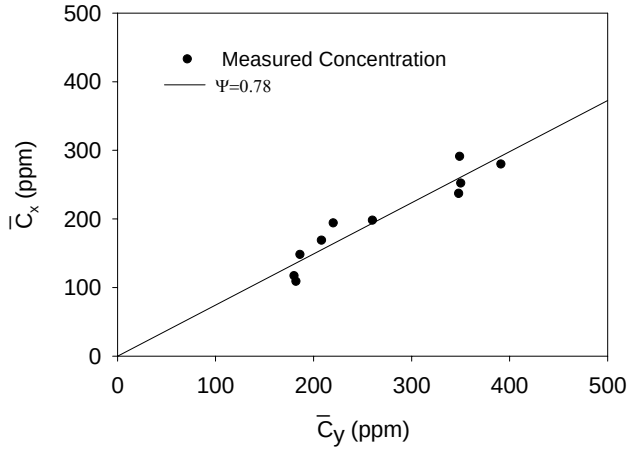

a) Relation Between Cross-Sectional Mean Concentration and Mean Concentrations on y-axis

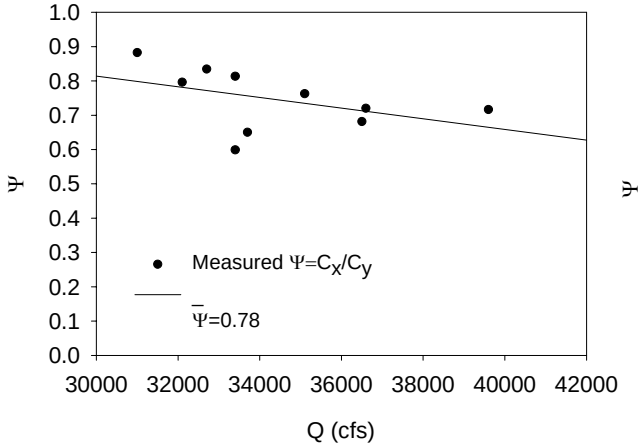

b) Relation Between Ψ and Q

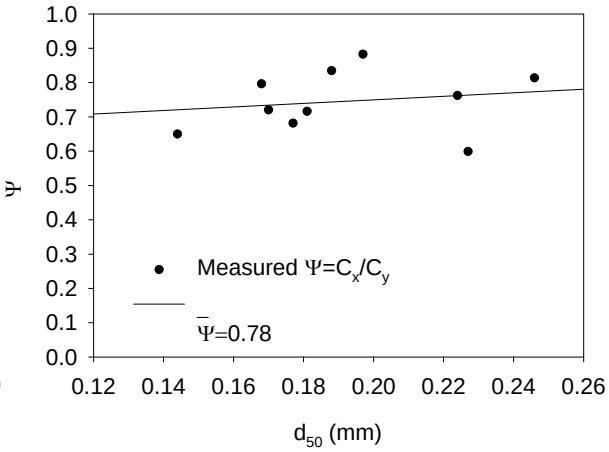

c) Relation Between Ψ and d_{50}

Figure 7-28 Relation of ψ to d_{50} and Discharge, Missouri River at Sioux City

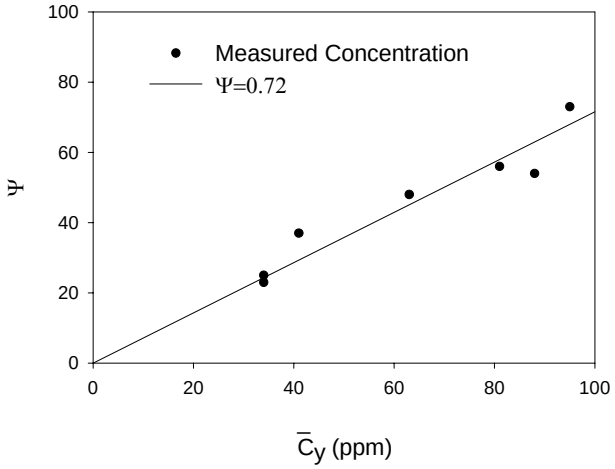

a) Relation Between Cross-sectional Mean Concentration and Mean Concentration on y-axis

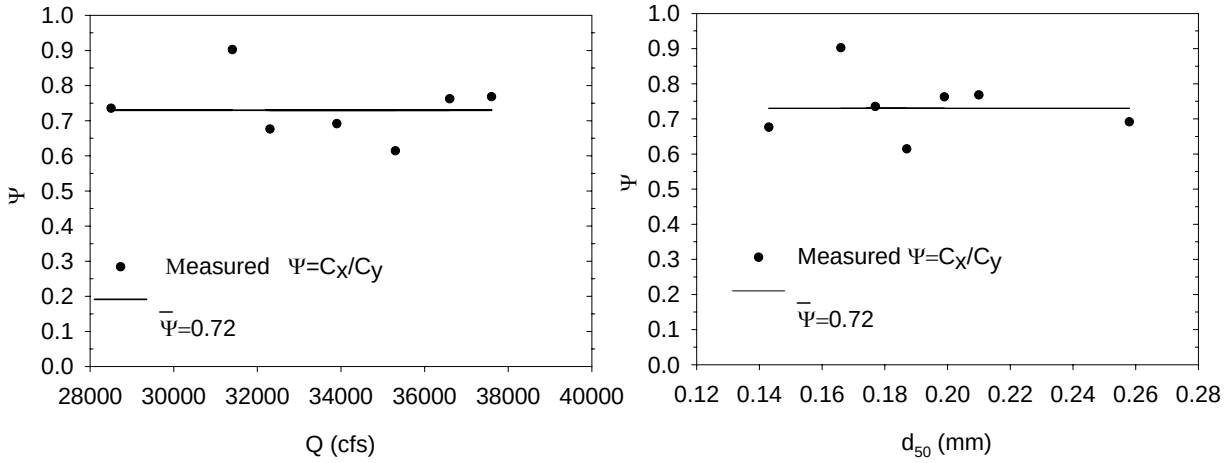

b) Relation Between Ψ and Q

c) Relation Between Ψ and d_{50}

Figure 7-29 Relation of ψ to d_{50} and Discharge, Missouri River at Gayville

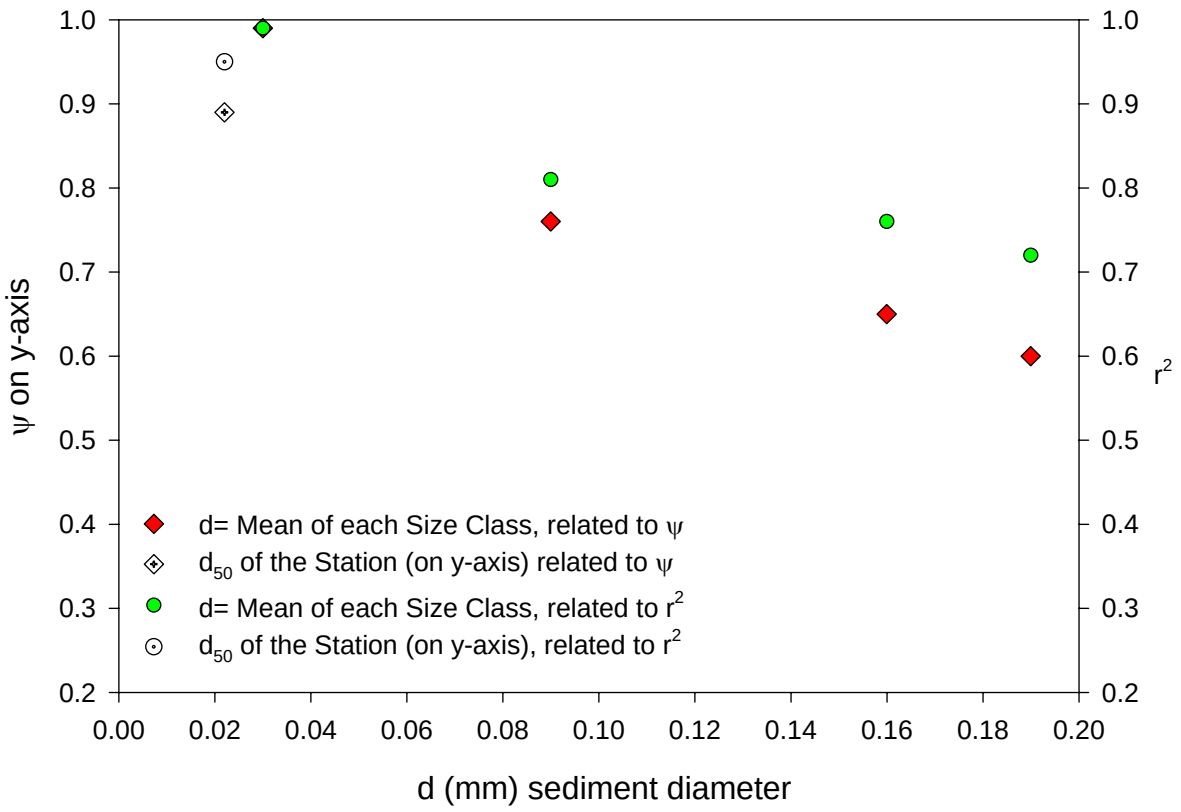

Figure 7-30 Relation of ψ to Sediment Diameter (d) and r^2, Mississippi River at Union Point, 1994-96

7.3 RELATION BETWEEN d_{50} AND WATER DISCHARGE

Hubbell and Matejka[37] found that "On streams such as the Middle Loup River, where sediment is relatively coarse and unlimited in supply and where the size distribution is evidently unrelated to water discharge and water temperature, the most representative size distribution can probably be determined from an average of all available samples." Also, they showed that d_{50} and water discharge do not have direct relation.

Kircher[26] investigated the relation between d_{50} and water discharge for Platte River in Nebraska and found that the median diameter decreases somewhat with discharge at Overton, but no trend is detected at Grand Island.

Colby and Hembree[29] indicated in their report on Niobrara River, that no relationships have been clearly defined for Niobrara River between water discharge and bed-material sizes. They also reported that at this station suspended sediment tend to become smaller at high flows.

To study the relationship between discharge (Q) and d_{50}, data sets on different rivers were analyzed as part of this research. Consequently, plots of Q against d_{50} on y- axis for different rivers did not reveal any trend, although poor relations for some datasets were found. Figures 7.31 to 7.35 show poor relations between Q and d_{50} on y-axis for various rivers.

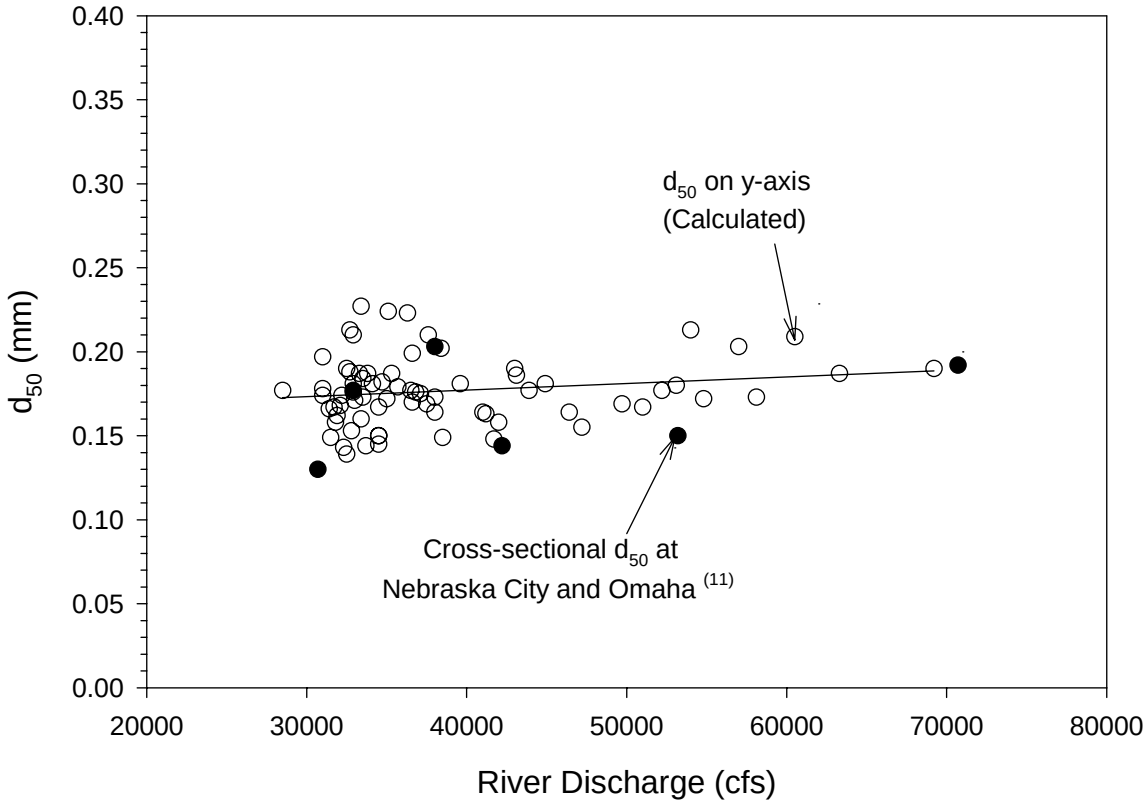

Figure 7-31 Relation between Discharge and d_{50} on y-axis, Missouri River at Ponca, Nebraska City, Omaha, Gayville and Sioux City

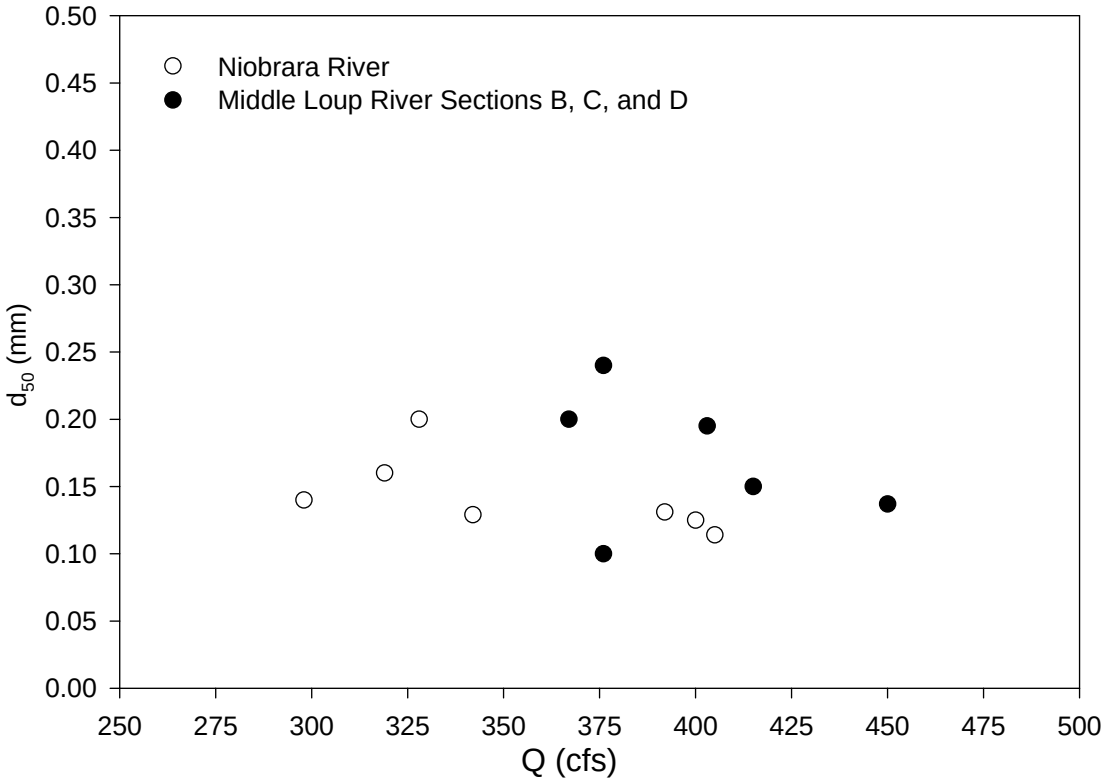

Figure 7-32 Relation between Discharge and d_{50} at y-axis, Niobrara River at Gaging Station (1950-52) and Middle Loup River (1948-60)

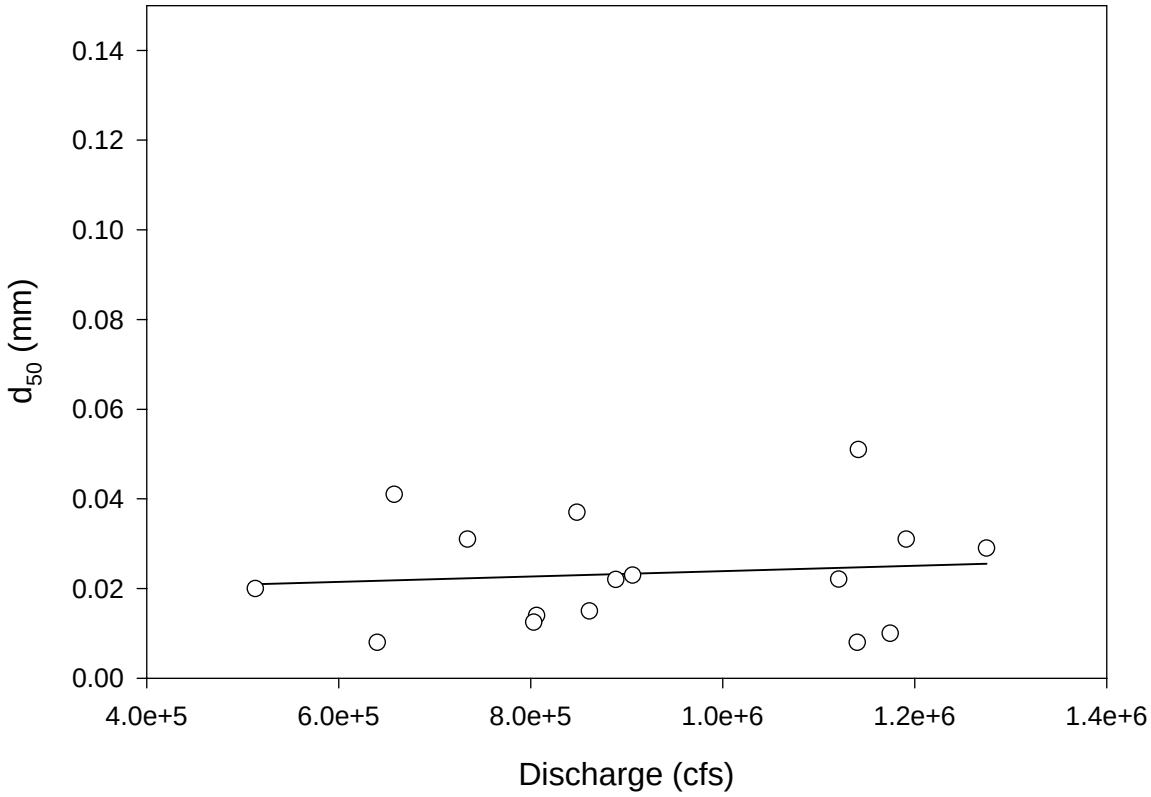

Figure 7-33 Relation between Discharge and d_{50} on y-axis and Discharge, Mississippi River at Union Point, 1995-96

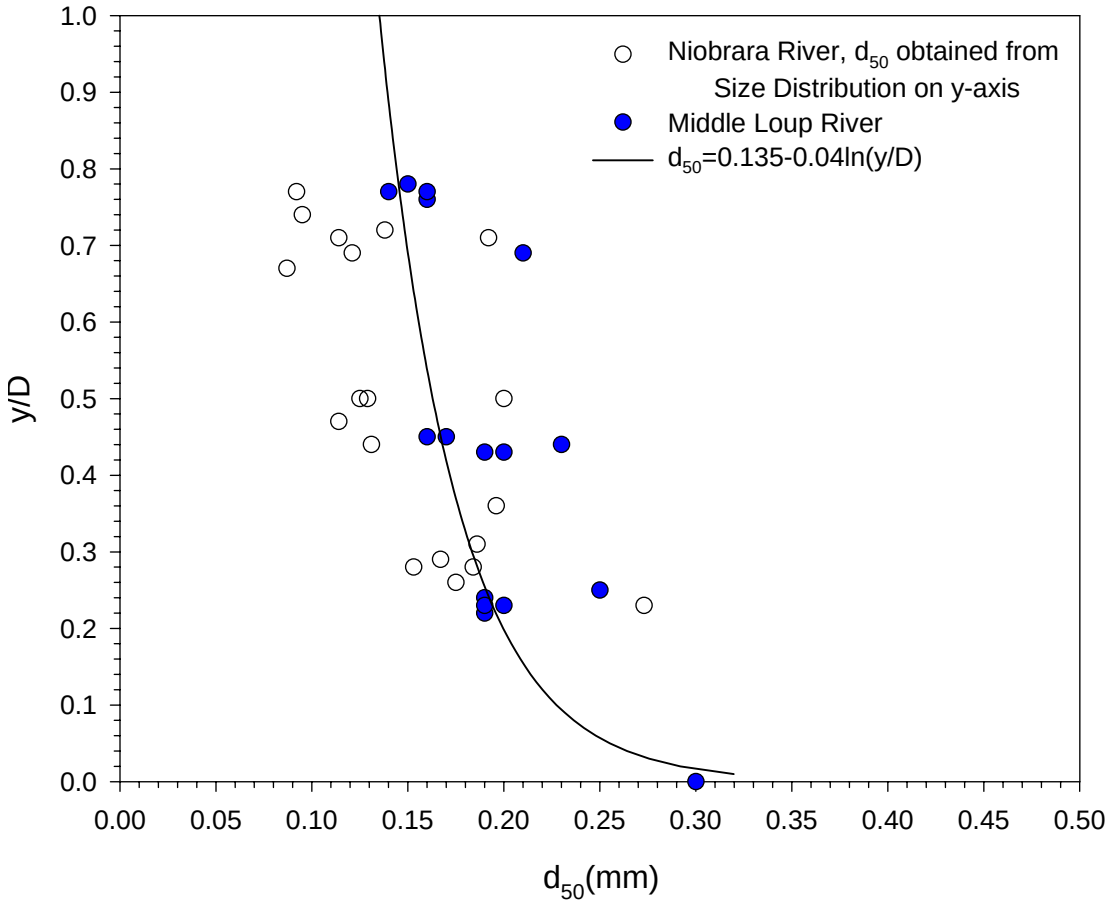

Figure 7-34 Relation between d_{50} and y/D, Niobrara River near Cody 3/3/1950-5/8/52 (Q=302–405 cfs); and Middle Loup River Section B at Dunning, 6/20/1950 (Q= 403 cfs)

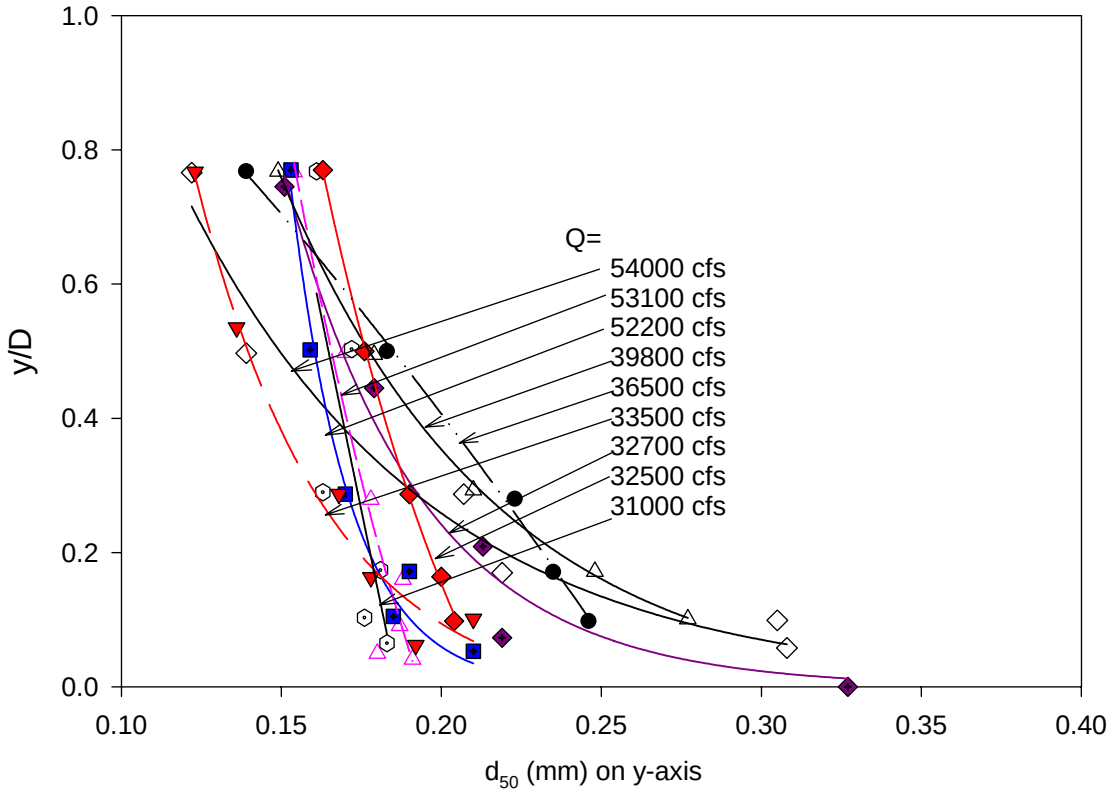

Figure 7-35 Relation between Discharge and d_{50} along y-axis, Missouri River at Ponca, 1977-81

7.4 MEAN SEDIMENT CONCENTRATION ON Y-AXIS USING CHIU'S EQUATION[2]

Method 1

Depth-averaged concentration (mean spatial concentration [35]) on y-axis is defined by:

$$\overline{C}_y = \frac{1}{D} C_0 \int_0^D C(y)dy \qquad (7\text{-}1)$$

Chiu's [2] equations are used in Equation (7-1). The depth-weighted mean concentration is generally higher than the velocity-weighted concentrations for the rivers analized in this research.

Method 2

The velocity-weighted, mean sediment concentration at y-axis for h>0 (maximum velocity below water surface):

$$\overline{C}_y = \frac{\int_0^D \left[\frac{u_{\max}}{M} \ln\left[1 + \left(e^M - 1\right) \frac{y}{D-h} e^{\left(1 - \frac{y}{D-h}\right)} \right] \right] C_0 e^{-\lambda' I(y)} dy}{\int_0^D \frac{u_{\max}}{M} \ln\left[1 + \left(e^M - 1\right) \frac{y}{D-h} e^{\left(1 - \frac{y}{D-h}\right)} \right] dy} \qquad (7\text{-}2)$$

Figure 7.36 shows calculated depth-averaged concentration is higher than the velocity-weighted concentration for Missouri River at Nebraska City and Sioux City. The same results were obtained for other river sections.

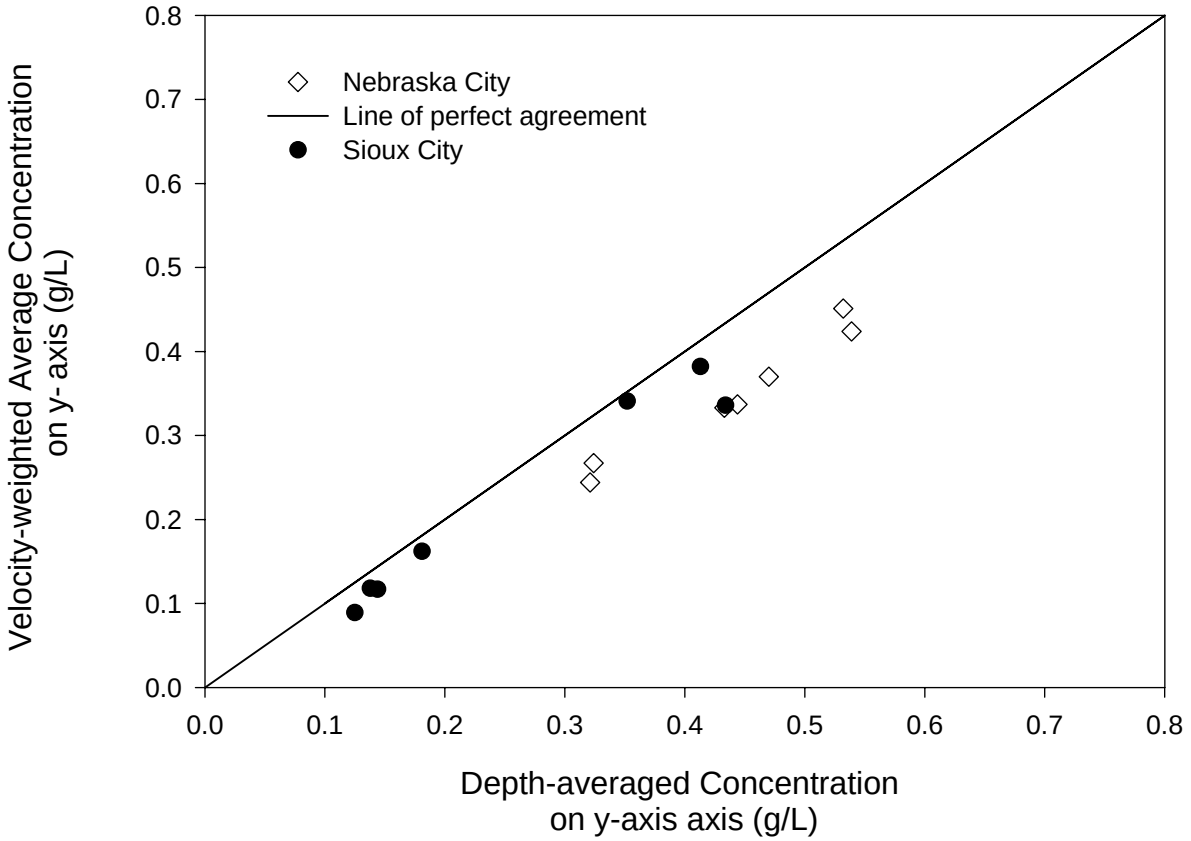

Figure 7-36 Comparison of Depth- and Velocity-weighted concentration, Missouri River

7.5 RELATION BETWEEN θ AND d_{50}

This research has improved the regression relationship between θ and d_{50} by analyzing a large number of sediment data on various rivers during different flow events. To establish the relation, first λ' is estimated by applying Chiu's sediment equations to multi-point sediment data on y-axis.

Then λ is calculated from the equation

$$\lambda' = \lambda \frac{1 - e^{-M}}{M\phi} \tag{6-15}$$

For each dataset, θ is calculated from

$$\theta = \lambda \frac{6(e^{M} - 1)}{\phi M (2 + e^{M})} \tag{6-17}$$

As part of this research, different d_{50} on y-axis of various rivers were calculated from particle size distribution related to different flow events. Also, different θ were calculated using above equations and the following regression relationship was determined Fig 7.37.

$$\theta = 22.54(d_{50} + 0.023)^{1.26} \tag{7-3}$$

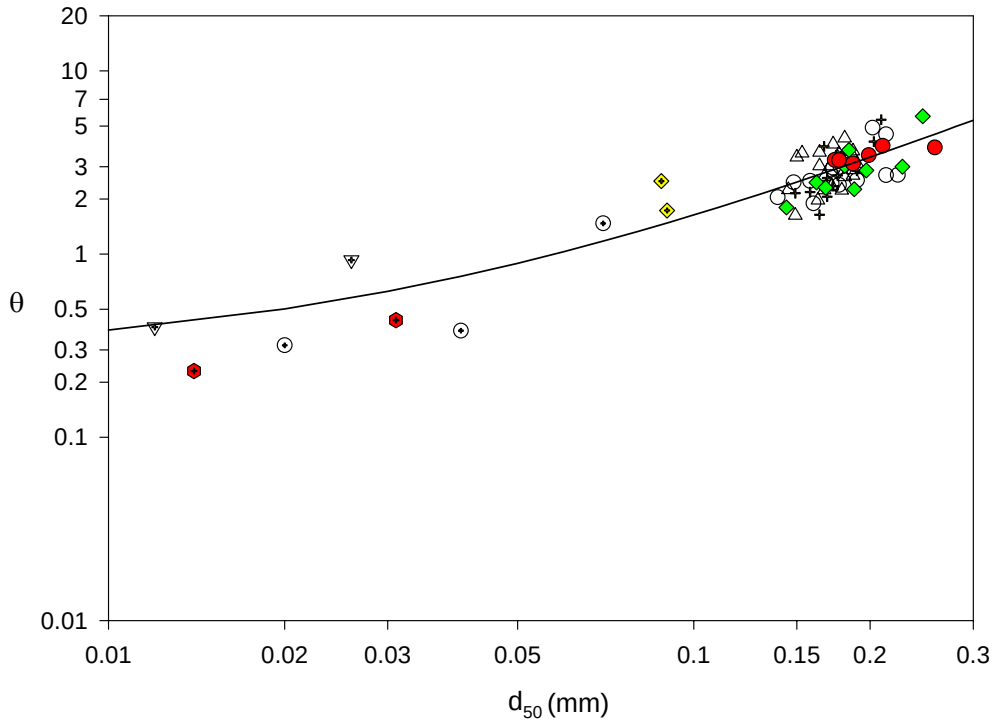

△ Missouri River at Omaha
10/6/1976 to 10/14/81, Q=31500 to 63300 cfs

○ Missouri River at Ponca
4/28/1977 to 7/23/81, Q=29800 to 54000 cfs

\+ Missouri River Nebraska city
10/5/1976 to 10/9/79, Q=36800 to 69200 cfs

◇ Missouri River at Sioux City
10/7/1976 to 10/15/1981, Q=31000 to 39600 cfs

⊙ Sacramento River, River Mile 35.64
3/19/1979, 2/29/1980; and RM 37.85, 1/19/79, Q=16800 to 76200 cfs

◈ Rio Grand Conveyance Channel
Sections 2243+62, and 2249+93, 12/21/1965, Q=1860 cfs

⬢ Mississippi River at Union Point
3/28/1995, Q=806,000 cfs, and 6/6/1995 Q=1,191,000 cfs

▽ Mississippi River at Tarbert
2/9/1995, Q=651,000 cfs and 12/30/96, Q=829,000 cfs

● Missouri River at Gayville
4/22/1980 to 7/21/1981, Q=28500 to 37600 cfs

—— $r^2=0.8,\ \theta=22.54(d_{50}+0.023)^{1.26}$

Figure 7-37 Relation between θ and d_{50} on y-axis

7.6 COMPUTATION STEPS FOR DETERMINING LOCATION OF MEAN SEDIMENT CONCENTRATION ON Y-AXIS

For a channel section with known M and median sediment size (d_{50}) on y-axis the location of mean concentration on y-axis ($\bar{y}_c$) is computed as follows:

h/D is a function of M and is calculated by using the following equations (Chiu and Tung) [7]:

$$\frac{h}{D} = -0.2 \ln \frac{j(M)}{58.3} \tag{4.31}$$

$$j(M) = \frac{e^M - 1}{M\phi} \tag{4.32}$$

$$\phi = \frac{e^M}{e^M - 1} - \frac{1}{M} \tag{4-24}$$

$$\lambda = G'(M)\theta \text{, and } G'(M) = \frac{\phi M(2 + e^M)}{6(e^M - 1)} \tag{6-17}$$

Figure 7.37 yields

$$\theta = 22.54(d_{50} + 0.023)^{1.26} \tag{7-3}$$

λ can be obtained from either Equations (4-24), (6-17) and (7-3) or Figure 7.38.

Figure 7.38 gives the relation between λ and d_{50} for different M values. It can be used to obtain λ in a channel section with known values of M and d_{50}.

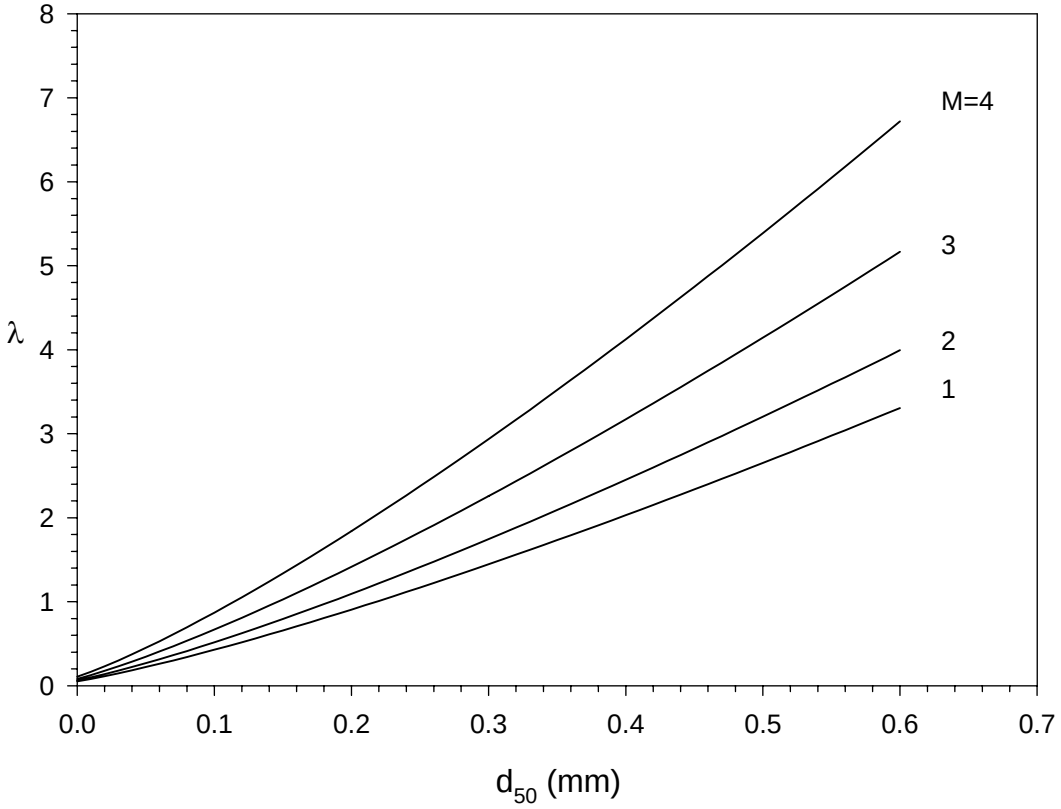

Figure 7-38 Relation between λ and d_{50}

For M=1.0 -5.6 and h/D>0, maximum velocity [28] is below water surface, Chiu's sediment transport equation is:

$$\frac{C}{C_0} = \exp\left[-\lambda' I(\frac{y}{D}, \frac{h}{D}, M)\right] \tag{6-21}$$

where λ' = Chiu's sediment distribution parameter and is a function of M and λ

$$\lambda' = \lambda \frac{1-e^{-M}}{M\phi} \tag{6-15}$$

Equations (4-11), (6-18), (6-22) and (6-23) can be written for y/D

$$I(\frac{y}{D}) = \frac{e^M}{\xi_{\max}} \int_0^1 h_\xi^{-1} \left[1 + (e^M - 1) \frac{\xi}{\xi_{\max}} \right]^{-1} (\frac{\tau}{\tau_0})^{-1} \; d(\frac{y}{D}) \tag{7-4}$$

$$\frac{\tau}{\tau_0} = \frac{h}{D} \left(1 - \frac{\frac{y}{D}}{1 - \frac{h}{D}} \right) + \left(1 - \frac{h}{D} \right) \left(1 - \frac{\frac{y}{D}}{1 - \frac{h}{D}} \right)^2 \tag{7-5}$$

$$\xi(\frac{y}{D}) = \frac{\frac{y}{D}}{1 - \frac{h}{D}} e^{\frac{(1 - \frac{y}{D})}{1 - \frac{h}{D}}} \tag{7-6}$$

$\xi_{\max} = 1$

$$h_\xi(\frac{y}{D}) = \left[\frac{\xi(\frac{y}{D})}{\frac{y}{D}} \left(1 - \frac{\frac{y}{D}}{1 - \frac{h}{D}} \right) \right]^{-1} \tag{7-7}$$

$\bar{y}_c$ = Location of the point on y-axis, where the concentration is equal to $\overline{C}_y$.

if $\frac{y}{D} = \frac{\bar{y}_c}{D}$ is substituted in the concentration equation, $\overline{C}_y$ can be calculated from:

$$\overline{C}_y = C_0 \exp\left[-\lambda' I(\frac{\bar{y}_c}{D}) \right] \tag{7-8}$$

On the other hand the depth-averaged concentration on y-axis

$$\overline{C}_y = C_0 \int_0^1 C(\frac{y}{D}) dy(\frac{y}{D}) \tag{7-9}$$

And the velocity-weighted average concentration

$$\overline{C}_y = \frac{\int_0^1 \left[\frac{u_{\max}}{M} \ln \left[1 + \left(e^M - 1\right) \frac{\frac{y}{D}}{1-\frac{h}{D}} e^{\left(\frac{1-\frac{y}{D}}{1-\frac{h}{D}} \right)} \right] \right] C_0 e^{-\lambda' I(\frac{y}{D})} d(\frac{y}{D})}{\int_0^1 \left[\frac{u_{\max}}{M} \ln \left[1 + \left(e^M - 1\right) \frac{\frac{y}{D}}{1-\frac{h}{D}} e^{\left(\frac{1-\frac{y}{D}}{1-\frac{h}{D}} \right)} \right] \right] d(\frac{y}{D})} \tag{7-10}$$

Therefore,

$$C_0 \, e^{\left[-\lambda' I(\frac{\overline{y}_c}{D}) \right]} = C_0 \int_0^1 C(\frac{y}{D}) d(\frac{y}{D}) \tag{7-11}$$

Consequently, $\frac{\overline{y}_c}{D}$ can be computed for each d_{50}

Figure 7.39 is the plots of sediment concentration normalized by depth-averaged concentration against their relative depths. In this figure, λ was calculated from Equations (6-17) and (7-3) or Figure 7.38; and h/D from Equation (4-31). It is evident that the location of mean concentration on y-axis is lower for larger sediment diameters.

A comparison of Figure 7.40 by Chiu [2] and the simulated plots in Figure 7.39 indicates that Figures 7.39 and 7.40 both give the same $\frac{\overline{y}_c}{D}$ for C=$\overline{C}_y$. h/D is a function of M, therefore in Figure 7.40, for M =3, the plots corresponding to h/D = 0.4 is to be used.

Figure 7.41 presents the relation between M and G'(M). It can be used to calculate λ.

In Figure 7.43, concentration is normalized by depth-averaged concentration. It suggests that when d_{50} is kept constant in different channel sections, M will affect slightly the distribution of sediment concentration and the location of sampling. On the other hand, when λ is kept constant,

as M increases, $\frac{\bar{y}_c}{D}$ will increase, because, d_{50} will decrease, as it is evident from Equation (6-17). Both Figure 7.41 and Equation (6-17) show that G'(M) will increase as M increases. Figure 7.42 indicates when λ is kept constant, $\bar{y}_c$ is located closer to the channel bed for lower M values.

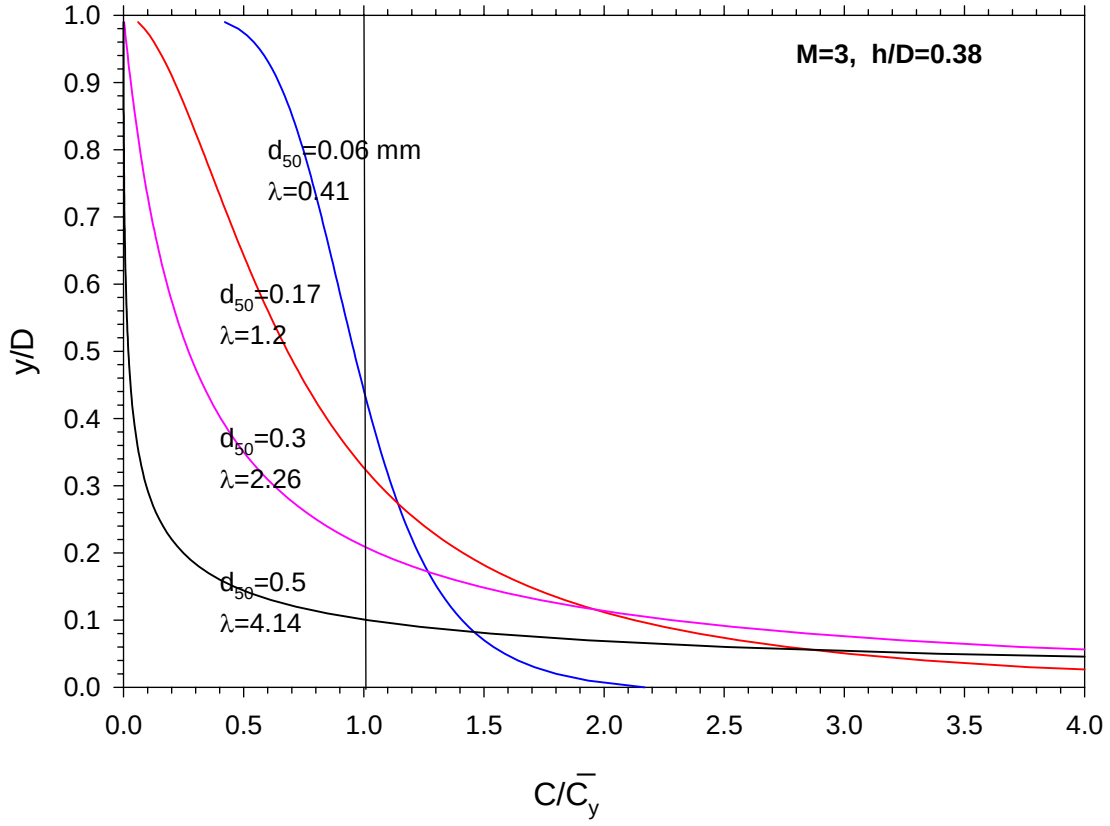

.

Figure 7-39 Effect of Sediment Size on Sediment Concentration

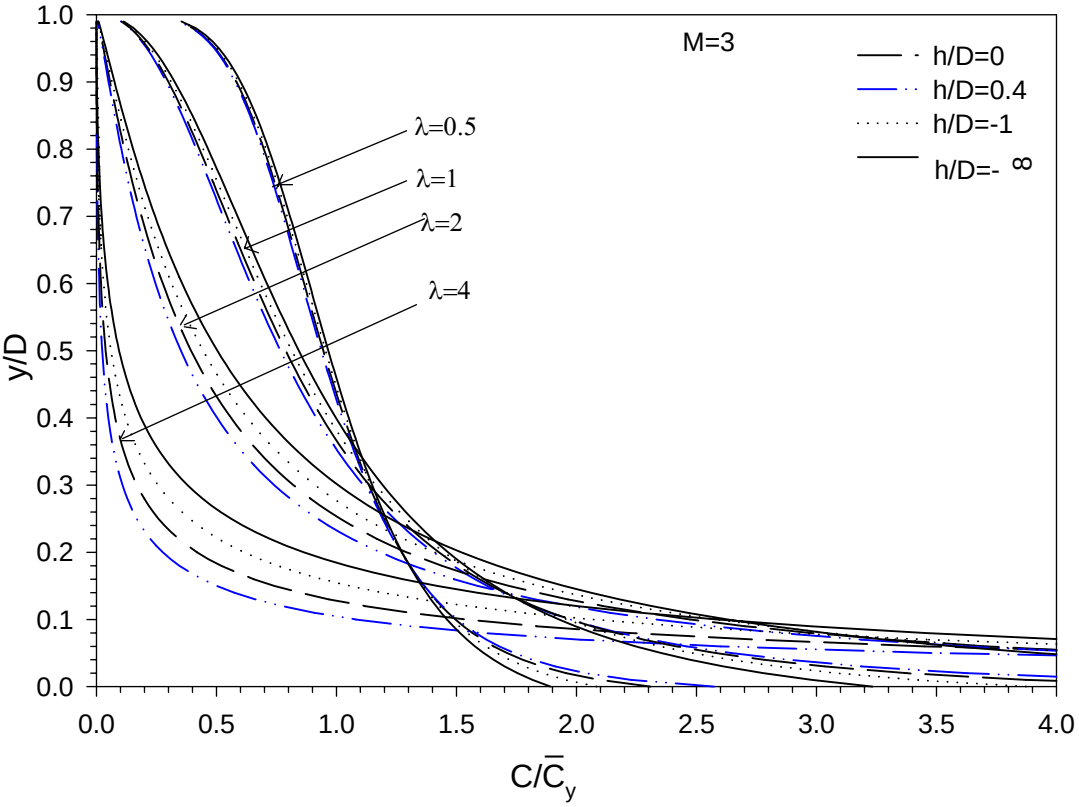

Figure 7-40 Effect of λ and h/D on Sediment Distribution, Chiu [2]

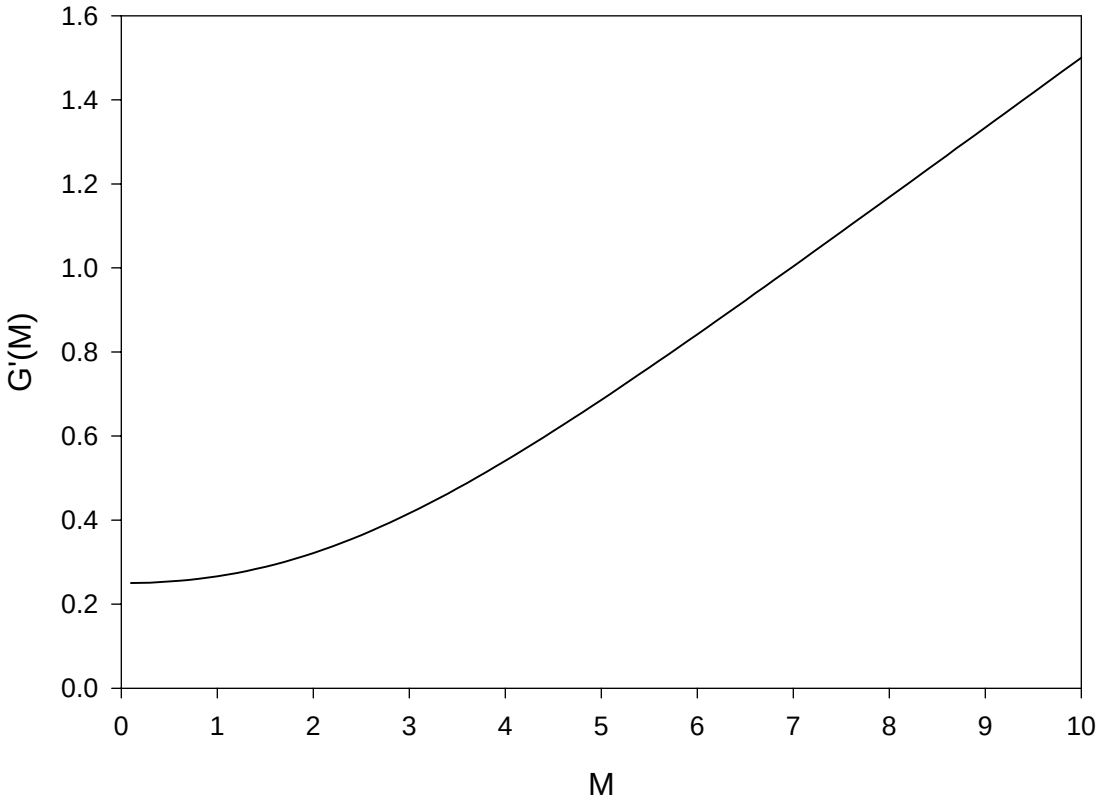

Figure 7-41 Relation between G'(M) and M

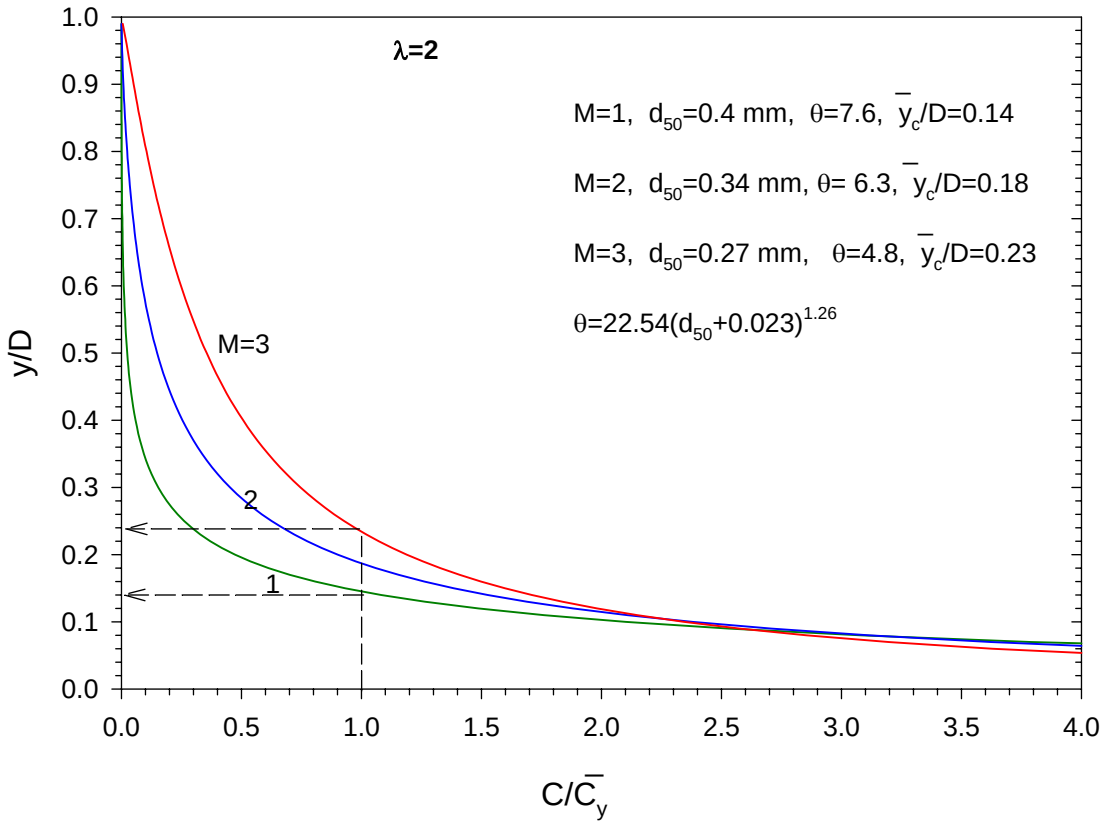

Figure 7-42 Effect of M on Sediment Distribution for λ = 2

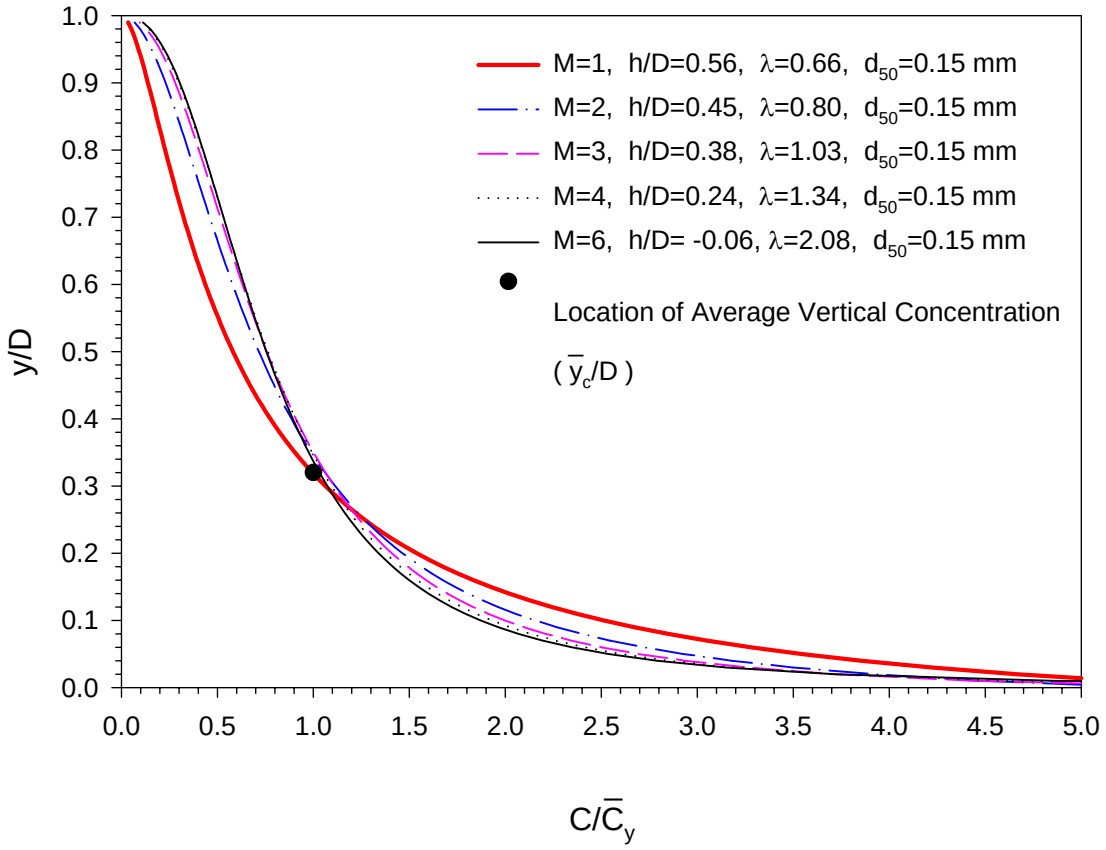

Figure 7-43 Effect of M on Location of Mean Concentration (on y-axis) for Constant d_{50}

Figure 7.44 compares observed data with the simulated sediment distributions when M and d_{50} are used as input. Both distributions fit the data. The difference between the two distributions is due to the methods of calculations of θ and h/D for each point. Figures 7.45 to 7.49 are also Chiu's sediment concentration distributions. The location of mean concentration on y-axis is at a depth where concentration is equal to the average vertical concentration.

Figure 7.45 is the sediment distribution applied to observed data of Omaha Station. This figure was plotted based on the parameters obtained from applying Chiu's equations to the observed

data on y-axis. Figure 7.46 is the simulation using the input of M and d_{50} related to Figure 7.45. The simulation uses the regression relation Equation (7-3) for θ and Equation (4-31) for calculating h/D. Figure 7.48 shows Chiu's Equation (6-20) applied to the sediment data on Missouri River at Nebraska City (4/25/1978). The location of mean vertical concentration is also shown.

Figure 7.49 shows Chiu's sediment concentration distribution applied to the observed data at Line 13, Mississippi River (d_{50} = 0.02 mm). The mean concentration on y-axis is located at y=0.48D.

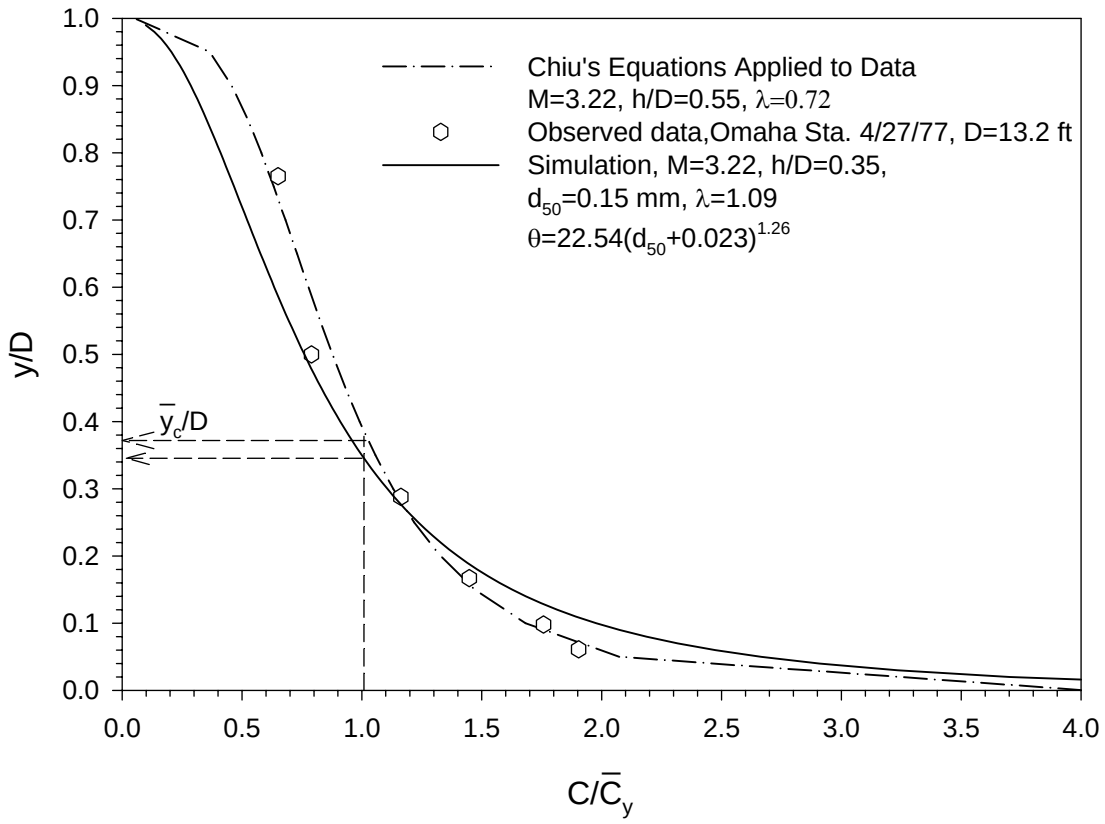

Figure 7-44 Location of Mean Concentration on y-axis by Simulation and Observed Data, Missouri River at Omaha, D=16.6 ft, 9/14/1977

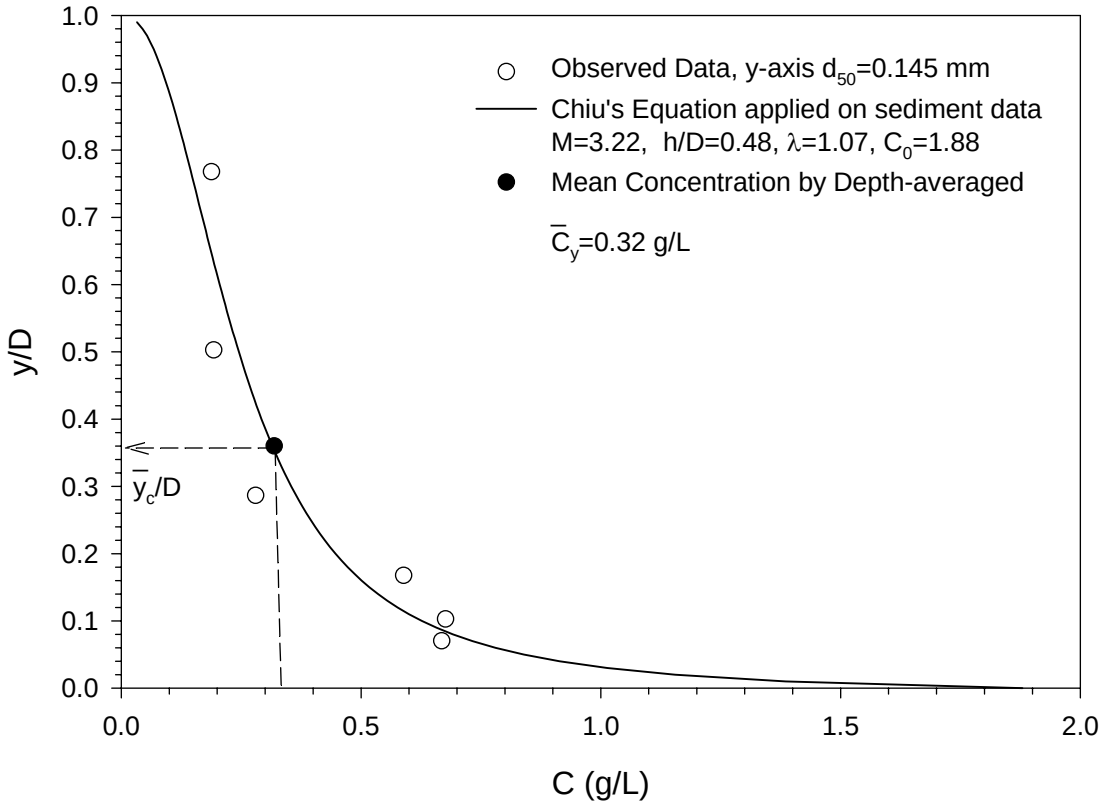

Figure 7-45 Location of Mean Concentration on y-axis, Missouri River at Omaha, 4/26/1978

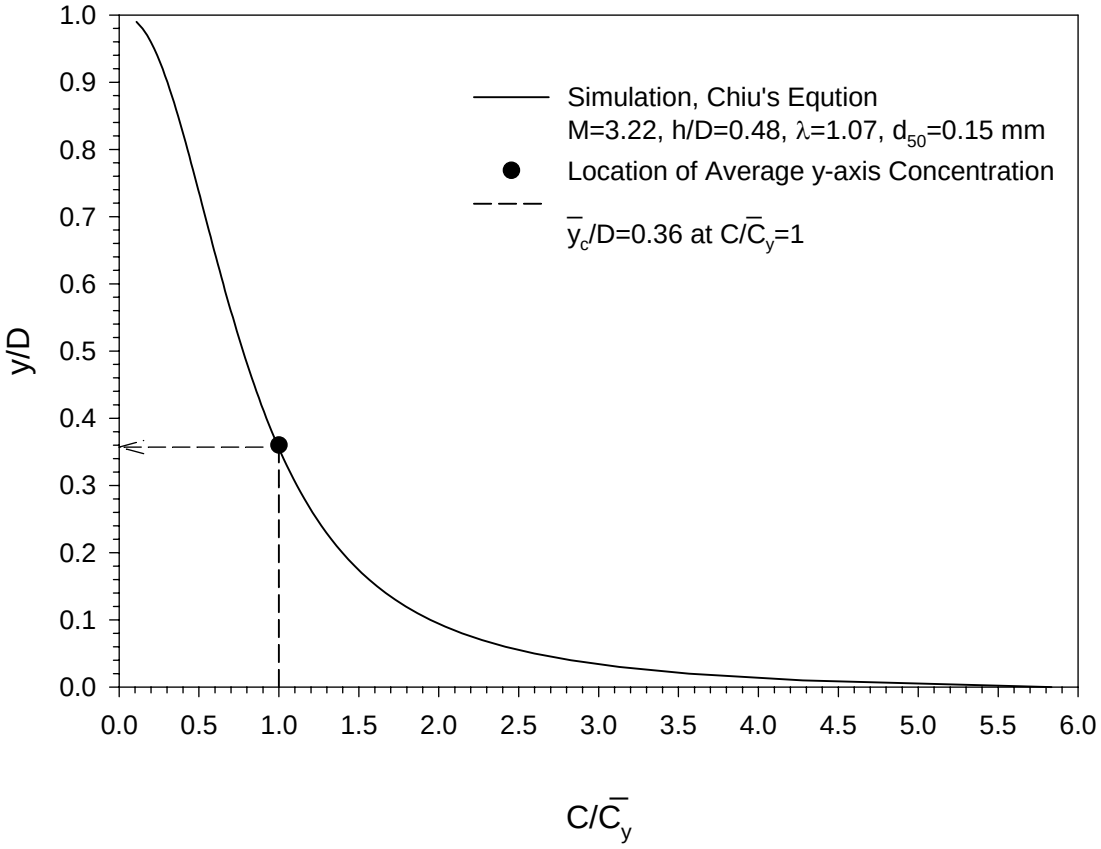

Figure 7-46 Location of Mean Concentration on y-axis (Simulation with M and d_{50} as input), Omaha Station 4/26/1978

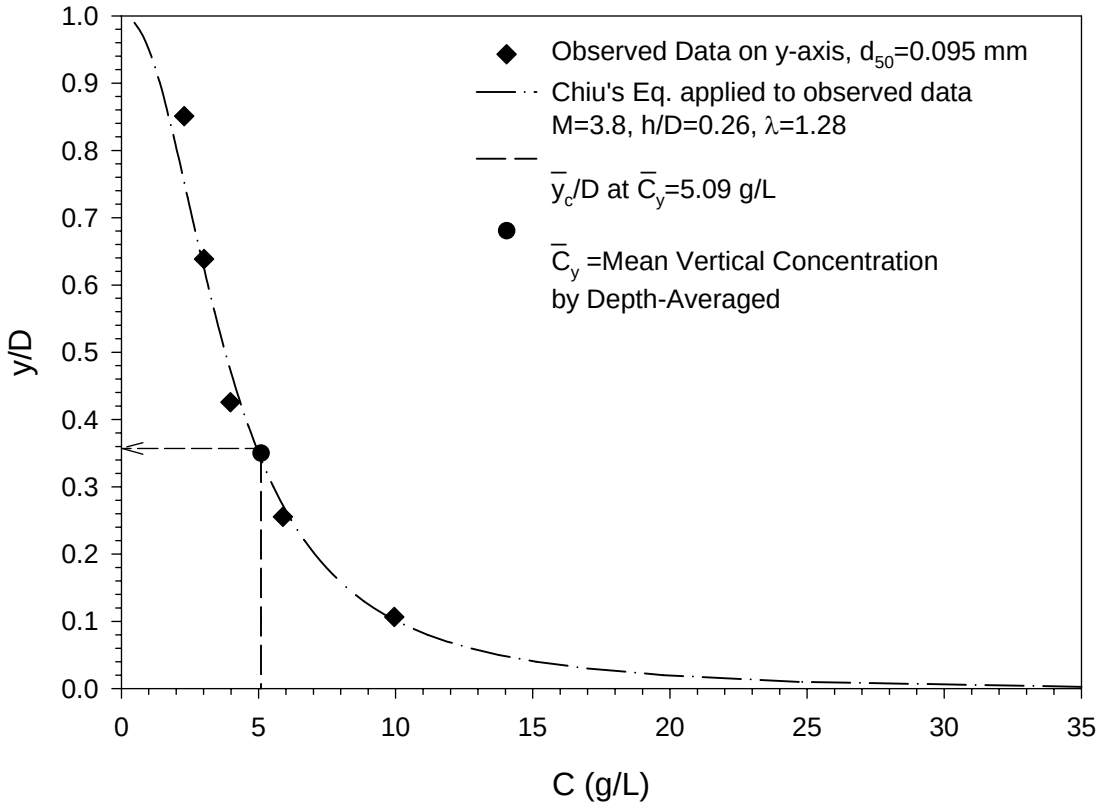

Figure 7-47 Location of Mean Concentration on y-axis, Rio Grande Channel, Section 2249, 12/21/1965

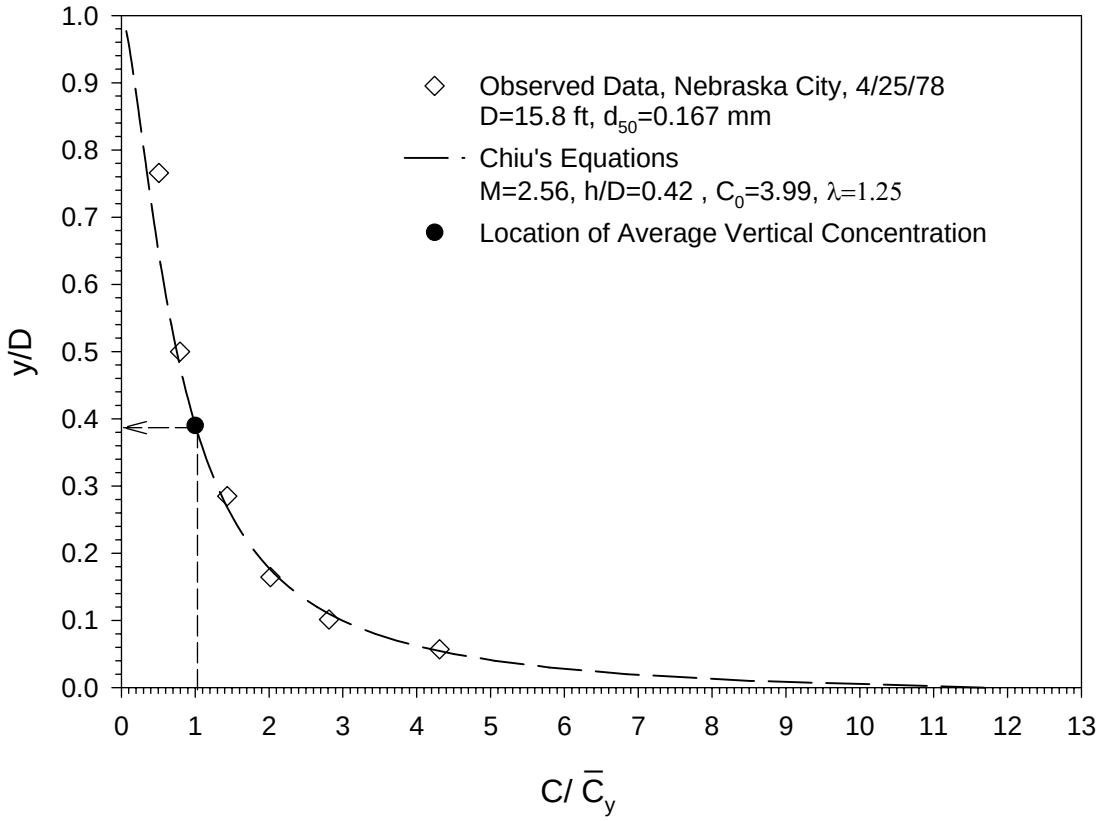

Figure 7-48 Location of Mean Concentration on y-axis, Missouri River at Nebraska City

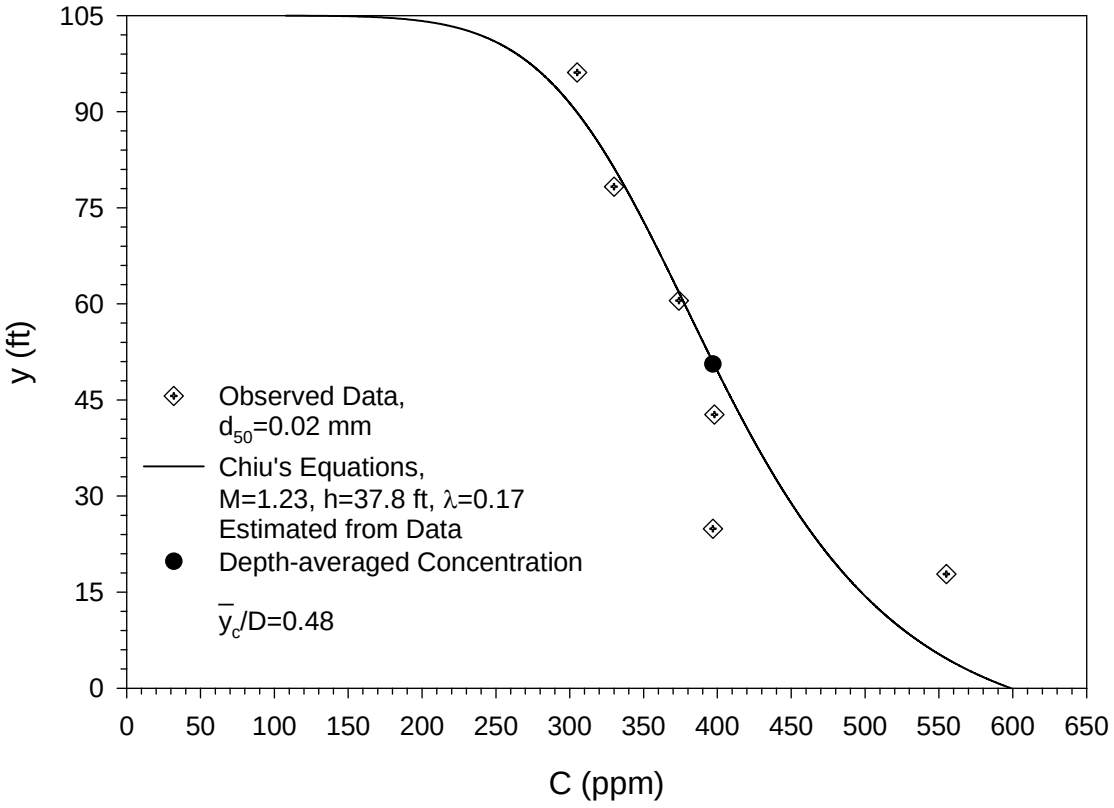

Figure 7-49 Location of Mean Concentration on y-axis, Mississippi River at Line 13, 4/17/1998

7.7 RELATION OF M TO $\frac{\overline{y}_c}{D}, \frac{\overline{y}_v}{D}$ AND $\frac{\overline{y}}{D}$

For a channel section with known M and d_{50}, the location of a single sampling point on y-axis ($\frac{\overline{y}_c}{D}$) can be determined from $\frac{\overline{y}_c}{D}$ - M relations. The collected sample at this location represents the average concentration on y-axis ($\overline{C}_y$). For comparison, the locations of average velocities on y-axis and cross-sectional average velocities have been plotted based on their relations with M.

Figure 7.50 shows the relation of M to locations of average concentration on y-axis for different λ and d_{50}. The figure indicates that $\frac{\bar{y}_c}{D}$ is a function of d_{50}.

The plots of M against $\frac{\bar{y}_c}{D}$ show that when M increases, for a given d_{50}, $\frac{\bar{y}_c}{D}$ tends to be insensitive to variation of M for fine sediment ($d_{50} \leq 0.06$ mm). $\frac{\bar{y}_c}{D}$ varies slightly (5%) with M for coarse sediment (d_{50} =0.3 mm). Therefore, it can be said that $\frac{\bar{y}_c}{D}$ is not a function of M, but depends on d_{50}. If d_{50} (y-axis) of a river is known, location of the single-point sampling can be obtained by referring to related plots presented here (Figure 7.50).

On the other hand, location of average velocity on y-axis $\left(\frac{\bar{y}_v}{D}\right)$ and location of cross-sectional average velocity $\left(\frac{\bar{y}}{D}\right)$ are functions of M and do not change in a channel section (Figures 7.51 and 7.52).

Figures 7.51 and 7.52 give the location of mean concentration on y-axis $\left(\frac{\bar{y}_c}{D}\right)$ in a channel section with known M. Figure 7.53 compares $\frac{\bar{y}_c}{D}$ obtained from depth-and velocity-weighted averaging. This figure demonstrates that as d_{50} reduces, the distributions of sediment concentration determined from depth- and velocity-weighted methods become closer.

Figures 7.54 and 7.55 suggest that data support the results obtained from Figure 7.50.

Ingram [15, 18] studied the sampling depths of several rivers and found that the sampling point in the Middle Loup River and Rio Grande Conveyance Channel were located at between y = 0.19D and to 0.33D.

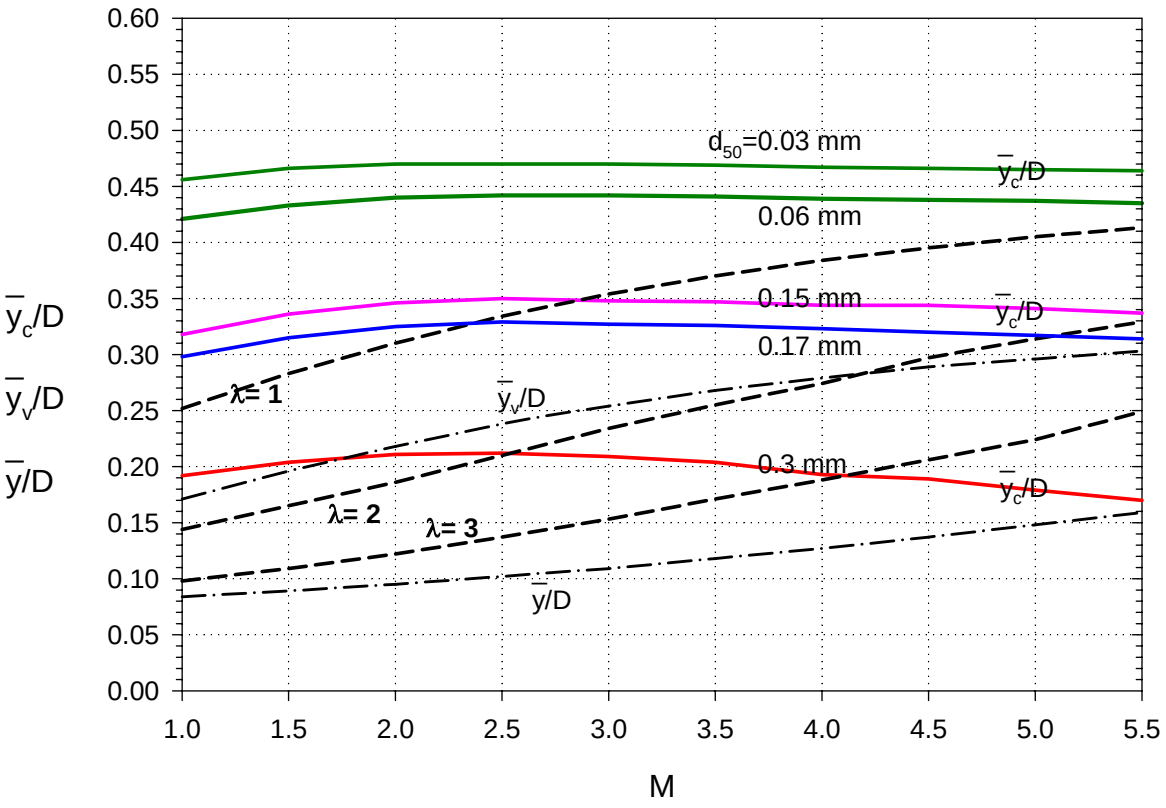

Figure 7-50 Relations among Locations of Mean Concentration on y-axis, Cross-sectional Mean Velocity and Mean Velocity on y-axis

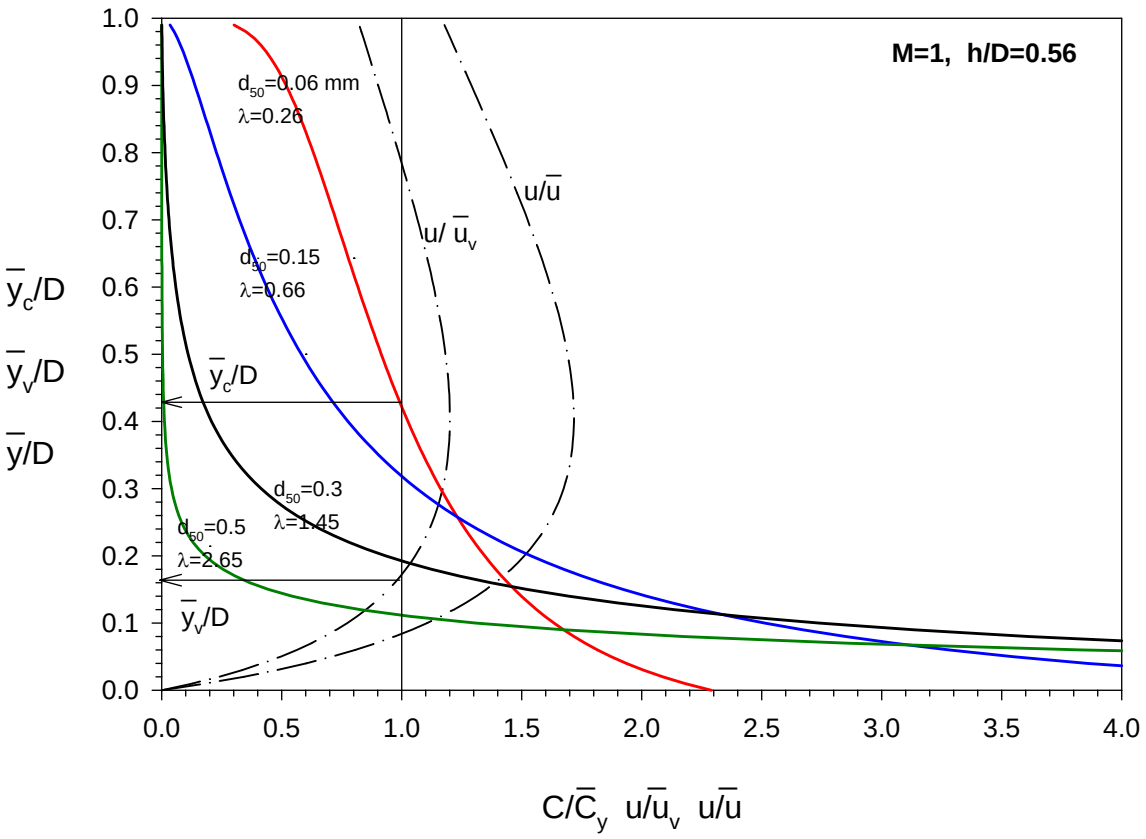

Figure 7-51 Locations of Mean Concentration and Velocity on y-axis and Cross-sectional Mean Velocity for M=1

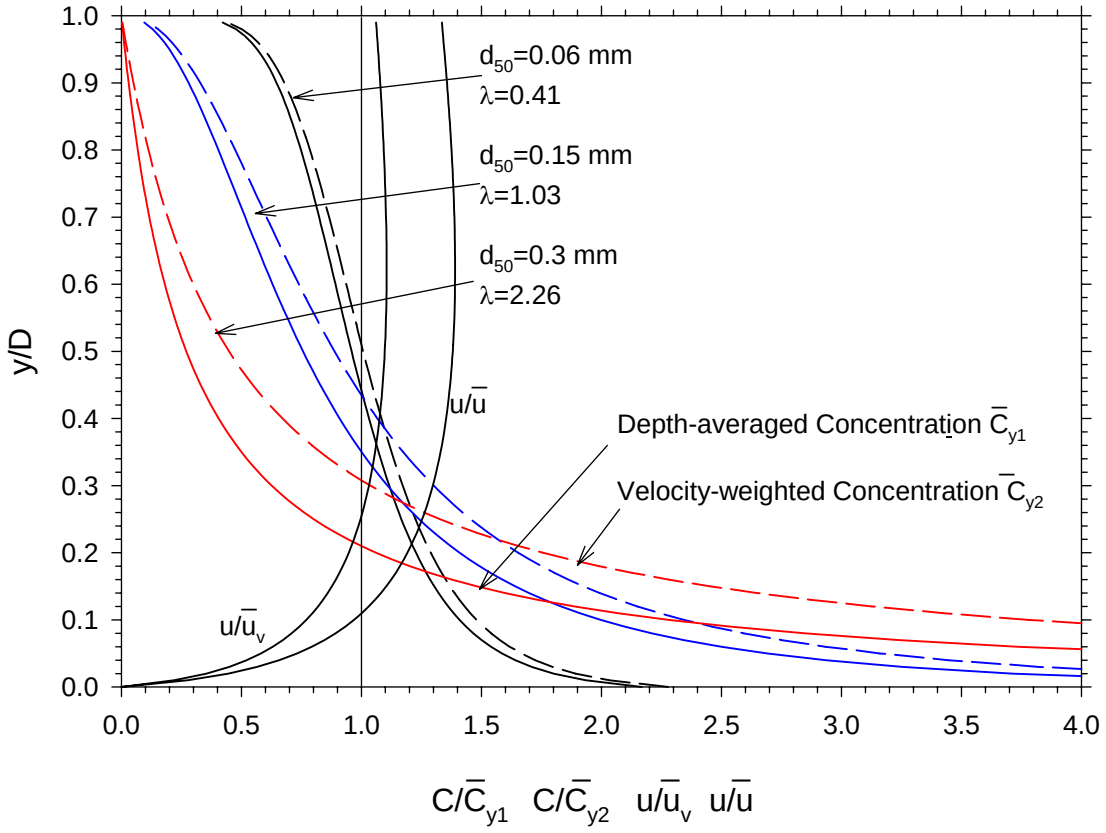

Figure 7-52 Locations of Mean Concentration on y- axis (by two methods), Mean Velocity on y-axis and Cross-sectional Mean Velocities for M=3

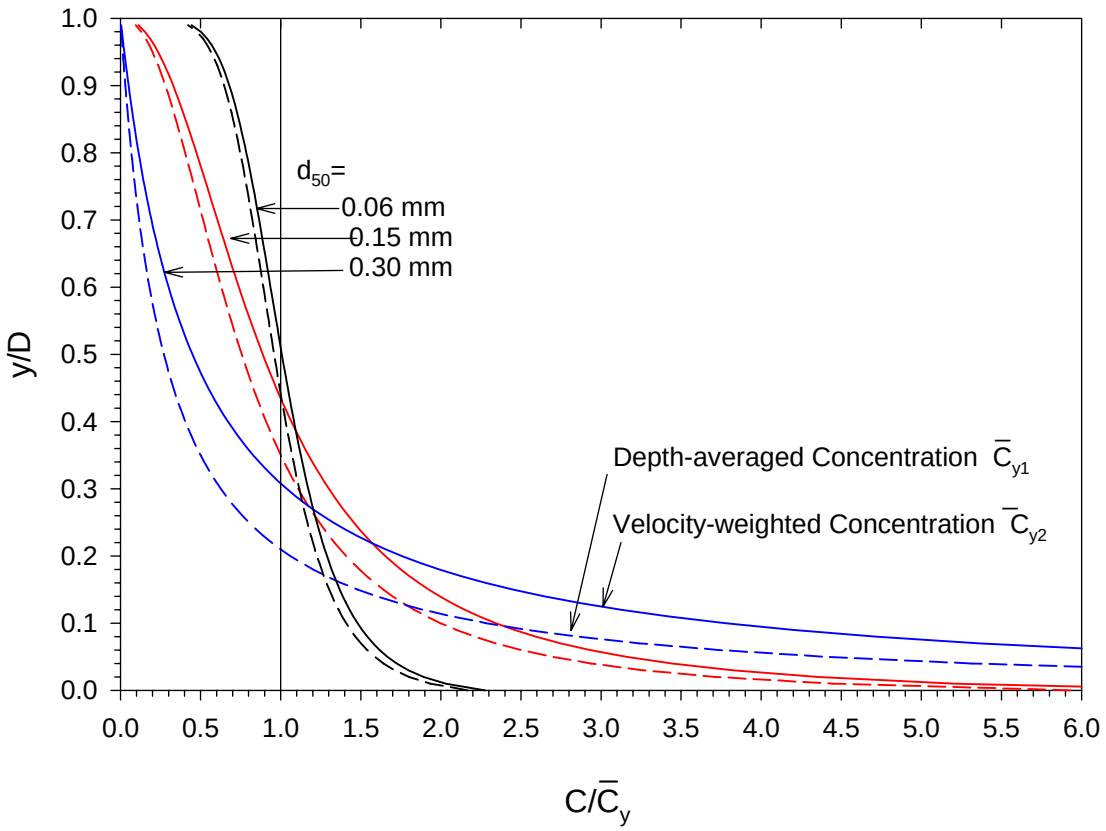

Figure 7-53 Locating Mean Concentration on y-axis by Depth- and Velocity-weighted Methods for M=3

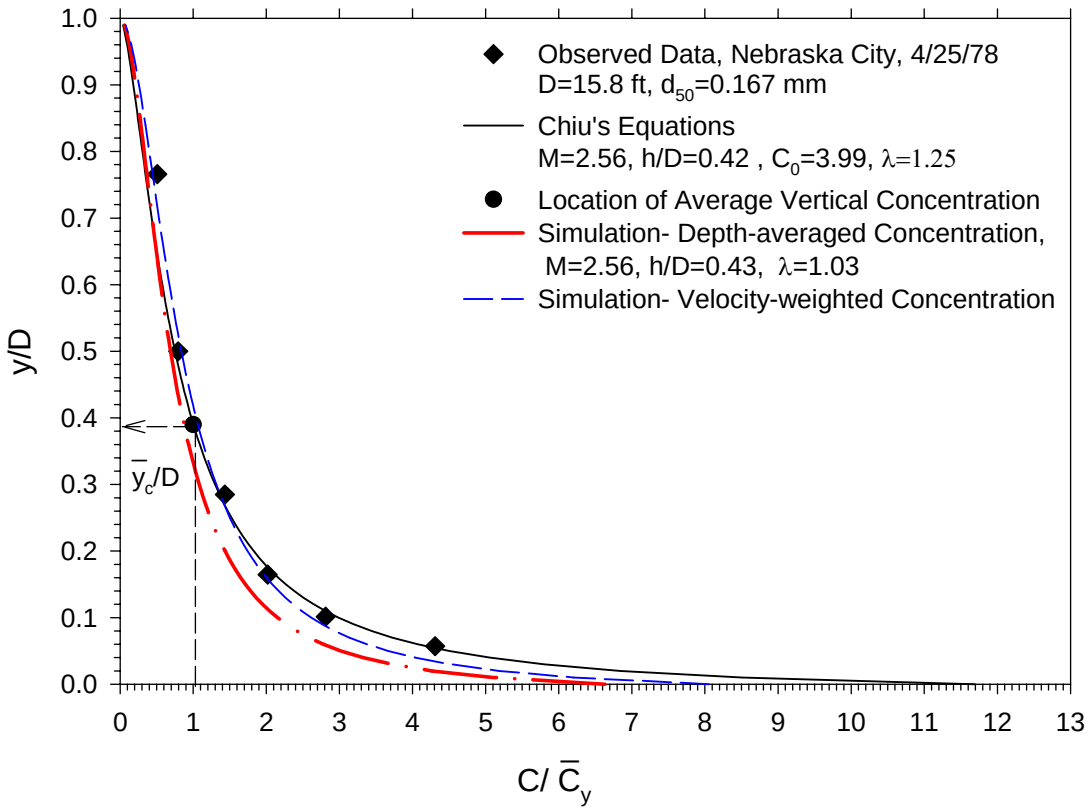

Figure 7-54 A comparison of Normalized Chiu's Sediment Distribution Applied to Data and two Simulations Normalized by Depth-and Velocity-weighted Averages, Missouri River

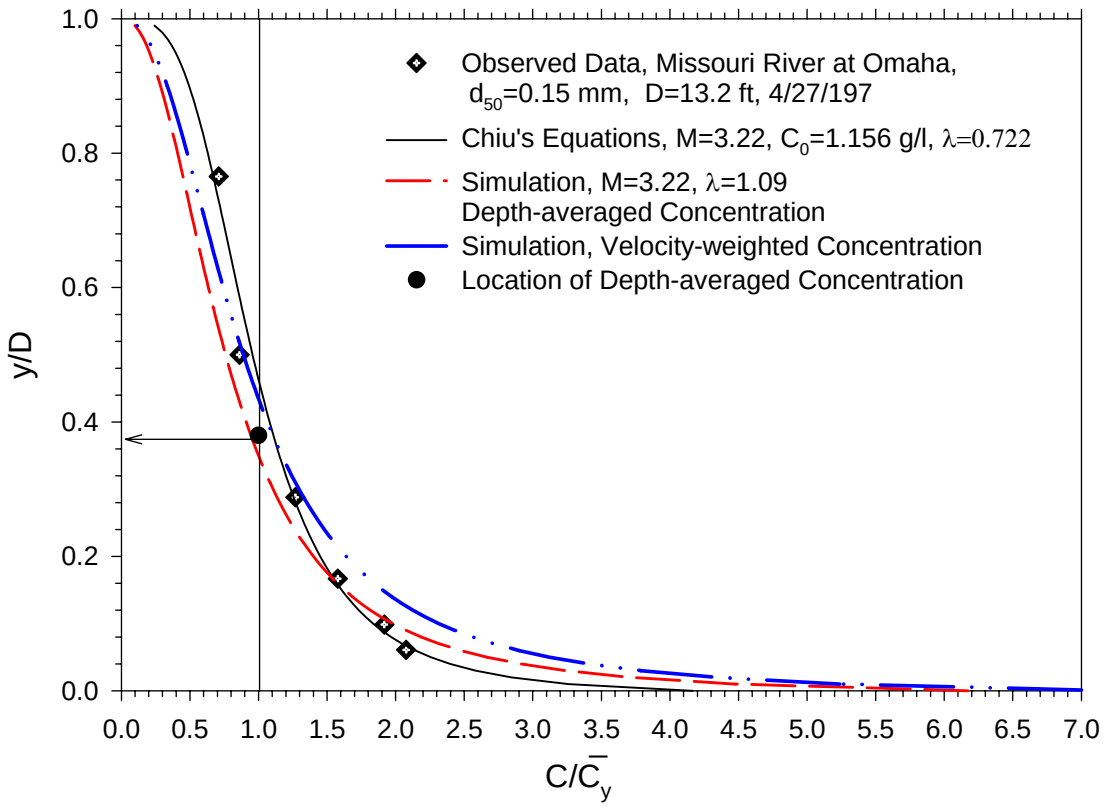

Figure 7-55 Sediment Concentration Distribution Normalized by Depth-and Velocity-weighted mean Concentration

7.8 RELATION BETWEEN M AND Ψ

Relations between Ψ and M for different river sections were determined by data analysis. Figure 7.56 shows relations between M and Ψ for river sections with fine size sediment d_{50} <0.1 mm, and coarse size sediment $0.19 \geq d_{50} \geq 0.13$ mm.

The scatter of the points indicates two separate relations due to difference in d_{50} of different river sections. For the sections with larger sediment size d_{50}=0.13-0.19 mm, the values of Ψ were found to be between 0.50 and 0.75, while for the sections having finer sediments d_{50}=0.007-0.095 mm, the Ψ values were between 0.80 and 0.99 (Figure 7.56).

In order to use these relations, d_{50} on y-axis in the channel section must be determined from sediment size distribution either from the long term historic data (for established stations) or by taking several samples on y-axis (for new stations).

Figure 7.57 shows the relations between M and Ψ for a range of particle diameters (0.06-0.36 mm). For the data analyzed in this research, the sediment diameters of 0.15 to 0.18 mm have the highest coefficient of determination r^2 and fine sediment with diameter of 0.06 mm has the lowest r^2.

Table 7.1 shows the computed values of M and Ψ related to a channel section. It indicates a trend that Ψ will increase with M, but does not vary with discharge.

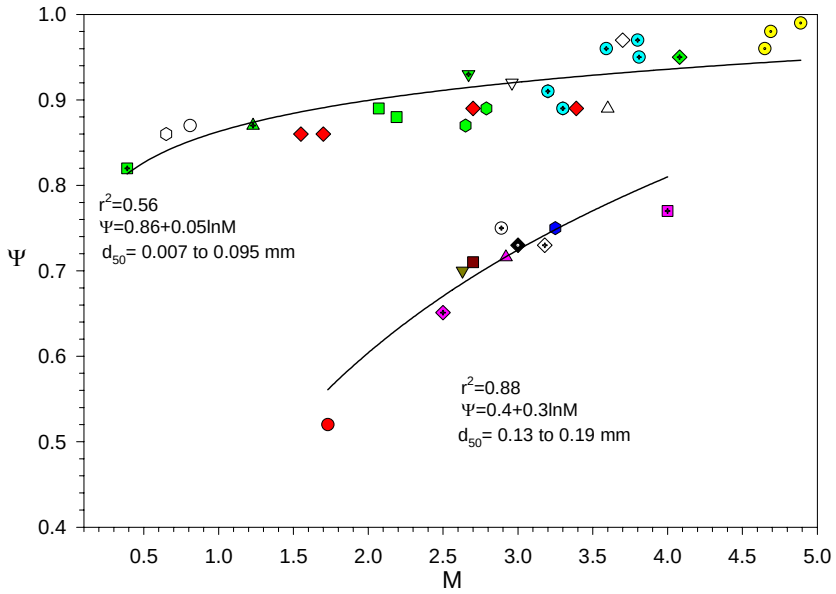

- Misssouri River at Nebraska City, 12 Sets (d_{50}=0.17mm)
- Niobrara River at Gaging Station 6 Sets (d_{50}=0.16mm)
- Missouri River at Ponca 14 Sets (d_{50}=0.17mm)
- Missouri River at Gayvill 8 Sets (d_{50}=0.18mm)
- Missouri River at Maskell 7 Sets (d_{50}=0.15mm)
- Missouri River at Sioux City 11 Sets (d_{50}=0.182mm)
- Middle Loup River at Dunning Section B 6 Sets (d_{50}=0.16 mm)
- Mississippi River at Line 6, RM 307 (d_{50} =0.02mm)
- Mississippi River at Line 13, RM 313 (d_{50}=0.02mm)
- Mississippi River at Low Sill Channel (d_{50}=0.02mm)
- Mississipi River at ORC Outflow Channel (d_{50}=0.02mm)
- Rio Grande Channel Sections 245, 255, 2249, 2243 and 1318 (d_{50}=0.09mm)
- Sacramento River at River Miles 38.45, 37.85, 37.16, and 35.64 (d_{50} =0.01-0.06 mm)
- Mississippi River at Union Point RM=265, 32 Sets and RM 323 (d_{50}=0.02 mm)
- Mississippi River at Range 362.2, 9 Sets (d_{50}=0.007mm)
- Mississippi River at Tarbert RM306, 35 Sets and RM 304 (d_{50}=0.012mm)
- Atchafalaya River at Simmesport, 15 Sets (0.026mm)
- Flume Data, Coleman 3 Runs (d_{50}=0.05mm)
- Missouri River at Omaha 16 Sets (d_{50}=0.17mm)
- Mississippi River at Auxiliary Channel (d_{50}=0.02mm)
- Mississippi River at Outflow Auxiliary Structure (d_{50}=0.09mm)
- Mississippi River at Hydroinflow Channel (d_{50}=0.02 mm)
- Middle Loup River at Dunning, Section C (d_{50}=0.13 mm)
- Middle Loup River at Dunning, Section D (d_{50}=0.19 mm)
- Regression Lines

Figure 7-56 Relation between M and ψ

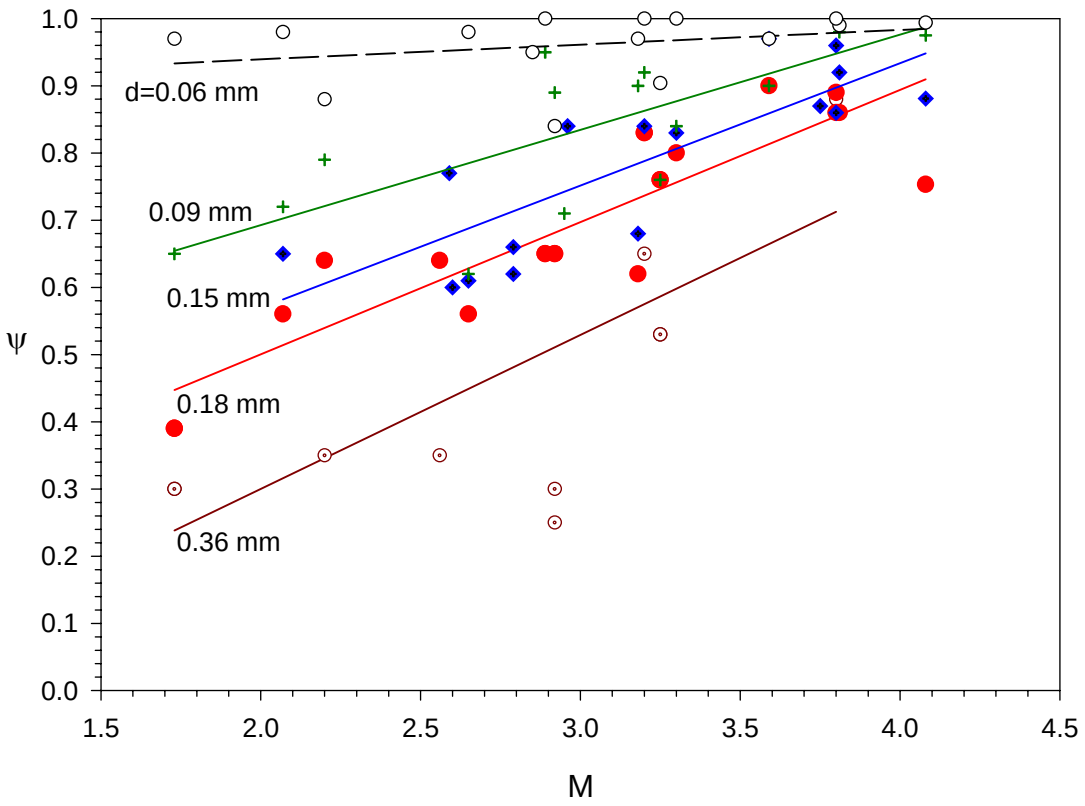

d=0.36 mm: ψ=0.23M-0.16, r^2=0.52
0.18 mm ψ=0.2M+0.11, r^2=0.79
0.15 mm ψ=0.18M+0.2, r^2=0.67
0.09 mm ψ=0.14M+0.41, r^2=0.58
0.06 mm ψ=0.02M+0.9, r^2=0.09

Figure 7-57 Relation between M and ψ for Different Sediment Diameters, Mississippi, Missouri, and Middle Loup Rivers, and Rio Grande Channel

Table 7-1 Relation between ψ and M

	Range Discharge	Range d_{50}	ψ	M
River Station	cfs	mm		
Missouri River at				
Omaha	31,500-63,300	0.149-0.19	0.75	3.22
Ponca	29,800-54,000	0.139-0.223	0.75	2.89
Nebraska City	36,800-69,200	0.115-0.237	0.68	2.56
Sioux City	31,000-39,600	0.162-0.246	0.78	4
Gayville	28,500-37,600	0.143-0.258	0.72	2.9
Niobrara River at				
Gaging Station	298-405	0.13-0.24	0.51	1.73
Middle Loup River at				
Sect.D	376-403	0.195-0.24	0.73	3.18
Sect.C	376-450	0.1-0.137	0.71	2.7
Sec.B	367-415	0.15-0.2	0.73	3
Mississippi River at				
Union Point	51,000-127000	0.022	0.89	2.07
Range 326.2	24,000-105,000	0.007	0.93	3.18
Tarbert	38,000-102,000	0.012	0.87	2.65
Atchfalaya River	12,000-57,000	0.026	0.95	0.96
Coleman Flume				
8/1/1990	0.27	0.03	0.95	4.65
8/2/1990	0.21	0.03	0.98	4.69
7/30/1990	0.54	0.03	1	4.89

Table 7-2 Location of Sampling Point on y-axis

River	d_{50}	$\frac{\overline{y}_c}{D}$
	(mm)	
Missouri River Niobrara River Middle Loup River	0.13-0.18	0.32D-0.37D
Mississippi River at Union Point	0.022	0.48D
Mississippi River at Tarbert	0.012	0.48D
Sacramento River at Four Stations	0.06	0.45D
Rio Grande Channel at Sections 245 and1318	0.095	0.40D

8.0 SUMMARY AND CONCLUSIONS

- The proposed method is compatible with the efficient method of water discharge measurement based on probability concept pioneered by Chiu. Chiu's equations were used to determine the location of single sampling point on y-axis. It was found that the sample taken at a relative depth of $\frac{\bar{y}_c}{D}$ could represent the mean concentration on y-axis, $\overline{C}_y$. This sample concentration in turn can be converted into the cross-sectional mean concentration ($\overline{C}_x$) using their relations determined in this research. The cross-sectional mean concentration can be determined as $\overline{C}_x = \psi \overline{C}_y$. The sediment discharge in turn can be calculated as $Q_s = \overline{C}_x Q$, where $Q = A\bar{u} = \phi A u_{\max}$.
- The y-axis is a vertical on which the maximum velocity of the entire river section occurs. It was determined from the velocity data and verified from the pattern of the isovels. The location of y-axis is stable and does not change with time and discharge.
- The correlations between cross-sectional mean concentration and the mean concentration on each vertical across the channel sections of different rivers were determined. It was shown that the correlation is highest on y-axis and decreases toward the channel banks. Therefore, it provides a basis for collecting the sediment sample on the y-axis.

- The ratio of cross-sectional mean concentration ($\overline{C}_x$) to the mean concentration on y-axis ($\overline{C}_y$) is defined as $\psi = \frac{\overline{C}_x}{\overline{C}_y}$. This coefficient was calculated for each grain diameter (d) and median size (d_{50}) on y-axis. The ψ value representative of each river section was determined by regression.
- The coefficient of determination (r^2) of $\overline{C}_x$-$\overline{C}_y$ relation is higher for fine sediment particles (d_{50}<0.062 mm). It means that in rivers, that transport predominantly fine sediment, the sediment particles are uniformly distributed, and $\overline{C}_y$ is a good predictor of $\overline{C}_x$. The distribution of sediment concentration in river sections, with coarse sediment particles (d_{50}>0.062 mm) is not uniform and r^2 was found to have lower values.
- One needs to know d_{50} on the y-axis in order to choose an appropriate sampling depth. d_{50} affects the location of sampling on y-axis, but M affects it slightly.
- Table 7.2 summarizes the computed values of $\frac{\overline{y}_c}{D}$ and d_{50} of the suspended sediment for several rivers. For example, d_{50} on y-axis of Missouri, Niobrara and Middle Loup Rivers at different discharges used in this research are in the range of 0.13-0.18 mm. According to Figure 7.50 and Table 7.2 the sample point should be between y = 0.32D to 0.37D (32% to 37% of the depth from the channel bed).

- In this research, only the field data related to suspended sediment of different rivers were analyzed. Therefore, the estimated $\overline{C}_x$ determined from the relations of Ψ and M represents the mean suspended sediment concentration in the overall cross section.

BIBLIOGRAPHY

1. Chiu, C-L., and Said, C.A.A. "Maximum and Mean Velocities and Entropy in Open – channel Flow," Journal of Hydraulic Engineering, ASCE, Vol. 121, No.1 (1995), pp26-35.

2. Chiu, C-L., Jin, W., and Chen, Y-C., "Mathematical Models of Distribution of Sediment Concentration," Journal of Hydraulic Engineering, ASCE, Vol.126, No.1 (2000), pp.16-23.

3. Chiu, C-L., "Entropy and Probability Concepts in Hydraulics," Journal of Hydraulic Engineering, ASCE, Vol.113, No.5 (1987), pp.583-600.

4. Chiu, C-L., "Velocity Distribution in Open-channel Flow," Journal of Hydraulic Engineering, ASCE, Vol.115, No.5 (1989), pp. 576-594.

5. Chiu, C-L., "Application of Entropy Concepts in Open-channel Flow Study," Journal of Hydraulic Engineering, ASCE, Vol.117, Npo.5 (1991), pp.615-628.

6. Chiu, C-L. and D.W. Murray "Variation of Velocity Distribution along Non-uniform Open-channel Flow," Journal of Hydraulic Engineering, ASCE, Vol.118, No. 7(1992), pp.989-1001.

7. Chiu, C-L., and N-C. Tung, "Maximum Velocity and Regularities in Open-channel Flow," Journal of Hydraulic Engineering, ASCE, Vol. 128, No. 4 (2002), pp. 390-398.

8. Shen, H. W. and Wang W.C., "Missouri River, Sediment Transport Relationships," U.S. Army Corps of Engineers, Omaha District, MRD Sediment Series No.17 (1979).

9. Shen, H.W. and Wang W.C. "Missouri River Vertical Sediment Concentration Distribution for Different Sizes," U.S. Army Corps of Engineers, Omaha District, MRD Sediment Series No. 25 (1981).

10. Missouri River Special Point-Integrated Sediment Sampling Report, MRD Sediment Series No. 37(1991).

11. Mahmood, K., Missouri River User's Manual Sediment Transport Program, U.S. Army Corps of Engineers, MRD Sediment Series No. 26 (1982).

12. Mahmood, K., Verification of Sediment Transport Functions Missouri River, MRD Sediment Series No. 19 (1980).

13. Guy, H. P., "Fluvial Sediment Concepts," Techniques of Water Research Investigations of the United States Geological Survey (1970).

14. Edwards, T.K. and Glysson, G. D, "Field Methods for Measurement of Fluvial Sediment," U.S. Geological Survey, Open-File Report 86-531, 1988.

15. Ingram, J. J., Steven R., and Richardson, E. V. "Sediment Discharge Computation Using Point-Sampled Suspended-Sediment Data," Journal of Hydraulic Engineering, ASCE, Vol.117, No.6 (1991), pp. 756-771.

16. Walling, W. E., "Assessing the Accuracy of Suspended Sediment Rating Curves for a Small Basin," Water Resources Research, vol. 13 (June, 1977), pp. 531-538.

17. Harmon, J.G." Sediment and Stream-Velocity Data for the Sacramento River near Hood, California, May 1978 to September 1981", California Department of Water Resources.

18. Ingram, J. J. "Total Sediment Load Measurement using Point-source Suspended-sediment Data" Ph.D. Dissertation, Colorado State University, (1988).

19. McQuivey, R.S. "Summary of Turbulence Data from Rivers, Conveyance Channels, and Laboratory Flumes". U.S. Geological Survey Provisional Paper 802-B. (1973).

20. Crawford, Charles, "Estimation of Suspended-Sediment Rating Curves and Mean Suspended Sediment Loads," Journal of Hydrology, vol. 129 (1991), pp. 331-348.

21. Coleman, N. L. Personal Communication, (1990), Mid South Area National Sedimentation Laboratory, ARS, U.S. Department of Agriculture.

22. Yuqian, Long, Manual on Operational Methods for the measurement of Sediment Transport, World Meteorological Organization, No.29 (1989).

23. Horowitz, A.J., "The Use of Automatically Collected Point Samples to Estimate Suspended Sediment," Proceedings of The Oslo Symposium, August, 1992, IAHS, pub. No. 210, pp. 209-213.

24. Guy, H. P., An Analysis of Some Storm-Period Variables Affecting Stream Sediment Transport. Geological Survey Professional Paper 462-E, 1964.

25. Porterfield, George, Computation of Fluvial-Sediment Discharge. Book 3, U.S. Geological survey, 1972.

26. Kircher, James E., Interpretation of Sediment Data for the South Platte Rive in Colorado and Nebraska. U.S. Geological Survey, D series.

27. Catalyst-Old River Hydroelectric Limited Partnership, in Association with U.S. Army Corps of Engineers, Wicksburg, Mississippi, "Lower Mississippi River Sediment Study".

28. Hsu S-M., "Probability-Based Simulation of 2-D Velocity Distribution and Discharge Estimation in Open Channel Flow," Ph.D. Dissertation, University of Pittsburgh, 2004.

29. Colby, B.R. and C.H. Hembree, "Computation of Total Sediment Discharge, Niobrara River Near Cody, Nebraska," Geological Survey Water-Supply Paper 1357, 1955.

30. Garde, R.J. Mechanics of Sediment Transportation and Alluvial Stream Problems, (John Wiley & Sons, 1985).

31. Vanoni, V.A. Sedimentation Engineering. ASCE Manuals on Engineering Practices-No.4. (1975).

32. Graf, W.H. Hydraulics of Sediment Transport. Water Resources Publications. (1984).

33. Simon, D.B. Senturk, F. Sediment Transport Technology. (Water Resources Publication, Littleton, Colorado, 1992).

34. Morris, G. and Fan, J. Reservoir Sedimentation Handbook. (McGraw-Hill, 1997).

35. National Handbook of Recommended Methods for Water-Data Acquisition, (USGS, 1977).

36. Chow, V. T and Maidment, D. M, Applied Hydrology, (McGraw-Hill, 1988).

37. Hubbell, D.W. and Matejka, D.Q., "Investigations of Sediment Transportation Middle Loup River at Dunning, Nebraska, 1959", Geological Survey Water-supply Paper 1476.

38. Culbertson, J. K., Scott, C. H., and Bennett, J. P., "Summary of Alluvial Channel Data from Rio Grande Conveyance Channel, New Mexico, 1965-69", Open File Report, U.S. Geological Survey, Water Resources Division.